The Role of PTP1B in Anxiety-Related Behaviours in hAPP-J20 and PS19 Mouse Models of Alzheimer's Disease

FARIBA SHARMIN

This thesis is submitted as a partial fulfillment of the requirements of the

Master of Science Degree in Neuroscience

DEPARTMENT OF CELLULAR AND MOLECULAR MEDICINE
NEUROSCIENCE PROGRAM
FACULTY OF MEDICINE
UNIVERSITY OF OTTAWA
JANUARY 2022

Abstract

Alzheimer's disease (AD) is the most prevalent neurodegenerative disorder amongst older adults. Features of this disease include accumulation of amyloid-β (Aβ) plaques, neurofibrillary tau tangles (NFT), neuroinflammation, and neurodegeneration. These result in a progressive decline in memory and executive function in patients. Anxiety-related behaviours are disparaging comorbidities of AD, but how they arise in patients remains elusive. Protein-tyrosine phosphatase 1B (PTP1B) has been associated with Aβ pathology and with anxiety in separate paradigms, but whether PTP1B is involved in anxiety-related behaviours in AD mouse models is unknown. The objective of this project was to compare anxiety-related behaviours between the hAPP-J20 (Aβ pathology) and PS19 (Tau pathology) mouse models of AD and determine whether PTP1B is involved in these behaviours. Another major objective of this project was to investigate the role of PTP1B in tau pathology in the PS19 mouse model in anxiety-related brain regions, since this has not been previously examined. Using key anxiety-testing paradigms such as the elevated plus maze (EPM) and the open field test (OF), an age-based dimorphism in the onset of an inappropriately lowered anxiety response in the J20 and PS19 mouse models was identified. Furthermore, it was shown that this abnormal anti-anxiety baseline phenotype could be normalized with selective PTP1B inhibition by the drug trodusquemine and by genetic neuronal ablation. Finally, in PS19 mice at 8 months of age, it was shown that PTP1B blockade has the therapeutic effect of relieving neurotoxic phospho-tau burden and neuroinflammation. Together, these findings suggest that unleashed PTP1B may serve as a potential therapeutic target, with a possible role in AD-associated anxiety-related behaviours and AD pathology.

Acknowledgements

I would like to thank my supervisor, Dr. Hsiao-Huei Chen, for introducing me to this project and for providing me with invaluable feedback and direction throughout the entirety of my Master's experience. I would also like to thank all members of my laboratory, including Dr. Zhaohong Qin, Dr. Li Zhang, and Dr. Wei Lin for their continued assistance and advice for my project. In addition to this, I was fortunate to have a series of incredible former mentors in my laboratory, namely, Mr. Kaveh Farrokhi, Dr. Konrad Ricke, and Dr. Jonathan Weldrick, who equipped me with the technical skills I needed to succeed. My TAC members, Dr. Diane Lagace and Dr. Baptiste Lacoste, must also be acknowledged for their valuable constructive criticism on my project and guidance throughout my journey as a Master's student.

I am extremely indebted to my parents, Mr. Shahed Kamal and Mrs. Rubina Yesmin, and my sister, Faeza Afrin, for helping me keep a positive attitude as I worked towards completing this degree in the face of the difficult circumstances posed by the COVID-19 pandemic. Lastly, I am grateful for the support of my best friend, Ilham Rahman — thank you for always listening to my rants and keeping me motivated!

Division of Tasks:

In this project, I completed all animal behavioural experiments and performed the relevant statistical analyses. Animal breeding strategies were formulated by Dr. Chen and myself. Mouse colonies were maintained by Dr. Wei Lin, our lead laboratory technician. Drug injections were conducted by Dr. Wei Lin and Dr. Konrad Ricke, a former post-doctoral fellow in the lab. I planned and conducted all immunohistochemical (IHC) experiments in PS19 mice. Dr. Chen imaged the IHC preparations. I conducted Western blot experiments evaluating protein levels of PTP1B, p-GSK3β, and GSK3β, quantified protein levels, and statistically analyzed the results. I also planned the Western Blotting experiments designed to quantify pTau and total Tau levels in PS19 mouse brains. These experiments for pTau and total Tau were conducted in collaboration with Dr. Alex Stewart's laboratory.

Table of Contents

List of Abbreviations

2-AG: 2-arachidonoylglycerol
AD: Alzheimer's Disease
AEA: Anandamide
Akt (or PKB): Protein kinase B
APOE3: Apolipoprotein E3
APOE4: Apolipoprotein E4
APP: Amyloid precursor protein
Aβ: Amyloid- β
BLA: Basolateral amygdala
CeA: Central nucleus of the amygdala
DAGLα: Diacylglycerol lipase-α
ddH_2O: Double distilled water
EDTA: Ethylenediamine tetraacetic acid
EPM: Elevated Plus Maze
ER: Endoplasmic reticulum
GSK3β: Glycogen synthase kinase 3β
***i.p*:** Intraperitonial
IRS-1: Insulin receptor substrate 1
LMO4 KO: Lim domain only 4 knockout
LMO4: Lim domain only 4
LTP: Long-term potentiation
MAGL: Monoacylglycerol lipase
mGluR5: Metabotropic glutamate receptor 5
mPFC: Medial prefrontal cortex
NaCl: Sodium chloride
NaOH: Sodium hydroxide
NFT: Neurofibrillary tau tangle
NMDAR: N-methyl-D-aspartate receptor
nPKO: Neuronal PTP1B knockout
NSF: *N*-ethylmaleimide-sensitive factor
OF: Open Field
P13K: Phosphoinositide 3-kinase
PCR: Polymerase chain reaction
PDGFβ: Platelet-derived growth factor β-chain
PDK1: Pyruvate Dehydrogenase Kinase
PFC: Prefrontal cortex
p-GSK3β: Phospho-GSK3β
PHF: Paired helical filaments
PKCϵ : Protein kinase C epsilon type
PSEN1: Presenilin 1
PSEN2: Presenilin 2
pTau: Phospho-tau
PTP1B KO: PTP1B knockout
PTP1B: Protein tyrosine phosphatase 1B
SAP: Stretch-attend posture
STF: Short-term facilitation
Tris-HCl: Tris-hydrochloride
Veh. -treated: Vehicle-treated
WT: Wild-type

List of Figures

List of Tables

1. Introduction

1.1 Alzheimer's Disease

1.1.1 Overview

With over 40 million patients worldwide, Alzheimer's disease (AD) is the most common age-related neurodegenerative disorder amongst older adults[1–3]. AD is the most prevalent subset of both young onset (<65 years) and late onset (>65 years) dementia[2]. Clinically, the disease is defined as a progressive decline in cognitive and executive function which causes a disruption in daily life[3]. Impairments in specific cognitive domains, especially those related to memory, are a hallmark feature of AD[4]. Thereby, patients with AD display a loss of episodic memory and lose their ability to recall everyday events, which imposes devastating effects on the livelihoods of these patients [2]. Loss of memory is coupled with linguistic, visual, and executive problems, as well as a constellation of neuropsychiatric symptoms [3–5].

Both environmental and genetic risk factors have been identified in the future development of AD. Because AD develops over a long preclinical period of several decades, numerous lifestyle-related factors have been associated with disease prognosis, such as diabetes, obesity, physical and mental inactivity, depression, smoking, low educational attainment, diet and cardiovascular health status[6,7]. Only about 5% of AD cases are entirely caused by genetic and hereditary factors, rightly named familial AD[2]. Familial AD usually involves autosomal dominant mutations in APP (amyloid precursor protein), PSEN1 (Presenilin 1), or PSEN2 (Presenilin 2) genes[5]. These genes are involved in amyloid-β (Aβ) peptide metabolism, which is a key branch of AD pathology[5]. APOE4 (apolipoprotein E4) is another major genetic risk factor for AD, particularly sporadic AD, and is a gene involved in Aβ clearance in the brain, degeneration of blood vessels, leakage of the blood brain barrier, and neurodegeneration independent of Aβ[3]. Lifetime risk of AD is 50% higher for APOE4 homozygotes and 20-30% higher for APOE3 (apolipoprotein E3) and APOE4 heterozygotes[8]. Excluding these genes, more than 20 other genetic loci have been associated with increased AD risk in genome-wide association studies[9]. These novel genes are

key players in pathways implicated in the immune system, inflammatory responses, cholesterol and lipid metabolism and endosomal-vesicle recycling [9]. Although the large majority of AD cases are sporadic or non-hereditary, many of these genes may still influence sporadic AD onset[9].

More than these genetic and environmental predispositions, it is the pathophysiology of AD which is the greatest indicator of disease. Two hallmark biomarkers have repeatedly been implicated as pathognomonic of AD: Aβ plaques and neurofibrillary tau tangles (NFT), which can begin to form 2-3 decades prior to the onset of disease symptoms[1,5]. Other critical disease pathologies include neuroinflammation, neurodegeneration, synapse loss and vascular damage[10]. Studies have suggested that, of these pathologies, synapse loss and neurodegeneration most strongly correlates with dementia. This is because Aβ plaque accumulation does not correlate with cognitive impairments in patients, and tau tangles do correlate with cognitive decline and with neuron and synapse loss, but mutations in tau cause frontotemporal dementia, not AD[11–16].

1.1.2 Amyloid-beta Plaque Pathology and the hAPP-J20 Mouse Model

Amyloid-beta (Aβ) plaques are aggregates of Aβ peptides which deposit extracellularly between neurons and hinder neuronal function[17]. These neurotoxic peptides are produced from the defective endoproteolysis of the parental APP by groups of enzymes called α-, β-, and γ-secretases. In the amyloidogenic pathway, which leads to disease, APP is cleaved by β-secretease, resulting in the formation of sAPPβ and the 99-amino acid C-terminal fragment of APP called, C99[4]. C99, which is released intracellularly, is further cleaved by γ-secretase in complex with presenlin 1 and 2 proteins, releasing an intact Aβ peptide into the extracellular domain[4]. Among the Aβ peptide products, Aβ_{40} is the predominant hydrophilic form[18]. Aβ_{42}, Aβ_{43} and longer peptides are highly self-aggregating and are the main constituents of Aβ plaques[18]. Imbalance in the production and clearance of Aβ peptides may occur due to mutations in the APP, PSEN1, and PSEN2 genes, as many studies of familial AD have strongly suggested[1,4]. Cross-sectional studies of post-mortem human brain have shown that senile plaque deposition occurs early in the disease process and proceeds slowly in a top-down fashion, starting from

the neocortex and progressing through the allocortex, diencephalon, striatum, basal forebrain cholinergic nuclei, and finally into the brainstem and the cerebellum[19]. The neurites surrounding these dense plaques exhibit swollen, dystrophic morphologies and often contain aggregates of phospho-tau and other cellular components which may have deposited due to disrupted cellular transport[20,21]. Numerous studies have shown that plaques also disrupt the trajectories of nearby axons and dendrites, which may impede synaptic signal processing and transmission[22–24]. Severe gliosis and oxidative stress occurs around plaques, which participate in further impeding synapse structure and function[15,25,26]. More recently, soluble Aβ oligomers have been assigned as a major culprit behind the pathological cascade in AD, more so than Aβ plaques. These soluble Aβ species may arise in the form of dimers, trimers, dodecamers, and larger oligomers of Aβ peptides ranging from 90-650 kDa in molecular weight[27]. These oligomers have been linked to causing acute synaptotoxicity and inducing neurodegenerative processes[28–30]. One study by Shankar et al. showed that soluble Aβ_{42} oligomers that were isolated directly post-mortem from the cortex of AD patients dose-dependently decreased synaptic function and number, and impaired memory of learned behaviour in rats[31]. However, plaque cores isolated from the same AD brains and washed extensively *in vitro* did not impair long term potentiation in synapses[31]. Other studies have shown that injection of different soluble Aβ oligomeric species into rodent brains leads to reversible impairment of cognitive function and accumulation of biochemical damage within neurons, such as tau hyperphosphorylation[32–34].

In this project, hAPP-J20 transgenic mice will be used as a model Aβ pathology in AD. These transgenic mice overexpress human APP with two mutations (Swedish and Indiana) linked to familial AD. The transgene expression is driven by the platelet-derived growth factor β-chain (PDGFβ) promoter[35]. These mice show impairments in cognitive function, especially in spatial learning and memory, by 3-4 months of age in the radial arm and Morris water mazes[36,37]. As early as 1 month, Aβ puncta start to form in the hippocampus, one of the key brain regions involved in learning and memory[38]. By 8 months, widespread Aβ plaques develop[38]. Secondary phenotypes such as neuron/synapse loss,

gliosis, and impairments in synaptic transmission are also evident by this age[36,38,39]. These mice are invaluable models of AD in that they exclusively present with Aβ plaque formations without the presence of tau tangles and, thereby, are popularly used to model Aβ pathology.

1.1.2 Tau Pathology and the PS19 Mouse Model

The formation of neurofibrillary tangles of hyper-phosphorylated tau protein throughout various brain regions is another hallmark feature of AD pathogenesis. Tau is a microtubule-associated protein located mostly in the axons of neurons[40]. Under normal conditions, tau stabilizes microtubules and is involved in axonal growth and intracellular transport of motor proteins[41]. In tauopathies, including AD, tau becomes abnormally hyper-phosphorylated at multiple sites and becomes detached from microtubules to accumulate in the somatodendritic compartment in paired helical filaments (PHF) and straight filaments[42]. Tau is phosphorylated by several kinases, key among these is glycogen synthase kinase 3β (GSK3β), which is a constitutively active, proline-directed serine-threonine kinase[42,43]. In addition to tau phosphorylation, GSK3β is deeply involved in memory impairment, inflammatory responses, and increased production of Aβ[42]. Phospho-tau deposition begins in the entorhinal cortex and progresses through the hippocampus, association cortices, and primary sensory areas[44,45]. NFT deposition positively correlates with cognitive decline and neuronal loss in human AD brains. Since NFTs are intracellular components, it could be expected that they would have less impact on surrounding brain regions, however, significant gliosis has been observed in the vicinity of tangles that correlates with disease progression [13,14]. Hyper-phosphorylated tau tangles, in unison with Aβ plaques, disrupt neuronal function and plasticity and ultimately lead to cognitive impairment.

The P301S tau or PS19 mouse line used in this project has commonly served as an effective model of tauopathies. These mice express human tau protein, driven by the mouse prion protein (Prnp) promoter[46]. Widespread tangle-like inclusions in the neocortex, amygdala, hippocampus, brainstem and spinal cord first appear in these mice starting at around 6 months of age[47]. Accumulation of tau and associated neuronal loss is significantly apparent by 9-12 months[47]. Prominent hippocampal and

entorhinal atrophy also aggravates at this age[47]. Additional pathologies such as gliosis, synapse loss and changes in synaptic transmission, particularly in the hippocampus, have also been observed[47]. Behaviourally, these mice display selective deficits in spatial learning and memory, as demonstrated in the Morris water maze [48]. Additionally, motor deficits and a notable hunched-back posture has been reported in these mice around 7-10 months of age[48].

Although the hAPP-J20 and PS19 mouse models have been thoroughly purposed for the study of AD neuropathology and behavioural deficits related to cognitive impairment, the study of AD-related neuropsychiatric symptoms in these mice has received less research focus. Alzheimer's disease has been deemed one of the greatest health challenges of the 21st century[3], not only because of its complex neurobiological pathologies and cognitive implications, but also because of associated neuropsychiatric comorbidities. Despite long and expensive trials, no disease-modifying drug treatment for AD has yet been approved, and neuropsychiatric symptoms have largely been treated in disassociation from the disease[49,50]. This may be due to a lack in the understanding of underlying cellular mechanisms linking AD pathology with these neuropsychiatric comorbidities. Since these symptoms pose a significant burden on the livelihoods of AD patients, finding a molecular target for drug treatment which is common in both AD pathologies and associated neuropsychiatric symptomology is a critical goal towards effective AD treatment.

1.2. Anxiety and Alzheimer's Disease

1.2.1 Overview of Anxiety Behaviours in Alzheimer's Disease

Neuropsychological disturbances are being increasingly recognized as a common feature of AD. Sleep/appetite disturbances, apathy, delusional behavior, depression, agitation, irritability and anxiety all fall under the spectrum of AD-related neuropsychiatric symptoms[50–52]. These psychiatric impediments in AD are often concurrent with cognitive decline and exacerbate the adverse effects on the quality of life of AD patients and their caregivers[53]. These symptoms have also been shown to play a major role in the decision to seek institutionalization[53]. In a large cross-sectional study with data collected longitudinally

over 10 years from 3608 participants, Lyketsos et al. demonstrated that over 80% of dementia patients exhibited at least one neuropsychiatric symptom from the onset of cognitive decline and that there were no differences in prevalence of these symptoms between participants with Alzheimer's-type dementia and other dementias[54].

Of these symptoms, anxiety behaviour has been noted in 25-75% of AD cases early on in disease prognosis by a number of studies[55]. Anxiety is a feeling of nervousness, uneasiness or apprehension which may manifest in AD patients as increased irritability, agitation, or restlessness (i.e. wandering behavior)[56]. Teri et al. used a cohort of 523 community-dwelling AD patients and found that 70% suffered from comorbid anxiety symptoms, with 44% displaying anxious, fearful, or apprehensive behavior; 36% exhibiting irritability and aggression; 34% exhibiting agitation and restlessness; and 33% presenting with suspicion and paranoid behaviour[57]. Studies have also suggested that a history of significant anxiety appears in individuals who later develop AD and that anxiety symptoms positively correlate with AD severity[58,59]. Although this evidence suggests an association between AD and anxiety symptoms, it is not yet well understood what mechanisms underlie this association, which poses a challenge for effective treatment development.

1.2.2 Potential Etiology of Anxiety Behaviours in Alzheimer's

1.2.2.1 Psychological and Biological Factors

Although the underlying causes of anxiety in AD remain unclear, it has been agreed that these causes may be both psychological and biological. Patients with AD and other forms of dementia experience lowered ability to cope in daily life, often lose overview and control over life circumstances, and may experience fear of the future, which may all cumulatively contribute to increased anxiousness [60]. Additionally, anxiety in AD may be due to the stress of cognitive decline in vulnerable individuals who have inherent risk factors, such as a history of personal or familial psychiatric disorders[61]. Alternatively, direct pathological correlation between anxiety and AD is being recently established, with a study demonstrating that anxiety may be a risk associated with abnormal cerebrospinal fluid levels of $A\beta_{42}$ and

tau[62]. Altered glucose metabolism in various brain regions, as measured by PET has also been associated with neuropsychiatric symptoms in AD, including anxiety[63,64].

1.2.2.2 Brain Regions Implicated in Anxiety Behaviours and Alzheimer's

Researchers have identified several brain regions which are relevant in both anxiety-related behaviours and in AD. A neuroimaging study revealed decreased prefrontal cortex (PFC) gray matter in AD patients, especially in the inferior PFC[65]. In the medial prefrontal cortex (mPFC), which has been shown to be highly involved in the modulation of anxiety via reciprocal connections with the amygdala and other limbic structures[66], a tendency of volume loss and atrophy has been noted in AD patients following atrophy of other temporal and frontal regions[67]. However, subcortical regions, primarily limbic structures, are the major areas of focus when investigating affective disorders in AD.

Amongst subcortical regions, the amygdala is renowned in its roles in anxiety and fear conditioning and is also severely and consistently affected by AD pathology[68,69]. A study found that optogenetically stimulating the basolateral amygdala (BLA) terminals in the central nucleus of the amygdala (CeA) exerted an acute and reversible anxiolytic effect while optogenetic inhibition of these same projections increased anxiety-related behaviours, suggested that the BLA-CeA circuit is important in acute anxiety control in the mammalian brain[70]. In a study of 20 AD cases, the distribution of Thioflavin S-stained NFTs and neuritic plaques were prevalent in various nuclei that form the amygdala[71]. Large concentrations of NFTs and plaques were found in the accessory basal and cortical nuclei and the cortical transition area, while the mediobasal nucleus was relatively spared[69]. AD studies have also reported significant amygdalar atrophy, ranging from 26%-55%, which may in part contribute to the behavioural and cognitive decline in AD[71].

The hippocampus is another subcortical structure which is highly implicated in AD. Traditionally, the hippocampus is known to be heavily involved in cognition, specifically episodic memory and spatial learning[72]. However recent reports have linked the hippocampal formation to anxiety and mood behaviour[72]. The hippocampus achieves these dual functions via functional heterogeneity along its

dorsoventral axis, with the dorsal region contributing to cognitive functions while the ventral region contributes to emotional modulation[72]. Lesions to the ventral but not dorsal hippocampus have anxiolytic effects, with minimal effect on spatial learning[73]. The ventral CA1 region of the hippocampus is particularly relevant in anxiety because it integrates diverse cortical inputs from the entorhinal cortex to generate complex representations of the environment and aversive stimuli, and it makes dense projections to the amygdala[72]. Using freely moving calcium imaging and optogenetics, Jimenez et al. identified "anxiety cells" enriched within a population of ventral CA1 neurons projecting to the lateral hypothalamic area, and these cells are involved in representing anxiogenic environments and causally impact avoidance behaviour to rapidly control anxiety-like behaviours[72]. At early stages of AD, the CA1 hippocampal region is one of the most adversely affected areas. This region suffers high levels of AD-related neuronal loss and is also the site of initial NFT accumulation[74,75].

1.2.3 Assessing Anxiety Behaviours in Rodent Models of Alzheimer's

Two classical validated test paradigms used to assay anxiety-related behaviour in mice are the elevated plus maze (EPM) and open field (OF) tests. The EPM involves an elevated maze-like apparatus with four arms arranged in a plus formation, with two open arms and two enclosed arms. Unlike other assays which assess anxiety responses following exposure to noxious stimuli and produce conditioned anxiety responses, the EPM relies on a rodents' innate preference towards dark, enclosed spaces and an unconditioned fear of heights/open spaces[76]. Anxiogenic behaviour is characterized by increased duration or frequency of entries in the enclosed arms, while anti-anxiety behaviour is characterized by the opposite scenario[76]. As in the case of this project, the effects of drug treatment on anxiety behaviour can be easily studied using this paradigm[76]. In fact, the validity of the EPM is demonstrated by the fact that anxiogenic drugs reduce time spent in the open arms and anxiolytic drugs increasing the time spent in the open arms[77]. Additionally, other key indicator behaviours of anxiety in rodents, such as freezing and defecation, also occur more often in the open arms of the EPM compared to the closed arms, further validating the paradigm[77]. The OF paradigm is another assay for anxiety-related behaviour and

spontaneous locomotor activity in rodents[78]. This test involves a wall-enclosed box-like apparatus with an open ceiling into which the animal is placed. Similar to the EPM, this paradigm takes advantage of a rodent's natural aversion to large, brightly lit, open and unfamiliar environments[78]. Mice which frequent or remain in the dark corners of the field for extended periods of time or move close to the walls (i.e. thigmotaxis) are deemed to be exhibiting anxiogenic behaviour, whereas, the alternate scenario characterizes anti-anxiety behaviour[78]. Overall ambulatory behaviour in the OF may also be viewed as a form of affective behaviour[78].

Anxiety-related behaviour has been studied in several major mouse models of AD, including the hAPP-J20 and PS19 models. Several studies have noted that hAPP-J20 mice, ranging from 2-7 months of age, spend more time in the open arms of the EPM compared to WT littermates, suggesting abnormally lowered levels of anxiety or increased disinhibition[79,80]. These mice also display hyperactivity in the OF test[80]. Studies of anxiety-related behaviour in the PS19 tau mouse model have been relatively scarce. A recent study reported similar reduced anxious behaviour and hyperactivity in the PS19 tau mouse model[48]. Takeuchi et al. tested locomotion in 6-month-old mice in OF from 0-120 minutes and found increased total locomotive distance, increased stereotypic behaviour and increased time spent in the open relative to other regions of the OF arena[48]. However, they also noted motor deficits in older mice[48]. In the EPM, these mice displayed significantly reduced appropriate anxious behaviour, spending more time in the open arms of the maze compared to control non-transgenic mice[48]. Other studies, using different tauopathy mouse models, have reported similar observations[48,81].

The underlying neuropathology and cellular mechanisms directly linking AD and anxiety-related behaviours is largely unknown. Anxiety symptoms in AD are non-specific in humans and overlap with other psychiatric syndromes such as depression[57]. A better understanding of the full phenomenology of the anxiety construct in AD patients and its unique contribution to dementia-related behaviours, independent of other co-morbid psychiatric effects, is critical for the development of effective therapeutics[56].

1.3. A potential role of PTP1B in AD-associated anxiety behaviour

1.3.1 Overview of Protein Tyrosine Phosphatase 1B (PTP1B)

Protein tyrosine phosphatase 1B (PTP1B) may be proposed as a therapeutic molecular target for the amelioration of major AD pathology, cognitive decline and associated neuropsychiatric symptoms. PTP1B is a prototypical type 1 non-receptor tyrosine phosphatase that is attached to the cytoplasmic face of the endoplasmic reticulum (ER) membrane via a hydrophobic COOH-terminal anchoring sequence[82–84]. This protein plays a well-established role in limiting neuronal leptin and insulin signaling[85]. It is a highly validated therapeutic target for diabetes and obesity treatment[82]. However, it's implication in neurological disorders has been a comparatively novel concept.

The 50 kDa PTP1B enzyme is encoded by the *PTPN1* gene located to band 20q13 in the human genome[85,86]. The PTP1B enzyme harbors 10 conserved motifs, among which Motif 9, referred to as the PTP loop, is the catalytic domain[82]. The PTP loop contains a catalytic cysteine residue which executes nucleophilic attack of phospho-tyrosine residues on the substrate and becomes oxidized[82].

This phosphatase enzyme rose to prominence only recently over the past decade, as researchers discovered its pivotal role in leptin and insulin metabolism[82]. In insulin signaling, PTP1B inactivates the insulin receptor by dephosphorylation[87]. In PTP1B null mice, plasma insulin levels were significantly lower and glucose levels were slightly lower when compared with wild-type (WT) littermates[87]. PTP1B KO and heterozygous mice were also resistant to weight gain following a high-fat diet, whereas, WT littermates became insulin-resistant and rapidly gained weight[87].These findings established PTP1B as a key negative regulator of insulin signaling. In leptin metabolism, PTP1B attenuates leptin signaling by dephosphorylating the downstream effector Janus kinase 2[85]. Mice lacking leptin become morbidly obese, whereas mice with leptin and PTP1B ablation display reduced weight gain, lower amounts of adipose tissue and increased resting metabolic rates[88,89]. These studies demonstrate the PTP1B-mediated mechanism for the control of diet-induced obesity.

1.3.2 PTP1B Hyperactivity in Alzheimer's Disease

Increased PTP1B activity is associated with defective neuronal insulin and leptin signalling[89–91], pathways which are also impaired in AD [92,93]. Furthermore, PTP1B down-regulation restores hypothalamic insulin and leptin signalling[94,95]. Increasing evidence also suggests that insulin resistance is a risk factor associated with AD pathogenesis and may help explain why obesity is a prominent AD comorbidity[96,97]. Mice with ablated PTP1B in the hippocampus and cortex displayed improved performance in the Barnes maze, indicating that PTP1B is a negative regulator of spatial memory, which is compromised in AD[98].

In a novel study from our laboratory, Zhang et al. used hAPP-J20 mice to show that there are aberrations in cellular function that underlie cognitive behavioural impairments[99]. The study found that the presynaptic long-term potentiation (LTP) of CA3:CA1 synapses was severely hampered in hAPP-J20 mice, while paired-pulse ratio and short-term facilitation (STF) were abnormally increased[99]. The study further showed that these deficits were linked to reduced phosphorylation of the NMDAR GluN2B receptor and vesicle recycling protein, *N*-ethylmaleimide-sensitive factor (NSF)[99]. However, when PTP1B was blocked by a selective inhibitor drug, the synaptic and behavioural deficits were successfully rescued, indicating that active PTP1B impairs NMDAR-mediated plasticity required for spatial learning in the J20 mouse model[99]. Another recent report by Ricke et al. from our laboratory showed that drug-based inhibition of PTP1B prevents spatial memory deficits in hAPP-J20 mice of both sexes in the Morris water maze, while also preventing hippocampal neuron loss and neuroinflammation[100]. Most importantly, we found that neuronal ablation of PTP1B did not affect cerebral amyloid levels or Aβ plaque density in these mice, but significantly reduced plaque size[100]. Notably, however, neuron-targeted genetic ablation of PTP1B prevented hippocampal neuron loss and cognitive decline but did not reduce neuroinflammation, which suggests that PTP1B hastens neurodegeneration and cognitive decline in AD and the role of PTP1B in this process is segregated from neuroinflammation[100]. Together, these two publications show that impaired NMDAR-based synaptic plasticity via hyperactive PTP1B forms the

neuronal basis of cognitive impairment in the J20 mouse model, which can be reversed (along with pathological features) via PTP1B inhibition.

The role of PTP1B inhibition in amelioration of AD pathology in the PS19 tau mouse model has not been well studied. However, PTP1B activity prevents inhibition of GSK3β via its inhibition of the kinase Akt/PKB pathway and thereby may exacerbate tau pathology and other AD-associated effects[101]. Kanno et al. found that PKCϵ activated Akt and inactivated GSK3β via direct interaction with each protein, while PTP1B inhibition activated Akt and inactivated GSK3β via the IRS-1/P13K/PDK1/Akt signalling axis[102]. The combinatory effect of PKCϵ activation and PTP1B inhibition was greater on Akt activation and GSK3β inactivation, significantly suppressing tau phosphorylation and spatial learning and memory deficits in mice from the 5xFAD AD mouse model[102]. The effect of selective pharmacological and genetic inhibition PTP1B on tau hyper-phosphorylation in the PS19 model, particularly in brain regions implicated in anxiety-related behaviour, has not been studied.

1.3.3 PTP1B in Anxiety Behaviours in Rodents

In addition to its involvement in AD pathology, PTP1B hyperactivity has also been implicated in anxiety behaviour. Recently, Qin et. al. showed that PTP1B inhibition relieved anxiety symptoms in mice with ablation of the Lim domain only 4 (LMO4) protein[103]. LMO4 is an endogenous inhibitor of PTP1B, and its ablation results in PTP1B hyperactivity [90,91]. Qin et. al. demonstrated that elevated PTP1B activity in glutamatergic projection neurons in LMO4 KO mice increased de-phosphorylation/inactivation of the mGluR5 receptor, which negatively impacted the production of the endocannabinoid, 2-arachidonoylglycerol (2-AG), in the basolateral amygdala. This impaired eCB signalling led to the occurrence of an anxiogenic phenotype in LMO4 KO mice[103]. Pharmacological inhibition of PTP1B was able to rescue these behaviours[103]. Similarly, Mendes and colleagues found that knock-down of amygdalar PTP1B in diet-induced obese rats causes anxiolytic behaviour, while also improving insulin signalling and decreasing adiposity[104]. Whether and how anxiety behaviour is affected by pharmacological and genetic inhibition of PTP1B in the J20 and PS19 mouse models of AD is yet to be

elucidated. Since PTP1B activity has been commonly linked to AD and to anxiety-related behaviours, it may be implied that selective targeting of PTP1B may improve anxiety-related symptoms in the J20 and PS19 mouse models[99,100,103].

1.3.4 PTP1B as a Therapeutic Target

AD treatment is a complex challenge that is still far from being resolved. However, notable progress has been made in the development of therapeutics to target cognitive impairments and disease pathology in patients. As of 2016, two groups of approved treatments have been the standard of care to enhance cognitive function in AD patients: cholinesterase inhibitors and the NMDAR antagonist memantine[105]. Disease-modifying therapies have most commonly been directed at reducing Aβ burden, with many such programmes in phase 2 and phase 3 clinical trials[105]. Aducanumab, BAN2401, and gantenerumab all reduce Aβ plaques, while also reducing phospho-tau burden, neurogranin, and neurofilament light in the cerebrospinal fluid[106]. However, uncertainties in the clinical trials of these drugs have prevented them from obtaining approval for use on patients[105]. Therapies designed to modify tau pathology are also being developed. Monoclonal antibodies that sequester extracellular tau as it spreads from cell to cell are currently in trials[105]. Other small-molecule drugs which target tau aggregation and NFT formation are also being assessed. Still, these tau-targeted therapies come with numerous potential side effects[105]. Remedying other aspects of AD pathology, such as neuroinflammation, have also been a goal of current therapies. Oligomannate was a drug approved in China in 2019, after showing positive effect on cognitive function in Chinese phase 3 clinical trials[107]. The drug has been shown to reduce inflammation in AD through its effect on the gut microbiome[107]. It restores normal gut bacterial composition, reduces dysbiosis, and reduces peripheral inflammatory cell populations, which can contribute to central inflammation[107]. Global clinical testing for this drug to observe effects on diverse populations has been planned[105]. Aside from pharmacological treatments, experts are now stressing the importance of adopting holistic multi-modal preventative approaches to manage the risks of developing AD. The Finnish FINGER study promoted a combination of healthy balanced nutrition, regular physical

exercise, cognitive training and social activities, and vascular and metabolic risk management[108,109]. It was able to show a positive effect of these lifestyle-based interventions in reducing the risk of cognitive impairment in patients at risk[108]. Future studies are considering the combination of these lifestyle-based preventative approaches with pharmacological interventions which target biomarkers[105].

The treatment of neuropsychiatric symptoms of AD has largely occurred in segregation to disease-modifying treatment. Benzodiazepines have been widely used in the past for the treatment of anxiety and insomnia[110]. However, studies have shown that these drugs may negatively impact cognitive function in long term[111–113]. Often, physicians prescribe antidepressants (e.g. cholinesterase inhibitors) for their anxiolytic properties[55]. Donepezil is one such antidepressant which has been reported to decrease anxiety in patients with moderate to severe AD [114]. Another class of drug which is frequently used to ameliorate anxiety behaviours in AD are antipsychotics, such as Olanzapine. A study showed that AD patients receiving olanzapine treatment experienced significantly less anxiety compared to the placebo group[115]. Nevertheless, treatments which target AD pathology while concurrently relieving associated neuropsychiatric symptoms in patients are yet to be established.

As shown by the studies of Ricke et. al and Qin et. al, PTP1B may be a common therapeutic target for anxiety behaviours and AD pathology, as its blockade has shown beneficial effects in rodent models. Trodusquemine (a.k.a MSI-1436), used in the studies by Ricke et. al., Qin et. al., and Zhang et al., is a popular non-competitive and reversible PTP1B inhibitor[100,103,116,117]. It is a natural aminosterol derived from a spermine metabolite of cholesterol from dogfish shark liver[118,119]. This drug can be administered peripherally, is blood brain barrier-permeable, and has a half-life of more than 1 week *in vivo*[116,119,120]. From the studies of Ricke et al. and Qin et al., trodusquemine has shown some promise in targeting both AD pathology and anxiety behaviours in separate mouse models[100,103]. It must also be noted that this drug does not damage cerebral integrity or cognitive performance in WT mice[103]. Whereas, past treatments for anxiety, such as benzodiazepines, have had negative implications on cognition in AD and dementia patients[111,113]. Trodusquemine has also been shown to promote leptin and insulin signalling and

has already undergone clinical trials for safety in obesity treatment in humans[116,120–122]. Thereby, trodusquemine can be easily repurposed for use in AD and, perhaps, AD-associated anxiety-related behaviour. Another PTP1B selective inhibitor drug which was used in this study is ENT-03 (a.k.a Hu1436), which is similar to Trodusquemine. ENT-03 is an aminosterol derived from a bile acid conjugated to spermine extracted from the brain and liver tissue of neonatal mice (https://enterininc.com/lead-programs/). This drug represents the mammalian equivalent of trodusquemine and may be better metabolized in humans than its dog fish-derived counterpart (https://enterininc.com/lead-programs/).

Therapeutically targeting PTP1B may be an effective method to not only slow the progression of AD pathology and cognitive impairment, but also normalize associated anxiety symptoms. However, the role of PTP1B in anxiety-related symptoms of AD has not been thoroughly investigated in the hAPP-J20 AB and PS19 tau AD mouse models and thereby will comprise the subject of this study.

2. Objectives and Hypothesis

Although affective disorders, particularly anxiety symptoms, are prevalent comorbidities of AD, their underlying mechanisms have not been well studied. These neuropsychiatric symptoms reinforce the burdensome experience of AD patients and their caregivers, and contribute to the deterioration of livelihood in affected individuals. *In this project, the major objective was to compare anxiety-related behaviours between the hAPP-J20 and PS19 mouse models of AD and determine whether PTP1B is involved in these behaviours. Additionally, the effect of PTP1B inhibition/ablation on tau pathology in the PS19 mouse model was also examined, as this was not previously established. As PTP1B has been implicated in both AD pathology and anxiety behaviour, it was hypothesized that PTP1B activity may increase abnormal anxiety-related symptoms of the J20 and PS19 AD mouse models. It was also hypothesized that PTP1B blockade will have a therapeutic effect on AD pathology in the PS19 mouse model.*

The specific aims for this project were as follows:

1) Compare anxiety-related behaviours in the hAPP-J20 and PS19 AD mouse models and assess the effects of pharmacological inhibition and genetic ablation of PTP1B, and whether this can reduce anxiety-related behavioural abnormalities in AD.
2) Observe tau pathology, neuron loss, and neuroinflammation in the PS19 mouse line and investigate the effects of PTP1B inhibition on tau levels in brain regions associated with anxiety in this mouse model, which has not been previously examined.

3. Methods

3.1 Animals and Treatment

The transgenic mice used in the experiments of this project belong to the hAPP-J20 mouse line, on a C57BL/6 background, and the PS19 mouse line, on a (C57BL/6 x C3H) F1 mixed background, acquired from Jackson Laboratories. For each group, age-matched wild type littermates were also used for testing. A cohort of 6-month-old mice and another cohort of 8-month-old mice were assessed for age-based differences in anxiety-related behaviour. Both male and female mice were used in each cohort, with approximately equal numbers of both sexes. Male and female mice were housed separately, in groups of 3-4 mice per cage, with mouse chow and water available ad libitum.

Animals were genotyped via PCR using genomic DNA extracted from ear biopsy samples. Biopsy samples (approximately 0.2 cm) were lysed in Alkaline Lysis Reagent (25 mM NaOH, 0.2 mM EDTA, in ddH_2O) at 95°C for 45 minutes in a PCR machine. Samples were cooled to 4°C. Neutralization Reagent (40 mM Tris-HCl) was added to sample tubes to stop the lysis reaction. 2 uL of these DNA samples were used as template for PCR reactions. PCR reactions were conducted using GoTaq Green All-in-One Master Mix (Cat. #: PR-M7123, Thermo Fisher Scientific), which only required the addition of appropriate primers and nuclease-free water. Details of the primers used to detect PTP1B flx genes, PS19 transgene, APP transgene, and CamK-Cre mutant gene are listed in **Table 1**. PCR products were separated by size on 1.5% agarose gel containing 0.05% ethidium bromide for visualization. Gels were visualized under an ultraviolet light illuminator.

In each age cohort, a group of J20 and PS19 mice were either treated with saline or drug. Trodusquemine for injection was dissolved in ddH_2O at a concentration of 0.25 mg/ml. Trodusquemine-treated J20 and PS19 mice in each age group were subjected to 6 intraperitoneal (*i.p*) injections every 5 days over the span of 1 month, with a dosage of 2.5mg/kg of clinical grade drug (provided by Enterin Inc.). Due to a limitation in the provided drug resource at the time, we were unable to treat wild type mice

with trodusquemine, to generate a WT-trodusquemine treated control group. In a previously established cohort of 8-month-old J20 and PS19 mice, we also tested a dosage of 5.0 mg/kg trodusquemine. The last injection of the drug was administered 2 weeks prior to behavioural experiments. Vehicle (Veh.)-treated control mice were treated using the same administration protocol with sterile saline (0.9% NaCl in water). A new cohort of WT, J20, and PS19 mice, aged 6 months, were treated with either ENT-03 drug or saline using the same dosage and protocol as with trodusquemine administration. Only vehicle-treated WT, J20, and PS19 mice were used to compare anxiety-related behaviours between J20 and PS19 cohorts. The drug-treated groups were used later to analyze the effect of PTP1B on these behaviours.

Mouse lines with genetic ablation of PTP1B in projection neurons were bred into the hAPP-J20 and PS19 mouse models. hAPP-J20 mice were bred with PTP1Bflx/flx and Camk2α-Cre mice on a C57BL/6 background to generate hAPP-J20 mice with ablation of PTP1B in Camk2α-Cre -positive neurons (hAPP-J20 nPKO mice)[100]. The same breeding strategy was used to generate PS19 nPKO mice. It must be noted that this breeding strategy was not designed to yield global knockout of PTP1B, since Camk2α-Cre is primarily expressed in the hippocampus, cortex, and amygdala[123]. Thus, neuronal PTP1B ablation was mainly restricted to these brain regions.

3.2 Behavioural Experiments

3.2.1 Elevated Plus Maze (EPM)

The first anxiety assay that mice were subjected to was the EPM paradigm. The EPM is a plus-shaped maze, elevated 75 cm from the ground, with two open arms (6 cm x 35cm) and two wall-enclosed arms (6cm x 35 cm x 20 cm). Prior to testing, mice were habituated in the experiment room for 45-60 minutes **(Supplementary Figure 1A)**. Room lighting was set to 100 Lux. Experiments were performed between 9:00 a.m. and 6:00 p.m. EST. Each mouse was placed individually in the center zone of the maze diagonally such that the animal's nose was at the intersection between the open and closed arms. Mice were allowed to explore the maze for 10 minutes and their behaviour was monitored using the Ethovision

8 automated video tracking system (Noldus IT, The Netherlands). Parameters measured include: distance moved, duration/ frequency of entries to open arms, duration/ frequency of entries to enclosed arms, and duration/frequency of entries to the central zone. Using the frequency of entries measurements, the %Relative Entries to Open Arms was calculated using the following formula:

$$\%Rel.ent.Opn.Arms = \left(\frac{Frequency\ of\ entries\ to\ Opn.Arms}{Total\ Frequency\ of\ entries\ to\ Opn.Arms + Clsd.Arms + Cntr.\ zone}\right) \times 100\%$$

3.2.2 Open Field (OF)

On the day following EPM testing, mice were subjected to the OF test, which was used to assay motoric activity and anxiety-related behaviour. For the open field experiments, mice were first habituated in the experimentation room for 45-60 minutes prior to testing. Room lighting was set to 300 Lux. Experiments were performed between 9:00 a.m. and 6:00 p.m. EST. Each mouse was then placed in a box-like arena without a roof, with dimensions of 50 cm (length) x 50 cm (width) x 38 cm (height), and observed in the arena for 10 minutes **(Supplementary Figure 1B)**. The arenas were cleaned with 70% ethanol between each new trial. Mice were monitored using Ethovision 8 automated video tracking software (Noldus IT, The Netherlands). For each subject mouse, the parameters that were analyzed include: total distance moved (cm), duration/frequency of entries in the large center of the arena (i.e. open, well-lit center), duration/frequency of entries in the small center of the arena (i.e. the central-most region, which could further distinguish the degree of anti-anxiety behaviour), duration/frequency of entries in the four corners of the arena. Using the frequency parameters, two additional factors were calculated: %Relative entries to large center and %Relative entries to small center. These two parameters were calculated using the following formulas:

$$\%Rel.ent.Sml.Cntr. = \left(\frac{Frequency\ of\ entries\ to\ Sml.Cntr.}{Total\ Frequency\ of\ entries\ to\ Lrg.\ Cntr. + Sml.Cntr. + 4\ corners}\right) \times 100\%$$

$$\%Rel.ent.Lrg.Cntr. = \left(\frac{Frequency\ of\ entries\ to\ Lrg.Cntr.}{Total\ Frequency\ of\ entries\ to\ Lrg.\ Cntr. + Sml.Cntr. + 4\ corners}\right) \times 100\%$$

3.3 Biochemical Techniques to Observe Tau Pathology in PS19 Model

3.3.1 Tissue Collection for Histology and Western Blotting

Following behavioural experiments, PS19 mice were anesthetized by *i.p* injection of ketamine (65 mg/kg), xylazine (13 mg/kg), and acepromazine (2 mg/kg), and decapitated[100].

For immunohistochemistry, the brain hemispheres were fixed overnight in 4% paraformaldehyde in PBS (137 mM NaCl, 2.7 mM KCl, 10.1 mM Na_2HPO_4 dibasic anhydrous, and 1.8 mM KH_2PO_4 in double distilled H_2O, pH 7.4). Fixed tissue was then cryoprotected with increasing concentrations of sucrose (10% and 20%) over 5 days at 4°C in 0.1 M phosphate buffer (0.038 M NaH_2PO_4 monobasic and 0.162 M Na_2HPO_4 dibasic, pH 7.4). The cryoprotected tissue was then flash frozen on dry ice and stored at -80°C. Brain tissue was sliced coronally into sections of 20 μm thickness using a microtome[100].

For immunoblotting, the remaining hemisphere from each mouse was flash frozen on dry ice and stored at -80°C for subsequent protein extraction.

3.3.2 Immunohistochemistry

Cryostat sections from each treatment group of mice (n = 3 mice/group) were washed in 1X PBS (3 x 3 min). The sections were then subjected to heat-induced antigen retrieval in Citrate buffer (0.1 M, pH 6.0) at 95°C for 20 min. Sections were then cooled on ice and blocked with Mouse on Mouse (M.O.M) IgG Blocking Reagent (Vector laboratories, Burlingame, CA, USA, cat. #: BMK-2202) and 10% sheep serum for 1 h at room temperature. Sections were then washed again in 1X PBS (3 x 3min) and incubated in primary antibodies for AT8 (phospho-tau Ser202/Thr205, 1:500, mouse, cat. #: MN1020, Thermo Fischer), NeuN (1:500, mouse, cat. #: MAB377, Sigma-Aldrich), GFAP (1:500, chicken, cat. #: AB5541, Sigma-Aldrich), Iba1 (1:1000, rabbit, cat. #: 019-19741, WAKO) in M.O.M diluent (Vector laboratories) overnight at 4°C. Co-staining combinations were NeuN, GFAP, Iba1 or AT8 alone. Following primary antibody incubation, sections were treated with M.O.M Biotinylated Anti-Mouse IgG reagent (Vector laboratories) for 10 min. at room temperature. Sections were then washed in

1X PBS (3 x 3 min) and incubated with species-appropriate secondary antibody (1:500) for 1h at room temperature. Sections were then washed in 1X PBS (3 x 3min), counter-stained with Dapi (1:5000) for 15 minutes at room temperature. Slides were washed in 1X PBS for a final three cycles before being mounted in Permount. Fluorescence microscopy images of the hippocampus (CA1) and basolateral amygdala were obtained using an inverted epifluorescence microscope (Axio Observer. ZI, Zeiss).

3.3.3 Western Blotting

Protein levels of PTP1B, p-GSK3β (Ser. 9), and GSK3β were quantified using Western blotting. To extract these proteins, brain hemispheres from each experimental group of mice were collected and homogenized via ultrasonification in RIPA buffer (150mM NaCl, 10mM Tris, pH7.2, 0.1% SDS, 1% Triton X-100, 1% sodium deoxycholate, and 5 mM EDTA in ddH_2O), with protease inhibitors (0.5 μg/ml leupeptin, 2 μg/ml aprotinin, 0.368 mg/ml sodium orthovanadate, and 1.74mg/ml phenylmethylsulfonyl fluoride), frozen on dry ice and stored at -80°C. Total protein concentration in each sample was quantified using the bicinchoninic acid assay Pierce BCA Protein Assay Kit (Thermo Fisher).

Western blotting experiments were performed according to protocols outlined by Ricke et al[100]. 3 mice were used per experimental group, and each sample had one identical technical replicate. 50 ug of each protein sample was loaded onto 10% SDS-polyacrylamide gels and run at 110 V for 1.5 hours in Tris-Glycine Running buffer (25 mM Tris base, 190 mM glycine, 0.1% SDS in ddH_2O at pH 8.3) until proteins were separated by size. Proteins were transferred from gels to PVDF membranes at 110V for 2.5 hours in Transfer buffer (25 mM Tris base, 190 mM glycine, 20% methanol in ddH_2O at pH 8.3). Membranes were blocked with 5% bovine serum albumin or 5% non-fat milk in TBST at room temperature. Each set of blots were separately stained for PTP1B (50 kDa, rabbit, 1:1000, Abcam, cat. #: ab245984), p-GSK3β (Ser. 9) (48 kDa, rabbit, 1:1000, Cell Signalling, cat. #: 5558), and GSK3β (48 kDa, rabbit, 1:1000, Cell Signalling, cat. #: 5558). After staining with one of these antibodies, blots were stripped with Stripping buffer (0.2 M glycine, 3.5 mM SDS, and 1% Tween 20 in ddH2O at pH 2.2) for 20 minutes at room temperature. Then, they were stained with β-Actin primary antibody (42 kDa, mouse,

1:1000, Sigma-Aldrich, cat. #: A5441). Following primary antibody incubation, blots were incubated in species-appropriate horseradish peroxidase (HRP)-conjugated secondary antibodies (1:10 000). Prior to imaging, each blot was incubated in 1 ml ECL Western Blotting HRP Substrate (Thermo Fisher, cat. #: 32109) for 1 minute prior to imaging using the Chemi Doc MP Imaging System (Bio Rad, Gel Doc XR+). Protein levels were quantified using ImageJ software.

Immunoblotting experiments were also performed to observe protein levels of phospho-tau and total non-phosphorylated tau in hemisphere tissue samples from 8-month-old PS19 mice. Proteins were extracted by homogenizing brain tissue in RIPA buffer (50 mM Tris, 150 mM NaCl, 0.1% SDS, 0.5% sodium deoxycholate, 1% NP40, 5 mM EDTA, and protease inhibitors), using 1 ml/g. Samples were then centrifuged at 40 000 g for 40 min at 4°C. Western blot experiments were carried out as outlined above and blots were probed using the AT8 antibody (phospho-tau Ser204/Thr205 60 kDa, mouse, 1:1000, cat. #: MN1020, Thermo Fisher) and total Tau (50 kDa, mouse, 1:1000, cat #: 835203, Biolegend Inc.). Following a stripping cycle, blots were stained with GAPDH primary antibody (37 kDa, mouse, 1:1000, cat. #: sc-59540, Santa Cruz Biotechnology). Following primary antibody incubation, blots were incubated in species-appropriate horseradish peroxidase (HRP)-conjugated secondary antibodies (1:10 000). Again, each blot was incubated in 1 ml ECL Western Blotting HRP Substrate (Thermo Fisher, cat. #: 32109) for 1 minute prior to imaging using the Chemi Doc MP Imaging System (Bio Rad, Gel Doc XR+). Protein levels were quantified using ImageJ software.

3.4 Statistical Analyses

All statistical analyses for behavioural and biochemical experiments are summarized in **Table 2** and **Table 3**.

4. Results

4.1 Age-Based Dimorphism in Onset of Anti-Anxiety Phenotype in J20 and PS19 Mouse Models

To test whether there are differences in anxiety-related behaviours between the hAPP-J20 and PS19 AD mouse models, EPM and OF behavioural experiments were conducted on vehicle-treated mice from each mouse model and their respective age-matched WT littermates at two independent cohorts aged 6 months and 8 months. In the 6-month age group, no significant difference was detected in the total distance moved within the EPM between the four groups **(Figure 1A$_1$)**. Compared to WT littermates, 6-month-old vehicle-treated J20 mice exhibited a significantly increased cumulative duration in both of the open arms of the maze **(Figure 1A$_2$)** and an increased frequency of entries into these open arms relative to total entries **(Figure 1A$_3$)**, displaying an anti-anxiety baseline phenotype. These differences were not found in the 6-month PS19 mouse line as compared to their respective WT littermates, neither was there any difference between vehicle-treated J20 and PS19 mice.

Interestingly, in the 8-month cohort, it was exclusively the PS19 mice which displayed an anti-anxiety behavioural profile in the EPM. As compared to both J20 vehicle-treated mice and WT littermates, vehicle-treated PS19 mice showed significant hyperactivity, with increased total distance moved within the maze **(Figure 1B$_1$)**. Additionally, PS19 vehicle-treated mice expended more time in the open arms of the maze compared to WT littermates and J20 counterparts **(Figure 1B$_2$)**. Compared to WT littermates, PS19 mice also entered the open arms at a significantly higher frequency relative to total entries **(Figure 1B$_3$)**.

These findings from the EPM experiments show a clear age-dependent dimorphism in the onset of abnormal anti-anxiety behaviour in the J20 and PS19 mouse models, with J20 mice displaying early-onset behavioural abnormalities while PS19 mice exhibit later-onset behavioural abnormalities.

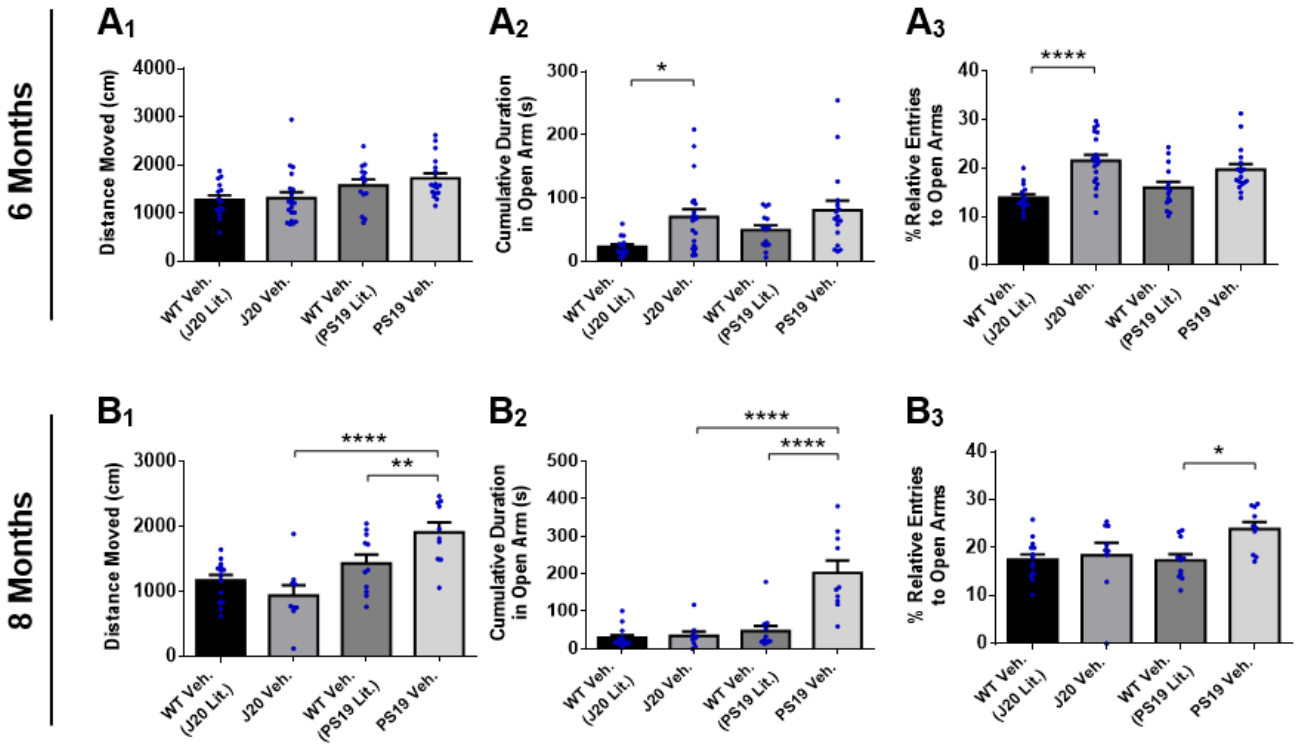

Figure 1. Age-based anxiety-related phenotypic differences in EPM parameters between hAPP-J20 and PS19 mice. No difference was detected in overall distance moved in the maze between all groups at 6 months of age (A1). 6-month-old J20 mice expended more cumulative time in the open arms of the maze and entered the open arms at a greater relative frequency than WT littermates (A2-A3). No effect was observed in PS19 mice at this age. In the 8-month age cohort, PS19 mice displayed increased total distance moved in the maze compared to WT littermates and J20 counterparts (B1). These mice also spent more time in the open arms of the EPM compared to WT and J20 mice (B2). Additionally, PS19 mice also frequented the open arms of the maze more that WT mice (B3). For A1-A3, n= 15, 20, 14, 17, respectively. For B1-B3, n= 14, 9, 11, 10, respectively. Data depicts mean ± SEM. For each analysis, one-way ANOVA was followed by Bonferroni's post-hoc pairwise comparisons. *p-value ≤ 0.05; **p-value ≤ 0.01; ***p-value ≤ 0.001; ****p-value ≤ 0.0001.

These first EPM tests were followed by a set of OF tests using 6-month-old J20, PS19, and WT littermate mice. There was no difference between groups in the total distance moved in the arena over the 10-minute testing period, no difference in the duration spent in the large and small centers of the arena, and no difference in the frequency of entries into the large and small centers relative to total frequency of entries **(Figure 2A_1-2A_5)**.

However, in the 8-month cohort of mice, distinct behavioural abnormalities were detected. Although, no statistically significant difference in motoric activity was found **(Figure 2B_1)**, 8-month-old

vehicle-treated PS19 mice spent more time in the large center of the open field arena compared to WT mice **(Figure 2B$_2$)**. There was trend towards PS19 mice spending more time in the small center of the arena as well, although this was not statistically significant **(Figure 2B$_3$)**. These mice also had a higher frequency of entries into the large and small centers relative to the total number of entries compared to WT littermates **(Figure 2B$_4$-2B$_5$, respectively)**. No such differences were found between vehicle-treated J20 mice and their littermate WT counterparts or between vehicle-treated J20 and PS19 mice in any of the OF test parameters in this age cohort.

Overall, **Figure 2** compliments the findings depicted in **Figure 1**, which illustrates an age-based dimorphism in the onset of an abnormal anti-anxiety baseline phenotype between J20 and PS19 mice. 6-month-old J20 mice, however, do not exhibit this behavioural phenotype in the OF test as they do in the EPM test in **Figure 1**. The anti-anxiety behaviour in PS19 mice at 8 months of age is apparent in both paradigms.

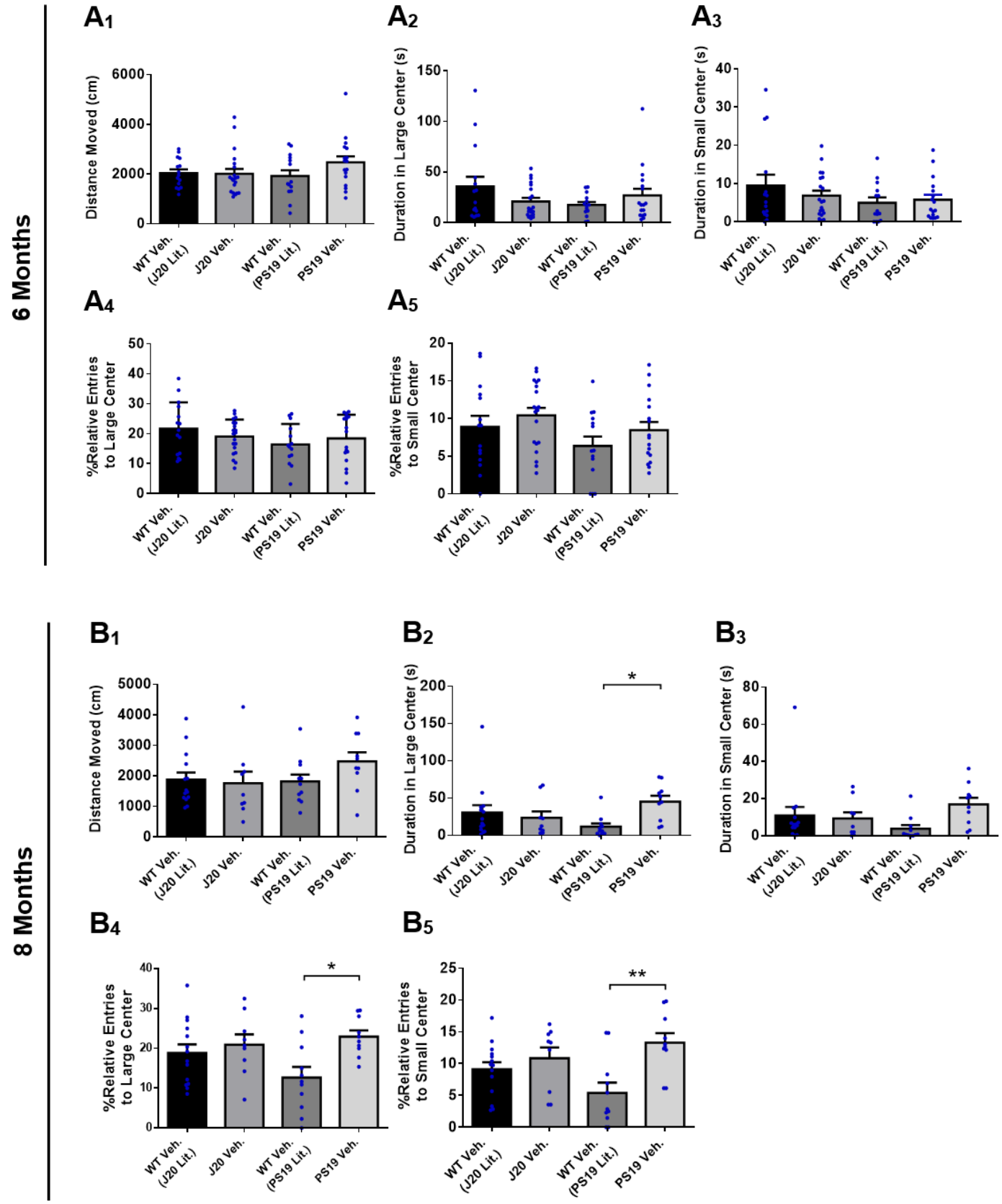
6 Months
A1
Distance Moved (cm)
6000
4000
2000
0
A2
Duration in Large Center (s)
150
100
50
0
A3
Duration in Small Center (s)
40
30
20
10
0
A4
%Relative Entries to Large Center
50
40
30
20
10
0
A5
%Relative Entries to Small Center
20
15
10
5
0
WT Veh. (J20 Lit.)
J20 Veh.
WT Veh. (PS19 Lit.)
PS19 Veh.
8 Months
B1
Distance Moved (cm)
5000
4000
3000
2000
1000
0
B2
Duration in Large Center (s)
200
150
100
50
0
*
B3
Duration in Small Center (s)
80
60
40
20
0
B4
%Relative Entries to Large Center
40
30
20
10
0
*
B5
%Relative Entries to Small Center
25
20
15
10
5
0
**

Figure 2. Age-based anxiety-related phenotypic differences in OF test parameters between hAPP-J20 and PS19 mice. No difference was detected in overall distance moved or anxiety-related behaviour in the OF test between J20 and PS19 mice or between these mice and their respective WT littermates at age 6 months (A1-A5). At 8 months of age, no statistically significant difference in motoric activity was detected between groups (B1). PS19 mice, but not J20 mice, expended more time in the large center of the OF arena compared to WT mice (B2). There was a tendency of this in the small center, although this was not statistically significant (B3). PS19 mice also entered the large and small centers of the arena at a greater relative frequency than WT littermates (B4-B5). For Figure A1-A5, n= 15, 20, 14, 17, respectively. For B1-B5, n= 14, 9, 11, 10, respectively. Data depicts mean ± SEM. For each analysis, one-way ANOVA was followed by Bonferroni's post-hoc pairwise comparisons. *p-value ≤ 0.05; **p-value ≤ 0.01; ***p-value ≤ 0.001; ****p-value ≤ 0.0001.

4.2 Selective Pharmacological Inhibition of PTP1B Normalizes Anti-Anxiety Behavioural Phenotype

Since PTP1B has been implicated in both AD and in anxiety behaviours, it was assessed whether PTP1B has a role in the behavioural abnormalities observed in J20 and PS19 mice. The same two anxiety-testing paradigms were used as in previous experiments, but with an added group of drug-treated transgenic mice. The effect of trodusquemine on behaviour was tested at two different dosages, 2.5 mg/kg and 5.0 mg/kg, using the same treatment protocol. Although both age groups for the 2.5 mg/kg dosage, only 8-month-old J20 and PS19 cohorts for the 5.0 mg/kg dosage. Upon consultation with my supervisor, it was decided that repeating the trodusquemine experiments at the 5.0 mg/kg dosage for 6-month-old mice was not needed.

First, it was examined whether selective inhibition of PTP1B by trodusquemine treatment could rescue the abnormally reduced levels of anxious behaviour observed in both J20 and PS19 mouse models using the EPM test. In reciprocation of previous results depicted in **Figure 1**, 6-month-old J20 vehicle-treated mice spent a greater cumulative duration in the open arms of the EPM, which was rescued in the J20 trodusquemine-treated group at a 2.5mg/kg dosage (**Figure 3A$_2$)**. These mice also entered the open arms of the maze at a greater relative frequency than WT counterparts, although this was not significantly ameliorated with trodusquemine treatment (**Figure 3A$_3$)**. There was no difference in distance moved in

the maze and trodusquemine treatment had no effect **(Figure 3A$_1$)**. No phenotype or rescue was observed in the 8-month-old J20 cohort of WT, J20 vehicle-treated, and J20 trodusquemine-treated mice **(Figure 3B$_1$-3B$_3$)**.

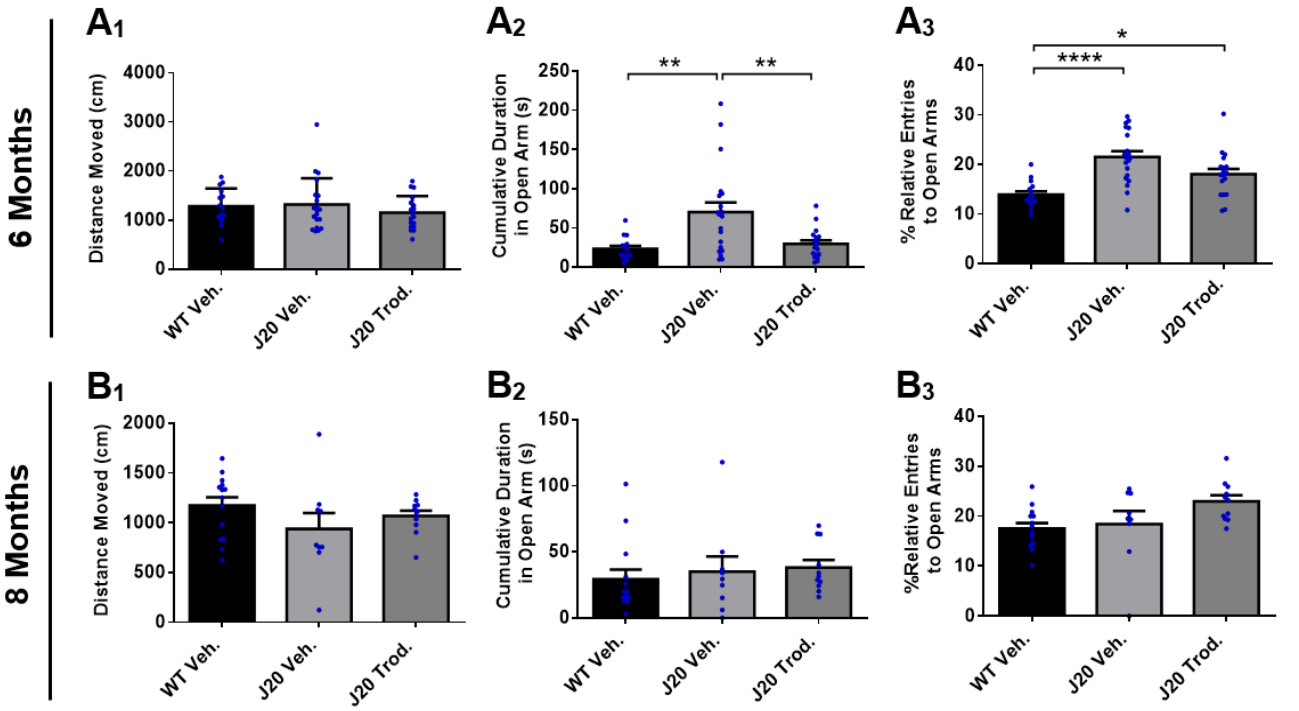

Figure 3. Selective inhibition of PTP1B via 2.5 mg/kg dosage of trodusquemine ameliorated inappropriately lowered anxious response in J20 mice aged 6 months in EPM. No difference was detected in overall distance moved in the maze between any of the treatment groups in both age cohorts (A1, B1). 6-month-old J20 mice expended more time in the open arms of the EPM and this was normalized by trodusquemine treatment (A2). J20 mice also entered the open arms of the maze more than WT littermates. Although there was a reduction of entries to the open arms in the trod. -treated group, this was not statistically significant (A3). In the 8-month cohort, no phenotype was detected and trodusquemine treatment did not affect behaviour. For A1-A3, n= 15, 20, 18, respectively. For B1-B3, n= 14, 9, 11, respectively. Data depicts mean ± SEM. For each analysis, one-way ANOVA was followed by Bonferroni's post-hoc pairwise comparisons. *p-value ≤ 0.05; **p-value ≤ 0.01; ***p-value ≤ 0.001; ****p-value ≤ 0.0001.

In the younger age group of PS19 mice, no behavioural phenotype or rescue was observed when comparing WT, PS19 vehicle-treated, and PS19 2.5 mg/kg trodusquemine-treated mice **(Figure 4A$_1$-4A$_3$)**. However, in the 8-month PS19 cohort, PS19 vehicle-treated mice expended more time in the open arms of the maze versus WT controls, and this effect was rescued in the PS19 trodusquemine-treated group **(Figure 4B$_2$)**. A similar phenotype was observed in the measure of %Relative entries to open arms of the maze (**Figure 4B$_3$)**, however this was not rescued by trodusquemine treatment. No difference was observed in the distance moved by these mice in the EPM **(Figure 4B$_1$).**

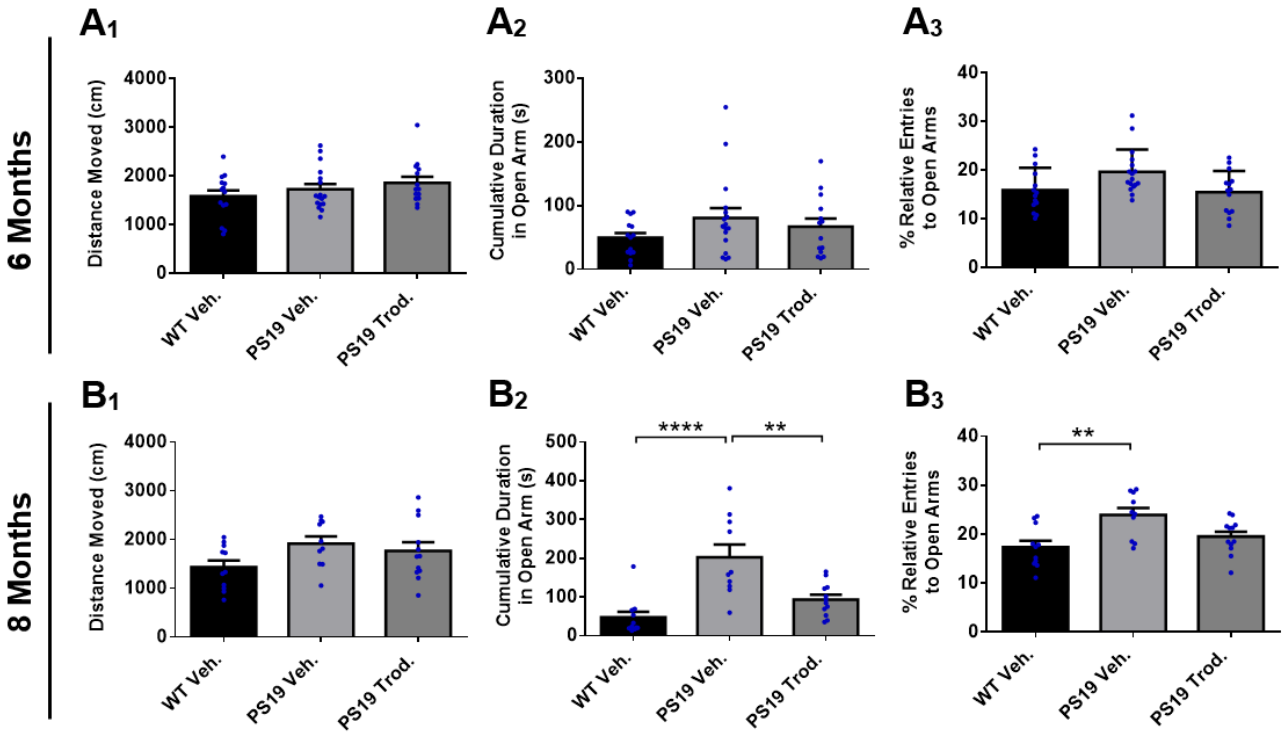

Figure 4. Selective inhibition of PTP1B via 2.5 mg/kg dosage of trodusquemine ameliorated inappropriately lowered anxious response in PS19 mice aged 8 months in EPM. No difference was detected in overall distance moved in the maze between any of the treatment groups in both age cohorts (A1, B1). In the 6-month cohort, no phenotype was detected and trodusquemine treatment did not affect behaviour (A2, A3). 8-month-old PS19 mice expended more time in the open arms of the EPM compared to WT mice, and this was rescued by trodusquemine treatment (B2). PS19 mice also entered the open arms of the EPM more frequently than WT mice, but this parameter was not sufficiently normalized by trodusquemine treatment (B3). For A1-A3, n= 14, 17, 14, respectively. For B1-B3, n=11, 10, 12, respectively. Data depicts mean ± SEM. For each analysis, one-way ANOVA was followed by Bonferroni's post-hoc pairwise comparisons. *p-value ≤ 0.05; **p-value ≤ 0.01; ***p-value ≤ 0.001; ****p-value ≤ 0.0001.

EPM experiments were repeated for 8-month-old J20 and PS19 cohorts treated with 5.0 mg/kg dosage of trodusquemine. As shown in **Supplementary Figure 2**, no difference in the total distance moved in the maze or in the anxiety-related behavioural parameters was detected between WT vehicle-treated, WT Trod. -treated, J20 vehicle-treated and J20 Trod. -treated mice at 8 months of age **(Supplementary Figure 2A-C)**. By contrast, in the 8-month PS19 cohort, PS19 Veh. mice moved a greater total distance within the EPM as compared to WT Veh. mice and this was normalized in the group of PS19 mice treated with 5.0 mg/kg trodusquemine **(Supplementary Figure 3A)**. PS19 Veh. mice spent significantly more time in the open arms of the maze versus WT controls, and this was rescued by trodusquemine treatment **(Supplementary Figure 3B)**. PS19 Veh. mice also frequented the open arms more than WT counterparts relative to other areas of the maze **(Supplementary Figure 3C)**. However, this was not rescued by trodusquemine treatment **(Supplementary Figure 3C)**.

In the OF test using WT vehicle-treated, J20 vehicle-treated, and J20 2.5 mg/kg trodusquemine-treated mice, no difference was found between groups in both the 6-month and 8-month age groups in any of the tested OF parameters **(Figure 5)**.

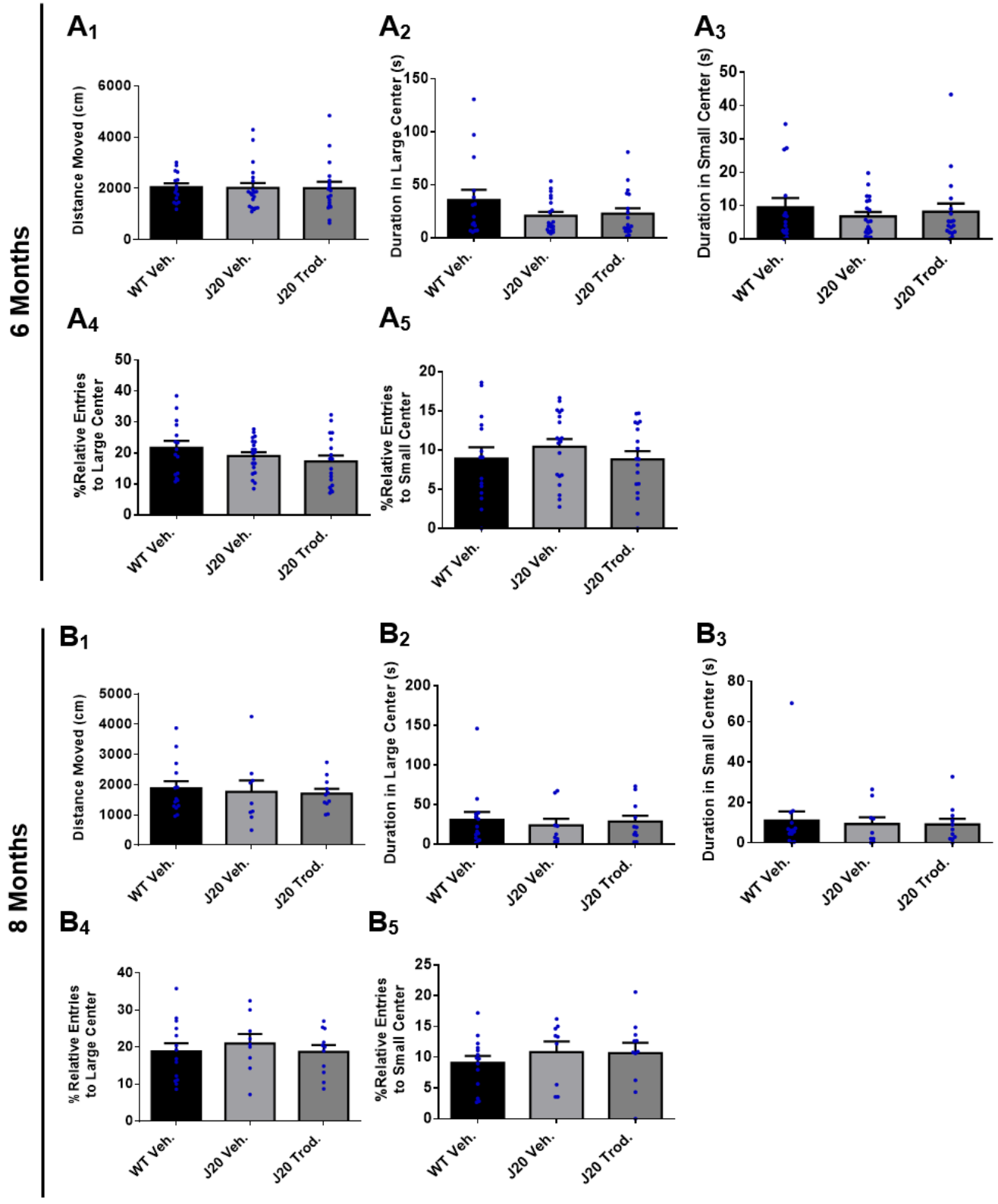
6 Months
A1
Distance Moved (cm)
6000
4000
2000
0
WT Veh.
J20 Veh.
J20 Trod.
A2
Duration in Large Center (s)
150
100
50
0
WT Veh.
J20 Veh.
J20 Trod.
A3
Duration in Small Center (s)
50
40
30
20
10
0
WT Veh.
J20 Veh.
J20 Trod.
A4
%Relative Entries to Large Center
50
40
30
20
10
0
WT Veh.
J20 Veh.
J20 Trod.
A5
%Relative Entries to Small Center
20
15
10
5
0
WT Veh.
J20 Veh.
J20 Trod.
8 Months
B1
Distance Moved (cm)
5000
4000
3000
2000
1000
0
WT Veh.
J20 Veh.
J20 Trod.
B2
Duration in Large Center (s)
200
150
100
50
0
WT Veh.
J20 Veh.
J20 Trod.
B3
Duration in Small Center (s)
80
60
40
20
0
WT Veh.
J20 Veh.
J20 Trod.
B4
% Relative Entries to Large Center
40
30
20
10
0
WT Veh.
J20 Veh.
J20 Trod.
B5
%Relative Entries to Small Center
25
20
15
10
5
0
WT Veh.
J20 Veh.
J20 Trod.

Figure 5. No anxiety-related behavioural abnormalities of J20 mice in both age groups in OF test, selective inhibition of PTP1B by 2.5 mg/kg dosage of trodusquemine had no effect. In both age groups, no difference in the total distance moved (A1, B1) or anxiety-related parameters was detected (A2-A5, B2-B5). For A1-A5, n= 15, 20, 18, respectively. For B1-B5, n= 14, 9, 11, respectively. Data depicts mean ± SEM. For each analysis, one-way ANOVA was followed by Bonferroni's post-hoc pairwise comparisons. *p-value ≤ 0.05; **p-value ≤ 0.01; ***p-value ≤ 0.001; ****p-value ≤ 0.0001.

Similarly, no difference in OF parameters was found at 6 months in the PS19 cohort between WT vehicle-treated, PS19 vehicle-treated, and PS19 2.5 mg/kg trodusquemine-treated groups **(Figure $6A_1$-$6A_5$).** In PS19 mice aged 8 months, no difference was detected between groups in the total distance travelled in the OF arena **(Figure $6B_1$).** Compared to WT littermates, PS19 mice expended more time in the large center, which was normalized by trodusquemine treatment **(Figure $6B_2$)**. These mice also expended more time in the small center of the arena, although this effect was not sufficiently rescued by drug treatment **(Figure $6B_3$)**. PS19 mice also entered the large and small centers at a greater frequency than other areas of the maze compared to WT counterparts **(Figure $6B_4 – 6B_5$)**. Although the increased relative entries to the large center of the arena was not rescued by trodusquemine treatment, the increased relative entries to the small center was **(Figure $6B_4 – 6B_5$)**. No phenotype in motoric activity was detected in these mice and there was no effect of trodusquemine treatment **(Figure $6B_1$)**.

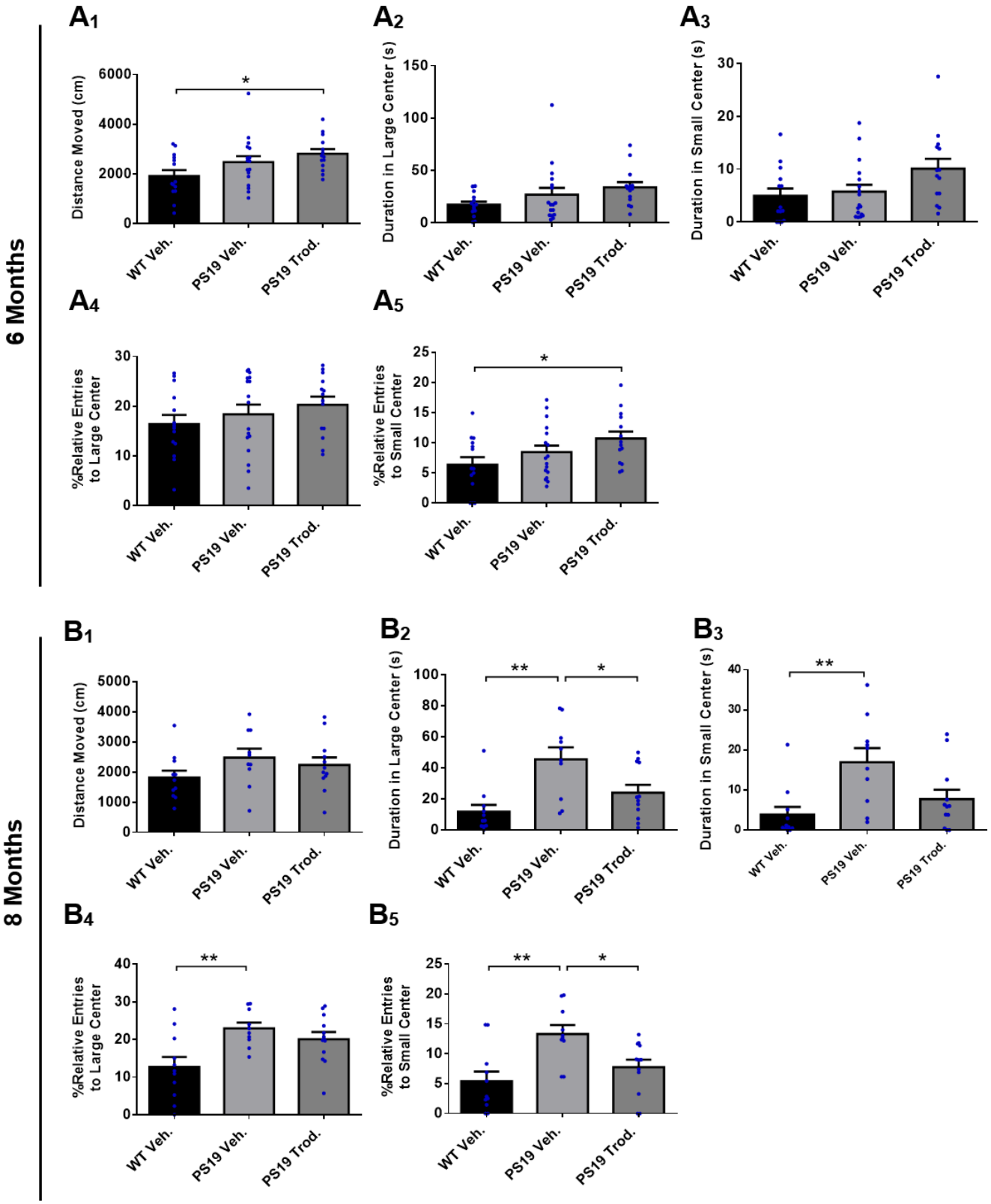
6 Months
A1
Distance Moved (cm)
6000
4000
2000
0
*
WT Veh.
PS19 Veh.
PS19 Trod.
A2
Duration in Large Center (s)
150
100
50
0
A3
Duration in Small Center (s)
30
20
10
0
A4
%Relative Entries to Large Center
30
20
10
0
A5
%Relative Entries to Small Center
25
20
15
10
5
0
*
8 Months
B1
Distance Moved (cm)
5000
4000
3000
2000
1000
0
B2
Duration in Large Center (s)
100
80
60
40
20
0
**
*
B3
Duration in Small Center (s)
40
30
20
10
0
**
B4
%Relative Entries to Large Center
40
30
20
10
0
**
B5
%Relative Entries to Small Center
25
20
15
10
5
0
**
*

Figure 6. Selective inhibition of PTP1B via 2.5 mg/kg dosage of trodusquemine ameliorated inappropriately lowered anxious response in PS19 mice at 8 months of age in OF test. No phenotype in distance moved (A1) or anxiety-related behaviour in the arena was detected in the 6-month cohort (A2-A5), and trodusquemine treatment did not affect behaviour in the majority of OF parameters. PS19 mice aged 8 months did not show any motoric phenotype (B1). However, these mice expended more time in the large and small center of the arena (B2-B3). The abnormally high amount of time in the large, but not small, center of the arena was rescued by trodusquemine treatment (B2-B3). PS19 mice also entered the large and small centers of the arena more than WT littermates (B4-B5). The high frequency of entries to the small center was rescued by trodusquemine treatment (B5). For A1-A5, n= 14, 17, 14, respectively. For B1-B5, n= 11, 10, 12, respectively. For each analysis, one-way ANOVA was followed by Bonferroni's post-hoc pairwise comparisons. *p-value ≤ 0.05; **p-value ≤ 0.01; ***p-value ≤ 0.001; ****p-value ≤ 0.0001.

When the OF test was repeated for J20 mice aged 8 months treated with 5.0 mg/kg dosage of trodusquemine, no anxiety-related phenotype was detected between WT vehicle-treated and J20 vehicle-treated groups, and 5.0 mg/kg trodusquemine treatment in the J20-trod. group did not show any effect on behaviour **(Supplementary Figure 4B-4E)**. However, a difference between the WT-Veh. and WT trod. -treated groups was noted, with the WT-trod. group exhibiting a lower total distance moved in the arena **(Supplementary Figure 4A),** less time spent in the large center **(Supplementary Figure 4B)**, and fewer relative entries to the large center **(Supplementary Figure 4D)**. This could possibly suggest that such a high dosage of the drug was inducing the mice to be slightly lethargic. An 8-month-old cohort of PS19 mice were also subjected to trodusquemine treatment at a dosage of 5.0 mg/kg. The anti-anxiety behavioural phenotype in PS19 vehicle-treated mice was again observed, which was normalized by 5.0 mg/kg trodusquemine treatment **(Supplementary Figure 5B-5E)**. It was also noted that WT trod. -treated mice moved a lower total distance in the arena compared to WT Veh. -treated mice **(Supplementary Figure 5A)**.

Next, these same behavioural experiments were repeated with new cohorts of J20 and PS19 mice at 6 months of age to test the efficacy of another drug, ENT-03 (a.k.a Hu1436), in normalizing AD-associated anxiety-related behaviours at a dosage of 2.5 mg/kg. Like trodusquemine, ENT-03 is also a selective PTP1B inhibitor (https://enterininc.com/lead-programs/). Again, EPM experiments were conducted on a cohort of WT, WT ENT 03-treated, J20 Veh. -treated and J20 ENT 03-treated mice aged

6 months. In the J20 mouse line at 6 months, a reduction of appropriate anxiousness was detected yet again when compared with WT control mice. J20 vehicle-treated mice spent more time in the open arms, which was rescued by ENT-03 treatment **(Supplementary Figure 6B)**. J20 Veh. -treated mice also exhibited a higher relative frequency of entries to the open arms of the maze versus WT controls **(Supplementary Figure 6C)**. However, this effect was not rescued by ENT-03 treatment. In the PS19 cohort at 6 months, no anxiety-related phenotype was detected in the EPM test, and ENT-03 treatment showed no effect **(Supplementary Figure 7B-7C).** In either of the two mouse lines, no differences in the distance moved within the EPM was detected **(Supplementary Figure 6A, 7A)**.

In the OF test, no significant differences were found amongst the four treatment groups of the J20 cohort at 6 months of age in any of the OF parameters measured, and ENT-03 treatment did not have any effect **(Supplementary Figure 8)**. Similar findings were noted for the PS19 cohort at this age **(Supplementary Figure 9)**.

Together, these data show that both trodusquemine and ENT-03 at a dosage of 2.5 mg/kg are sufficient to rescue the impairment of appropriate anxious behaviour in both the J20 and PS19 mouse models at the respective ages at which these behavioural deficits occur. Administration of trodusquemine at a higher dosage of 5.0 mg/kg also had a similar therapeutic effect on PS19 mice at 8 months of age but had no effect on J20 mice since they do not display behavioural deficits at this age.

4.3 Genetic Neuronal Ablation of PTP1B Normalizes Anti-Anxiety Behavioural Phenotype

Next, the same behavioural experiments were repeated using triple transgenic mice in the J20 and PS19 background with CamK2α-Cre-mediated genetic neuronal PTP1B ablation to observe whether neuronal PTP1B specifically is involved in the behavioural abnormalities observed previously.

First, triple transgenic mice in the J20 background were tested in the EPM at 6 months of age. There were no differences in the distance travelled in the maze between any of the groups in this J20 mouse cohort **(Figure 7A).** However, 6-month-old J20 mice exhibited their characteristic anti-anxiety phenotype, spending increased time in the open arms of the EPM compared to WT littermates and the nPKO control group **(Figure 7B)**. In the J20 nPKO group, the time spent in the open arms was lowered significantly to a level similar to WT littermates **(Figure 7B)**. J20 mice also entered the open arms of the maze more frequently than WT and nPKO mice **(Figure 7C)**. However, this parameter was not rescued in the J20 nPKO group **(Figure 7C)**.

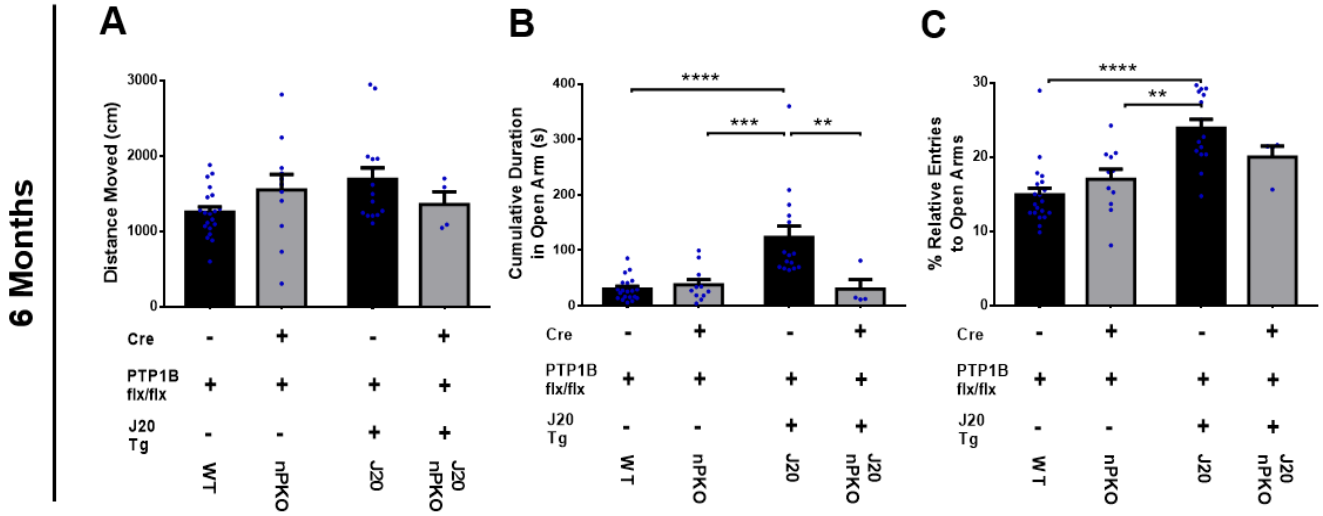

Figure 7. Genetic neuronal ablation of PTP1B (J20 nPKO) ameliorated inappropriately lowered anxious response of J20 mice at 6 months in EPM. There was no difference in distance moved in the EPM between groups (A). J20 mice expended more cumulative time in the open arms of the maze compared to WT and PKO control mice, and this was normalized in J20 nPKO group (B). The phenotype was also apparent in terms of relative entries to the open arms, although this was not sufficiently rescued by PTP1B ablation (C). For A-C, n= 20, 11, 15, 4, respectively. For each analysis, one-way ANOVA was followed by Bonferroni's post-hoc pairwise comparisons. *p-value ≤ 0.05; **p-value ≤ 0.01; ***p-value ≤ 0.001; ****p-value ≤ 0.0001.

Similarly, PS19 mice at 8 months of age also displayed an anti-anxiety profile in the EPM, consistent with previous experiments. These mice moved a greater distance throughout the maze than did WT mice and this phenotype was rescued in the PS19 nPKO group mice **(Figure 8A).** Compared to WT littermates and nPKO control mice, PS19 mice also spent more time in the open arms of the maze and entered the open arms at a greater frequency **(Figure 8B-8C)**. Both parameters were normalized in the PS19 nPKO group **(Figure 8B-8C).**

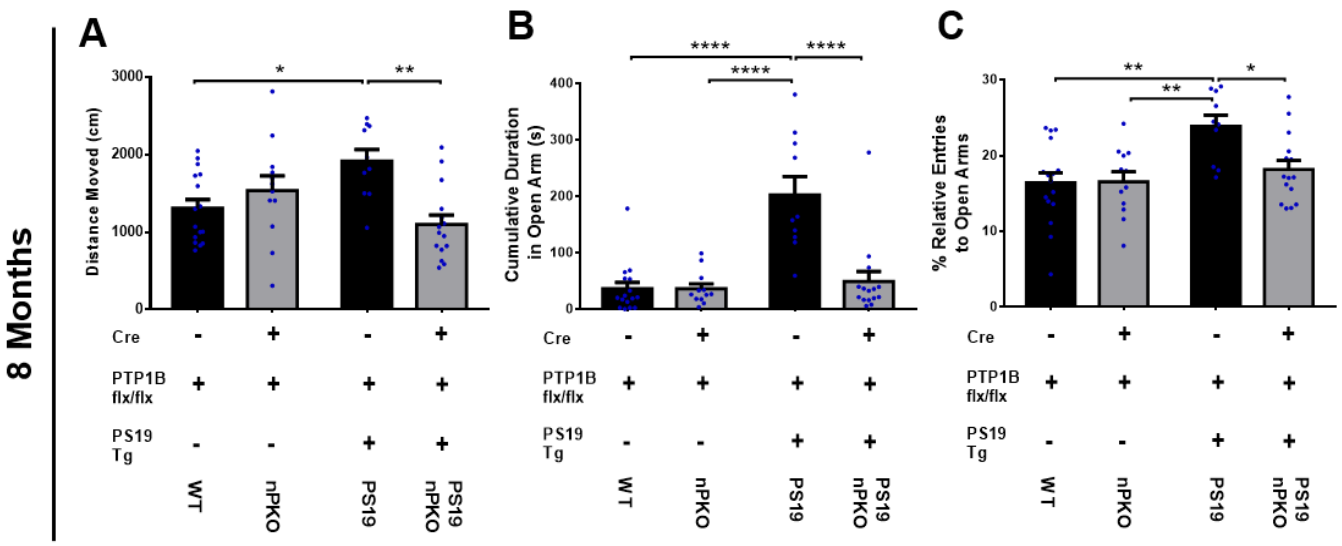

Figure 8. Genetic neuronal ablation of PTP1B (PS19 nPKO) ameliorated inappropriately lowered anxious response in PS19 mice at 8 months in EPM. PS19 mice moved an increased distance in the EPM compared to WT mice, which was normalized with neuronal PTP1B ablation in the PS19 nPKO group (A). PS19 mice also spent more time in and frequented the open arms of the maze more than WT mice (B, C). This was normalized with neuronal PTP1B ablation in the PS19 nPKO group (B, C). For A-C, n= 16, 12, 10, 15, respectively. For each analysis, one-way ANOVA was followed by Bonferroni's post-hoc pairwise comparisons. *p-value ≤ 0.05; **p-value ≤ 0.01; ***p-value ≤ 0.001; ****p-value ≤ 0.0001.

Next, it was examined whether similar anxiety-related behaviours can be observed in the OF test using these mice. At 6 months of age, J20 mice did not display any behavioural phenotype in this paradigm, consistent with previous OF experiments. The distance moved in the maze by J20 mice was not significantly different from WT littermates and the ablation of neuronal PTP1B in the J20 PTP1B KO group did not have any effect (**Figure 9A)**. Similarly, there was also no significant difference between WT and J20 mice in the duration in or relative entries to the center of the OF arena, and PTP1B knockout had no effect on these parameters (**Figure 9B-9E)**.

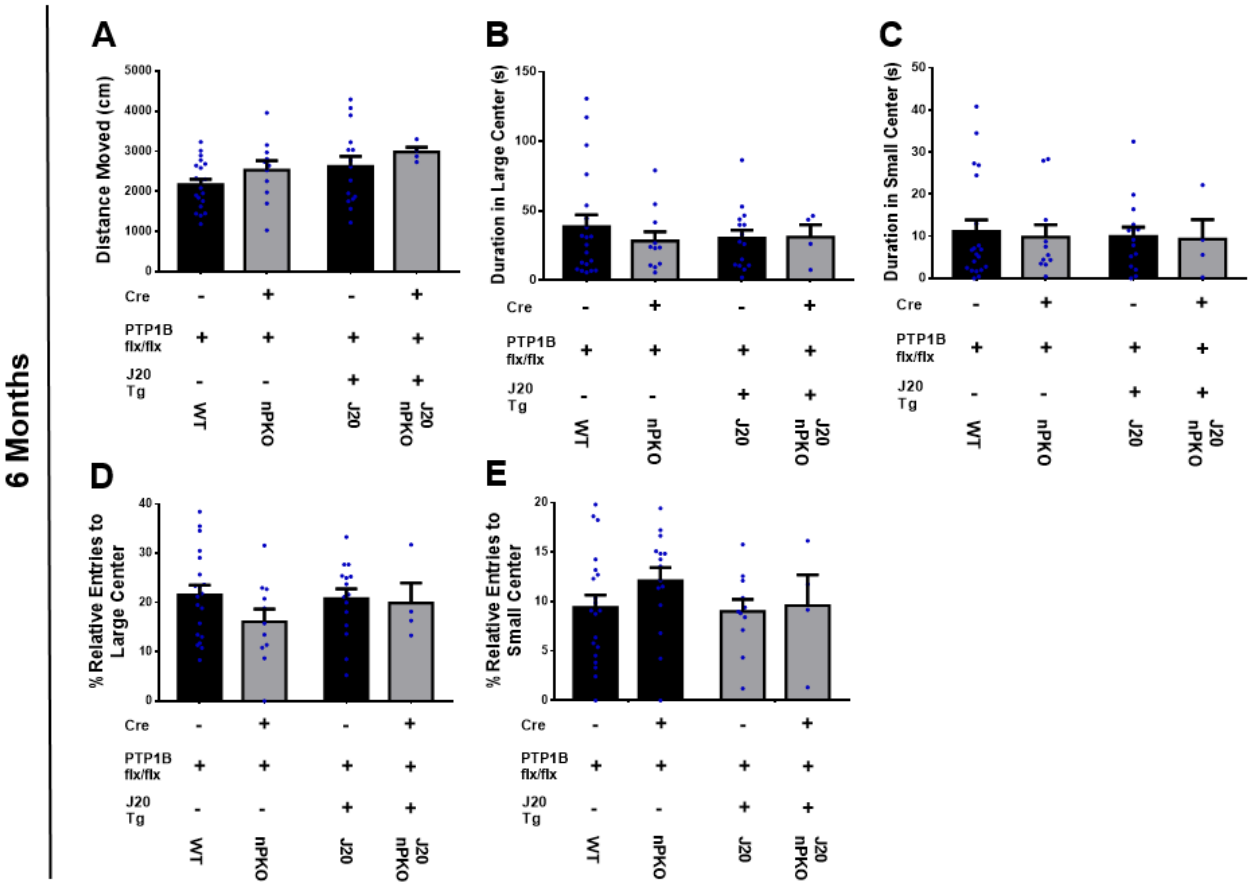

Figure 9. No anxiety-related phenotype detected in J20 mice in OF test; genetic neuronal ablation of PTP1B (J20 nPKO) had no effect. J20 PTP1B KO mice were tested at age 6 months. Each mouse was individually tested for 10 minutes. No phenotype was detected in distance moved (A). No phenotype was detected in anxiety-related parameters and neuronal PTP1B ablation did not have any effect (B-E). For A-E, n= 20, 11, 15, 4, respectively. For each analysis, one-way ANOVA was followed by Bonferroni's post-hoc pairwise comparisons. *p-value ≤ 0.05; **p-value ≤ 0.01; ***p-value ≤ 0.001; ****p-value ≤ 0.0001.

However, in the PS19 cohort at 8 months of age, a clear disinhibited behavioural phenotype was evident in the OF test. PS19 mice spent an increased duration of time in the large and small centers of the OF arena compared to WT littermates **(Figure 10B, 10C)**. PS19 mice also entered the small center of the arena more frequently than WT mice (**Figure 10E)**, although this was not noted for the large center of the arena (**Figure 10D)**. This behaviour was rescued in the PS19 nPKO group, which exhibited normalized duration in the large and small centers of the arena **(Figure 10B, 10C)** and normalized frequency of entries into the small center (**Figure 10E)**.

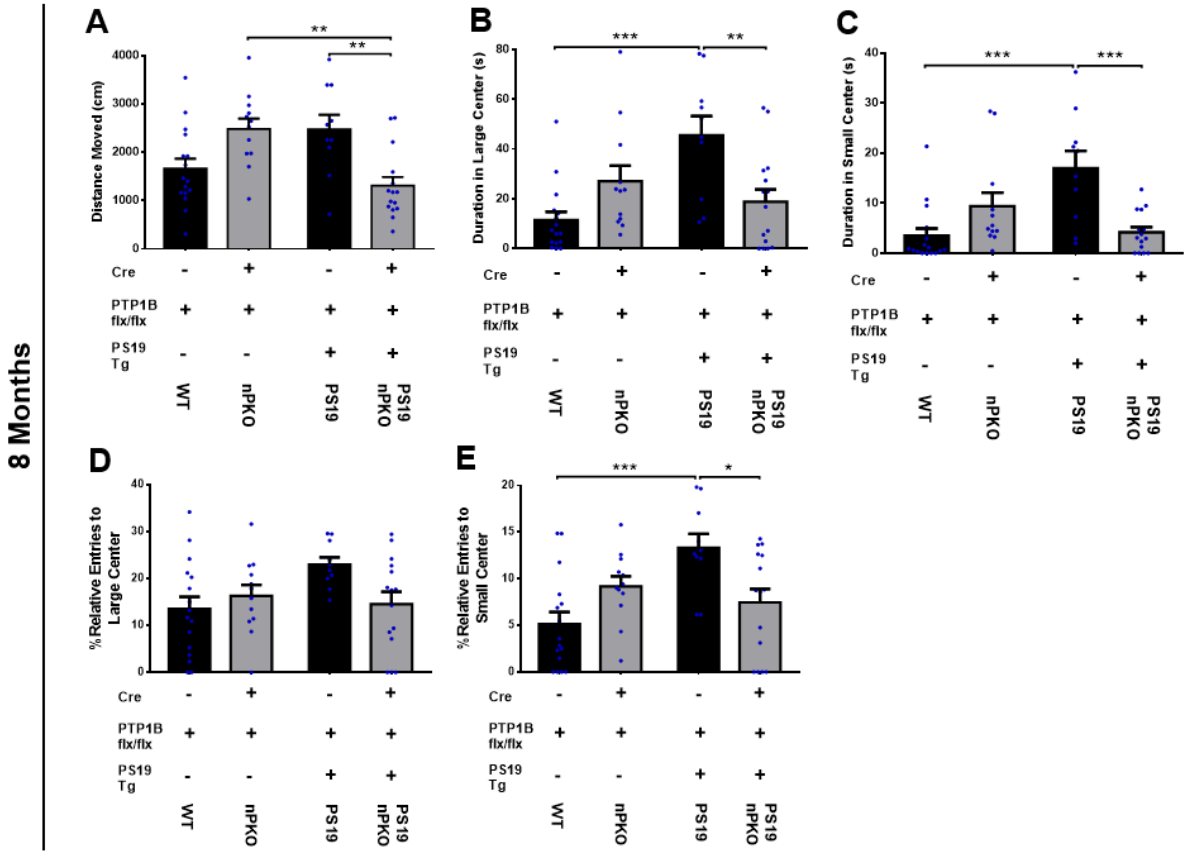

Figure 10. Genetic neuronal ablation of PTP1B (PS19 nPKO) ameliorated inappropriately lowered anxious response in PS19 mice at 8 months in OF test. No phenotype was detected in distance moved (A). PS19 mice spent more time in the large and small centers of the arena compared to WT littermates, and this was rescued by neuronal ablation of PTP1B in the PS19 nPKO group (B, C). No phenotype was detected in entries to the large center, but PS19 mice entered the small center more frequently than WT mice, which was normalized by PTP1B ablation (D, E). For A-E, n= 16, 12, 10, 15, respectively. For each analysis, one-way ANOVA was followed by Bonferroni's post-hoc pairwise comparisons. *p-value ≤ 0.05; **p-value ≤ 0.01; ***p-value ≤ 0.001; ****p-value ≤ 0.0001.

4.4 Therapeutic Effect of PTP1B Blockade on Tau Pathology in the PS19 Mouse Model

4.4.1 Immunohistochemistry

For Aim #2, IHC staining was used to observe AT8 phospho-Tau (pTau) deposition in the hippocampal CA1 region and basolateral amygdala (BLA) of PS19 mouse brains at 6 and 8 months of age and additionally observed the effect of selective PTP1B inhibition by trodusquemine (2.5 mg/kg). AT8 is a PHF-tau-specific monoclonal antibody which is popularly used to detected abnormally phosphorylated tau[124]. The antibody has binding epitopes at phospho-S202/phospho-T205[124]. Neuroinflammation, detected via GFAP and Iba1inflammatory marker immunofluorescence, were also studied in these areas. Finally, neuron loss was examined via immunofluorescence of the mature neuronal marker NeuN, with co-staining of Dapi to visualize cell nuclei.

In **Figure 11**, p-Tau immunofluorescence revealed p-Tau aggregation in the hippocampal CA1 region in PS19 mice at 6 and 8 months of age compared to WT littermates that do not express the human tau transgene. The aggregates appear to become more defined and numerous in the older cohort compared to 6-month-old counterparts. In both age groups, trodusquemine treatment reduced pTau levels.

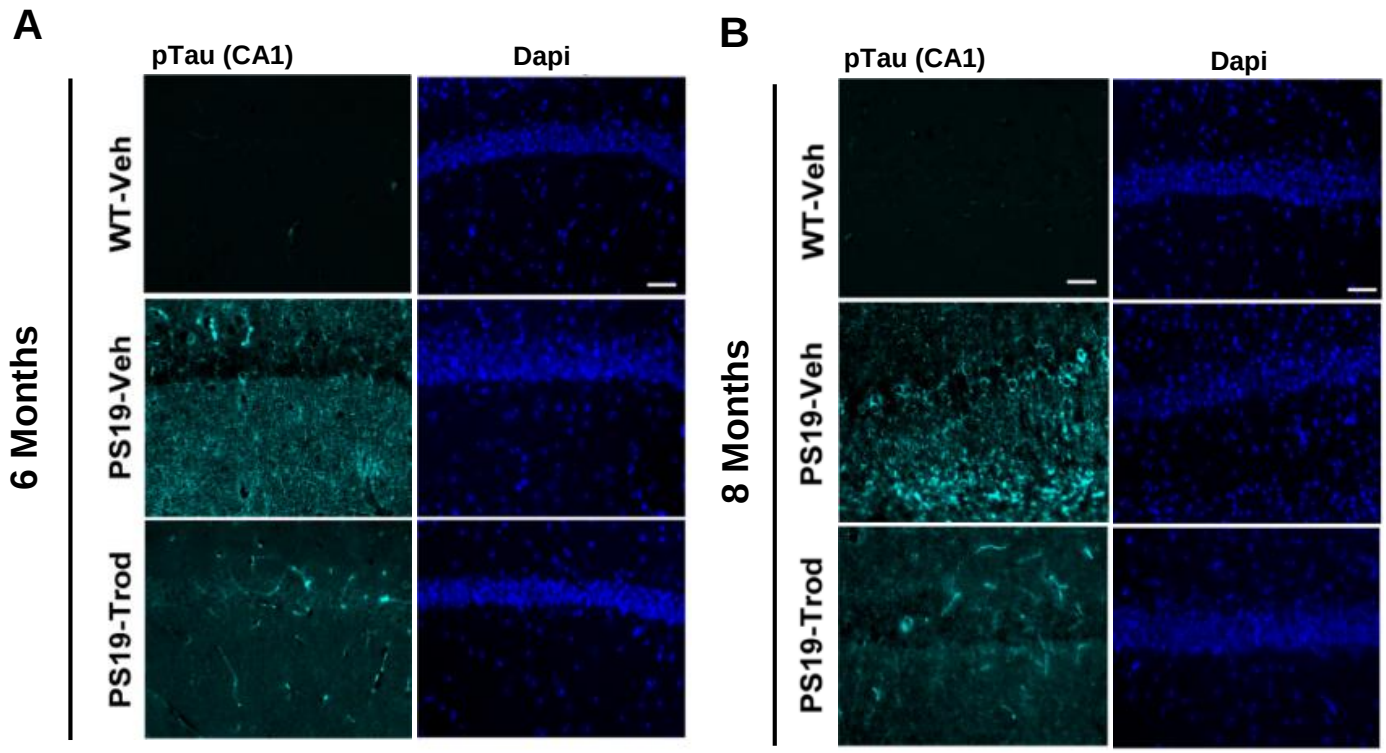

Figure 11. Immunofluorescence staining of hippocampal CA1 region shows increased pTau aggregation in PS19 mice aged 8 months compared to 6-month counterparts; 2.5 mg.kg trodusquemine treatment rescues this effect. PS19 mice at 6 months of age show increased pTau signal compared to WT littermates; this is reduced by trodusquemine treatment (A). PS19 mice at 8 months of age show increased pTau signal compared to WT littermates; this is reduced by trodusquemine treatment (B). The severity of these effects appears higher in 8 month PS19 mice compared to 6 month counterparts. Nuclei are counterstained with Dapi. Scale bars represent 50 μm. n=3 mice per group.

Similarly, pTau deposition in the BLA is also significantly apparent in PS19 mice by 8 months. This is rescued by CamK2α-Cre-mediated neuronal PTP1B ablation and with trodusquemine treatment **(Figure 12)**.

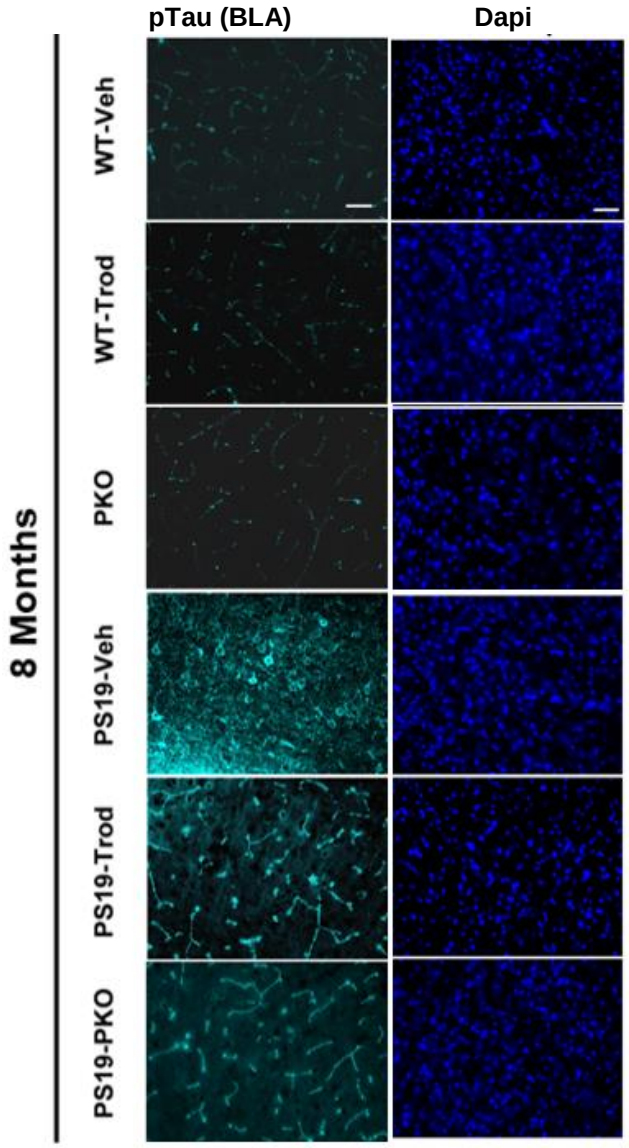

Figure 12. Immunofluorescence staining of basolateral amygdala (BLA) shows increased pTau aggregation in PS19 mice; 2.5 mg.kg trodusquemine treatment and neuronal PTP1B ablation rescues this effect. PS19 mice at 8 months of age show increased pTau signal compared to WT littermates and nPKO control mice; this is reduced by trodusquemine treatment and by genetic neuronal ablation of PTP1B. Nuclei are counterstained with Dapi. Scale bars represent 50 μm. n=3 mice per group.

Next, neuron loss and neuroinflammation in the hippocampal CA1 region and amygdala of PS19 mice at 6-month and 8-month age groups were measured. Overall, as depicted in **Figures 13-14**, neuron loss is not apparent in these regions in either of the age cohorts. However, increased neuroinflammation appears in PS19 mice in both age groups, and worsens in the older cohort. This is markedly attenuated by trodusquemine in all brain regions that were examined. **Figure 14**, shows that neuroinflammation in the BLA is not reduced as successfully with neuronal PTP1B ablation (PS19 nPKO) as with trodusquemine.

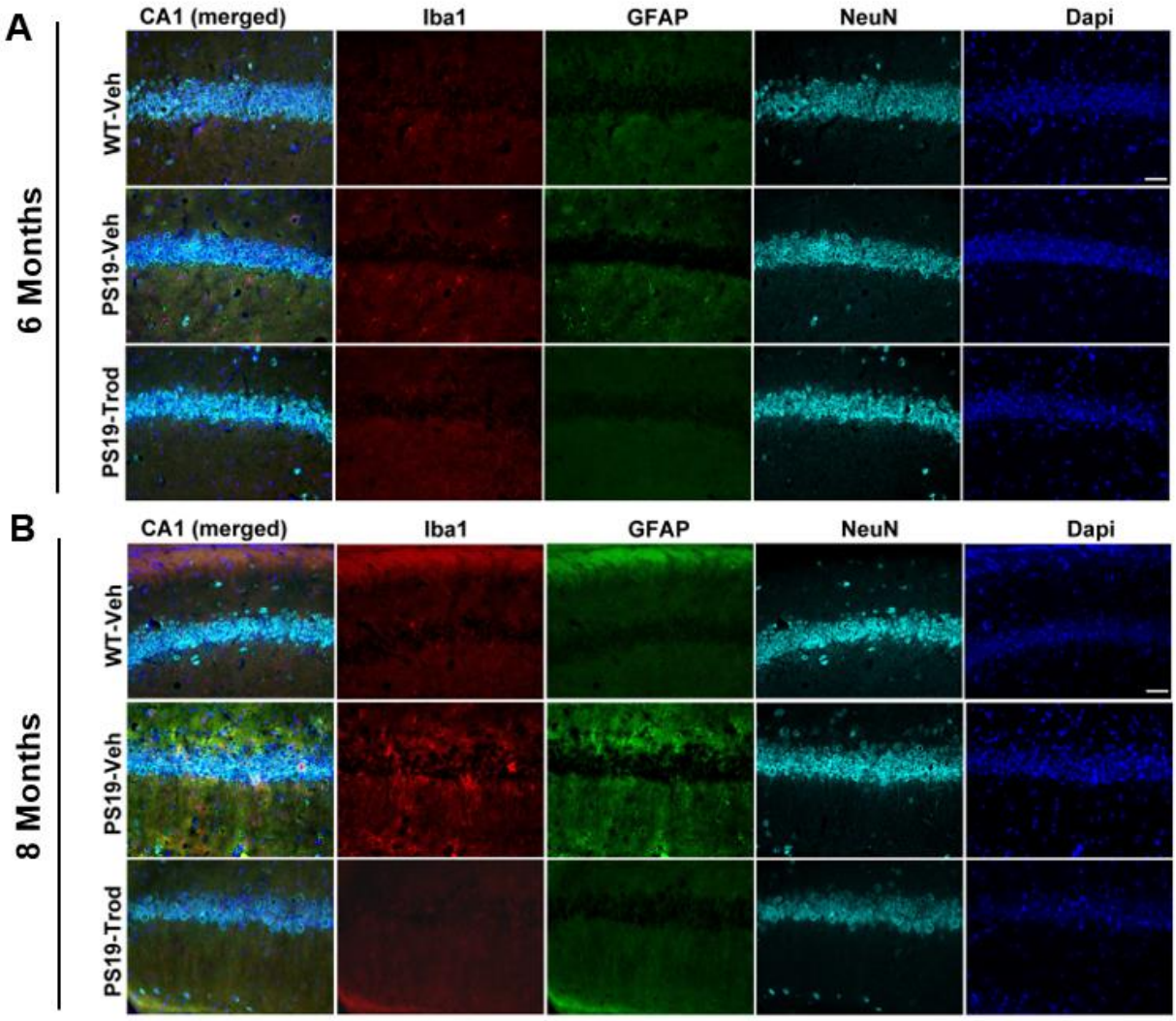

Figure 13. Immunofluorescence staining of hippocampal CA1 region of PS19 mice at 6 and 8 months of age shows increased neuroinflammation but no significant neurodegeneration; 2.5 mg.kg trodusquemine treatment had therapeutic effect on neuroinflammation and no effect on neuron numbers. PS19 mice at 6 months of age show increased signals of the neuroinflammatory markers GFAP and IBA1 compared to WT littermates (A). They do not display significant neuronal loss, as assessed by NeuN signal. Trodusquemine treatment had no effect (A). PS19 mice at 8 months of age display increased neuroinflammation but no significant neurodegeneration compared to WT littermates (B). Trodusquemine treatment had no effect (B). Nuclei are counterstained with Dapi. Scale bars represent 50 μm. n=3 mice per group.

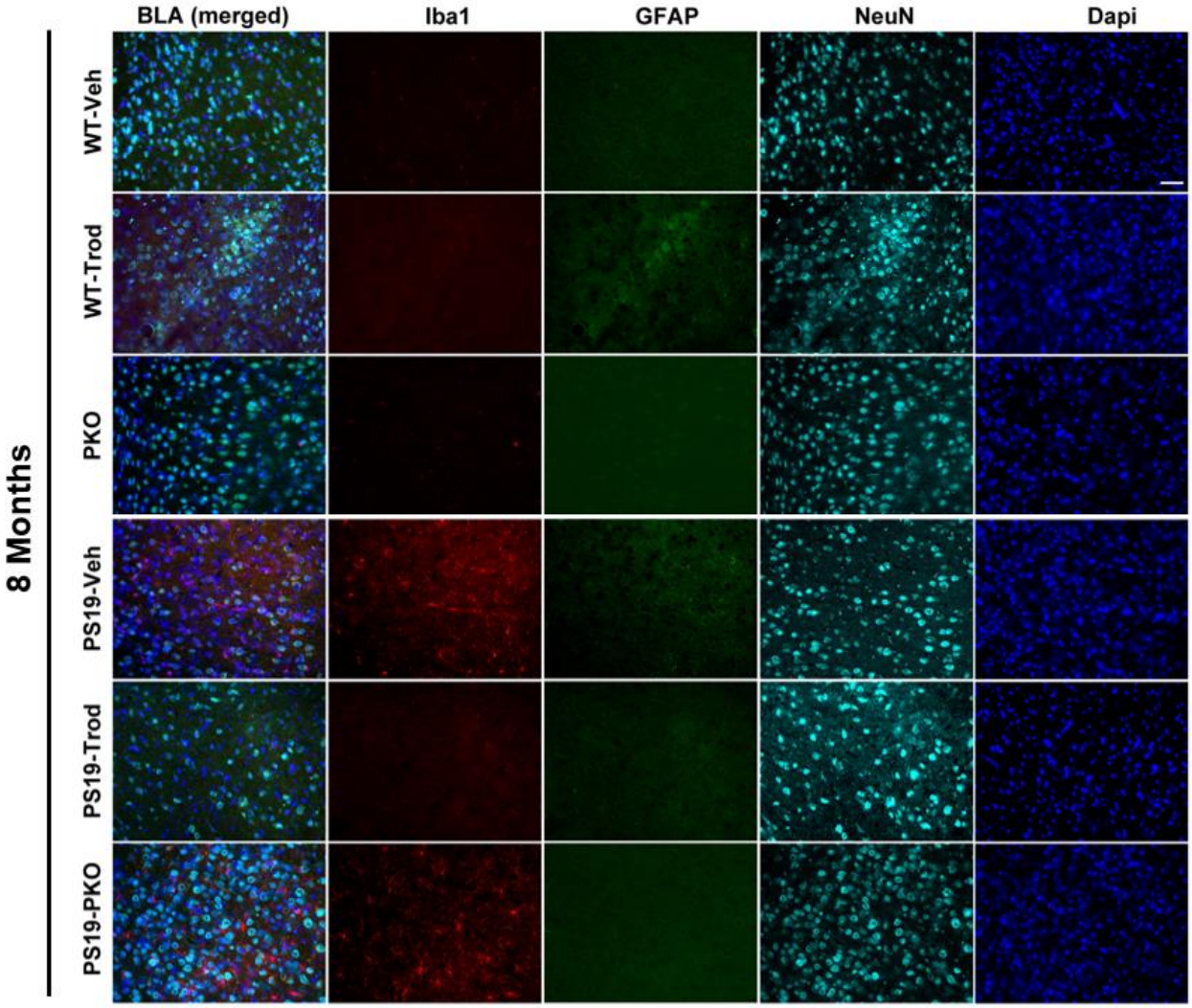

Figure 14. Immunofluorescence staining of basolateral amygdala (BLA) of PS19 mice at 8 months of age shows increased neuroinflammation but no significant neurodegeneration; 2.5 mg.kg trodusquemine treatment had therapeutic effect on neuroinflammation and no effect on neuron numbers; genetic neuronal PTP1B KO had no effect on neuroinflammaiton or neuron numbers. PS19 mice at 8 months of age show increased signals of the IBA1 neuroinflammatory marker compared to WT, WT-trod. and PKO control mice. They do not display significant neuronal loss, as assessed by NeuN signal. Trodusquemine treatment had no effect. PS19 nPKO group does not show rescue of neuroinflammation. Nuclei are counterstained with Dapi. Scale bars represent 50 μm. n=3 mice per group.

Taken together, these IHC experiments showed that pTau burden is apparent in PS19 mouse brains by 6 months of age and becomes more severe by 8 months of age in both the hippocampal CA1 region and the basolateral amygdala, which are both brain areas implicated in anxiety-related behaviours. Additionally, neuroinflammation, as depicted by GFAP and Iba1 immunofluorescence, is evident in both brain regions of diseased mice. Both pTau burden and neuroinflammation were relieved with PTP1B blockade, indicating a potential role of hyperactive PTP1B on tau pathology in this mouse model.

4.4.2 Western Blotting

Following IHC experiments, western blotting was used to characterize PTP1B, p-GSK3β (S9), GSK3β, and RIPA-soluble pTau protein levels in the brains of PS19 mice at 8 months of age. Whole-hemisphere brain samples from 8-month-old PS19 mice were used for western blotting experiments because AD pathology and behavioural abnormalities manifest more severely in this age group.

The first set of WB experiments were designed to compare PTP1B protein levels between experimental groups. **Figure 15** shows that PTP1B protein level is significantly lowered in nPKO and PS19 nPKO mice compared to WT and PS19 counterparts **(Figure 15A, 15B)**, which validates these knockout models. 2.5 mg/kg trodusquemine administration had no effect on PTP1B protein levels **(Figure 15A, 15C)**.

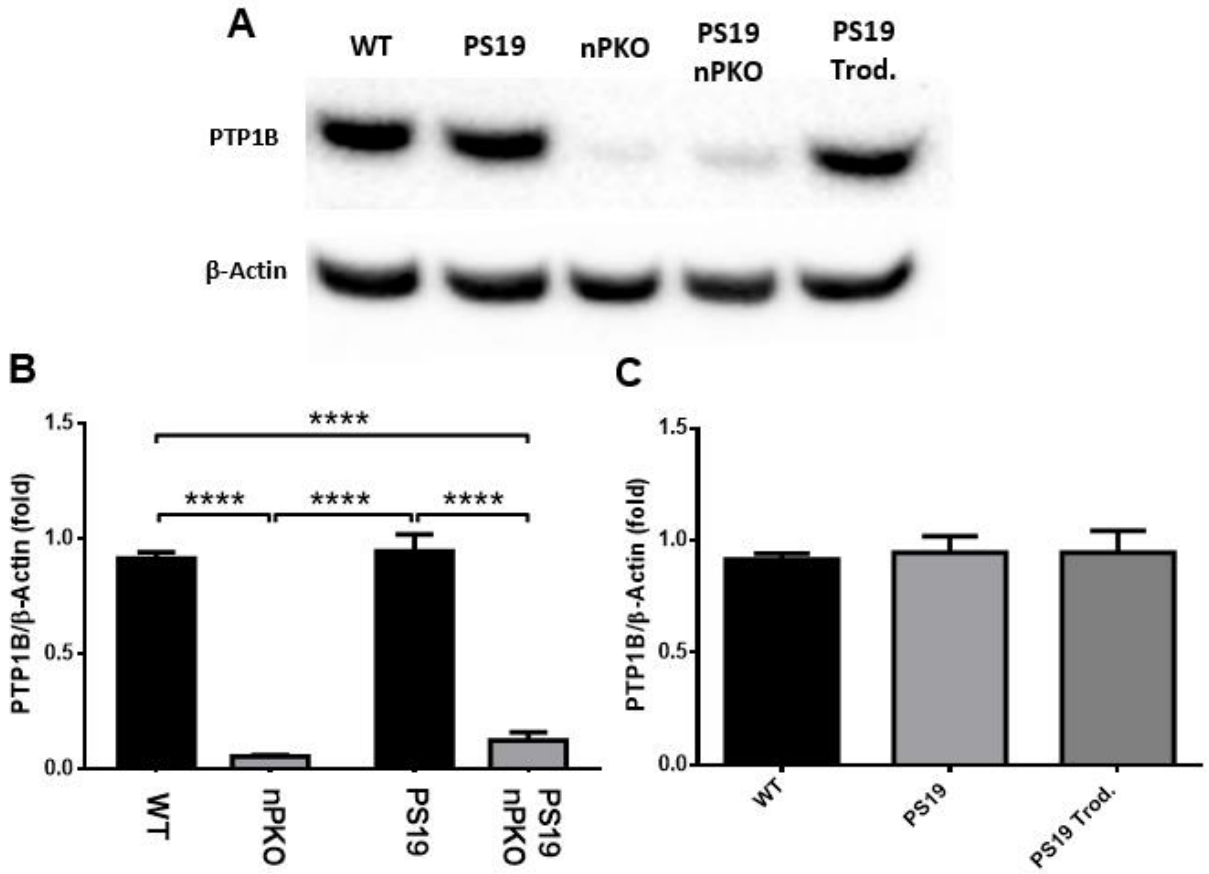

Figure 15. Immunoblotting shows significant decrease in PTP1B protein level in nPKO and PS19 nPKO mice at 8 months of age; 2.5 mg/kg Trodusquemine treatment showed no effect. Representative blot shows evident decrease of PTP1B protein level in nPKO and PS19 nPKO mice at 8 months of age compared to age-matched WT and PS19 mice. No effect is detectable in the PS19 trod. -treated group. PTP1B levels were normalized to β-Actin levels. (A). This is quantified in (B) and (C), using n=3 mice per group. For the analysis in (B), two-way ANOVA was followed by Bonferroni's post-hoc pairwise comparisons. In (C), one-way ANOVA was used due to the absence of the WT Trod. control group, followed by Bonferroni's post-hoc pairwise comparisons. *p-value < 0.05, mean values are reported, error bars represent SEM.

Next, protein levels of RIPA-soluble pTau (S202/T205) and total non-phosphorylated tau. WT and nPKO control mice did not exhibit any phosphorylated or non-phosphorylated tau because these mice do not express human tau protein **(Figure 16A)**. However, tau evident in PS19 mice **(Figure 16 A)**. Moreover, level of pTau was significantly reduced by neuronal PTP1B ablation and with 2.5 mg/kg trodusquemine treatment; with trodusquemine treatment showing a stronger effect **(Figure 16B)**. Levels of total non-phosphorylated tau, however, did not differ significantly between groups **(Figure 16C)**. The ratio of pTau to total Tau was also significantly lower in trodusquemine-treated PS19 mice compared to PS19 counterparts **(Figure 16D)**.

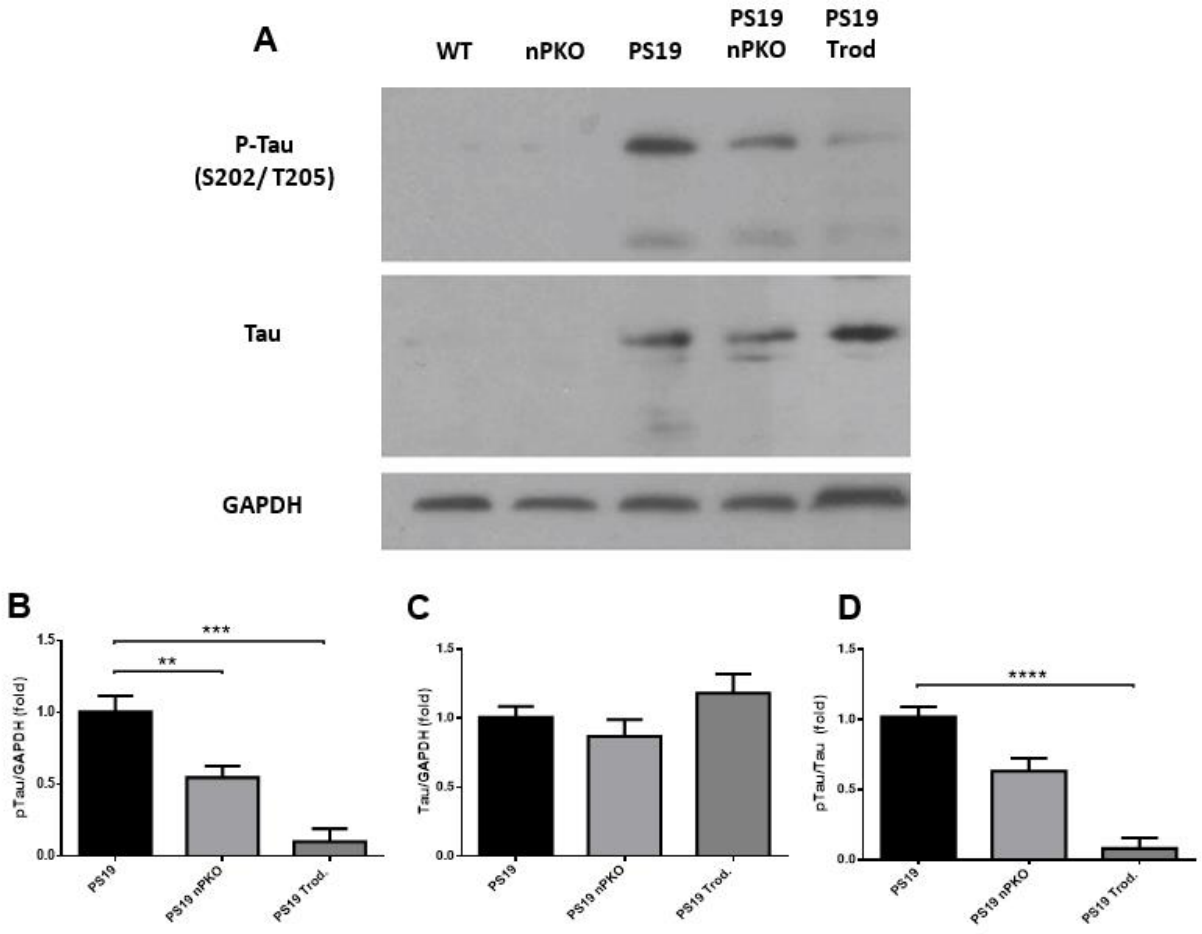

Figure 16. Immunoblotting shows decreased phospho-Tau levels in PS19 mice treated with 2.5 mg/kg dosage of trodusquemine and in PS19 nPKO mice. Representative blot shows significantly lowered levels of pTau in PS19 nPKO and PS19 trod. -treated mice compared to diseased PS19 mice. No differences detected in total Tau protein levels amongst groups. pTau and Tau were not detected in WT and nPKO control mice (A). This is quantified in (B), (C), and (D), using n=3 mice per group. GAPDH was used to control for loading. One-way ANOVA with Bonferroni's post-hoc pair-wise comparison. **, $p < 0.01$, ***, $p<0.001$. mean values ± SEM.

Finally, it was observed whether differences exist in phosphorylation status of GSK3β (i.e. p-GSK3β (S9)/GSK3β ratio) between WT and 8- month PS19 mice and whether PTP1B inhibition by trodusquemine or neuronal PTP1B ablation would have an impact on this phosphorylation status. This would provide insight into the activity level of the tau cascade in these mice, since GSK3β is a major tau kinase isoform. A lowered p-GSK3β/GSK3β (i.e. low level of p-GSK3β expression and high GSK3β expression) would indicate that GSK3 β is "unleashed" and potentially contributing to tau pathology. Interestingly, upon analysis, no difference was detected in the p-GSK3β/GSK3β ratio between WT mice and PS19 mice at 8 months of age **(Figure 17)**. In the PS19 nPKO group, the ratio was lower than in WT mice **(Figure 17 A, B)**. Trodusquemine administration (2.5 mg/kg) had no effect (**Figure 17 C)**.

Together, these western blot experiments were able to validate the PTP1B KO models used in the PS19 cohort and show that PTP1B inhibition and genetic ablation are both able to significantly reduce protein levels of soluble pTau, with drug treatment having a stronger therapeutic effect than genetic ablation. No difference was observed in the activity status of the major tau kinase GSK3β between groups.

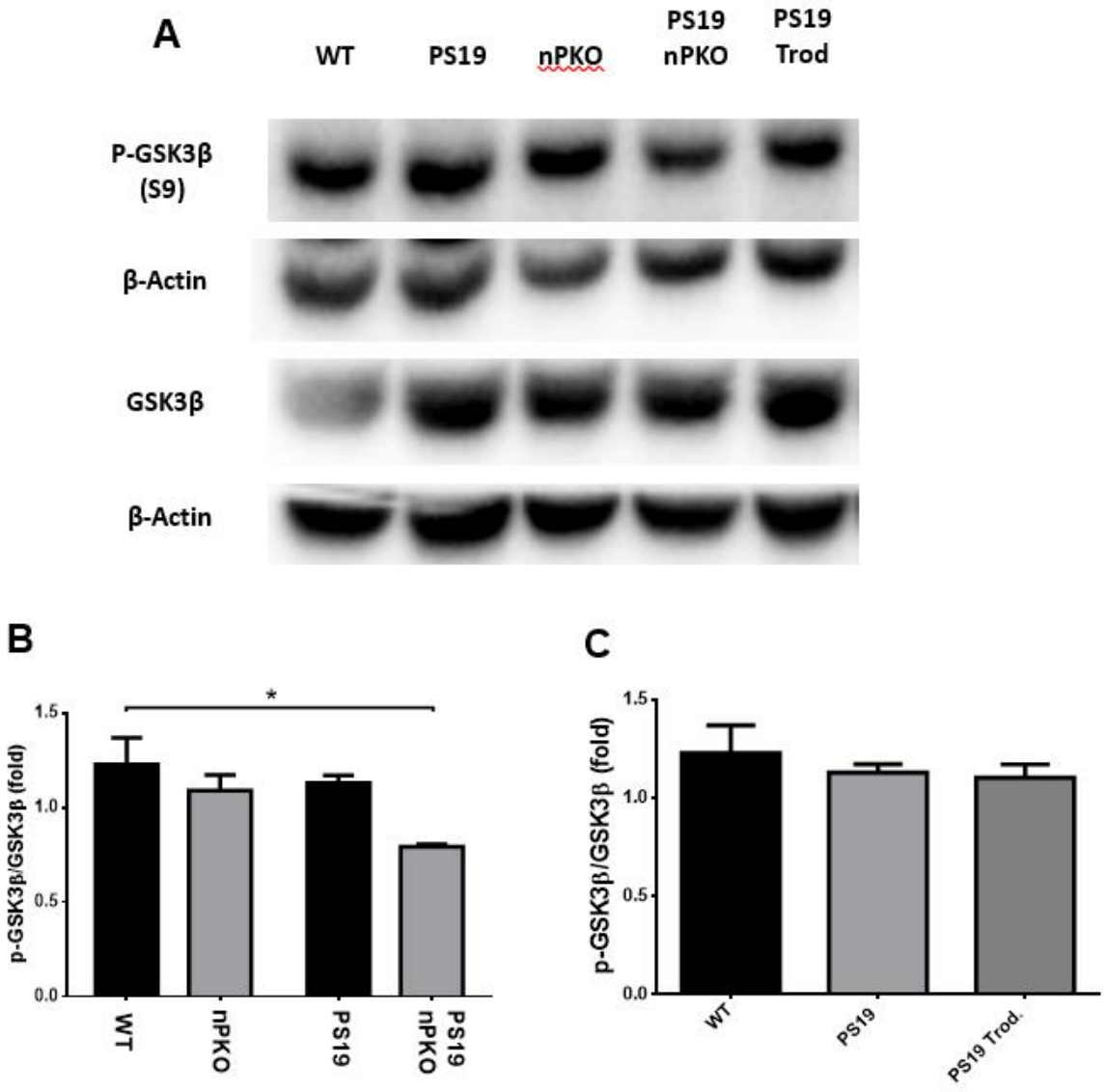

Figure 17. Immunoblotting shows no significant difference in p-GSK3β/GSK3β protein level ratio between WT and PS19 mice at 8 months of age; decrease in ratio observed in PS19 nPKO mice but no effect observed in trodusquemine-treated mice (2.5 mg/kg).
Representative blot shows no difference in p-GSK3β/GSK3β protein level ratio between WT and PS19 mice, although a significant decrease is evident in the PS19 nPKO group. No effect is detectable in the PS19 trod. -treated group (A). This is quantified in (B) and (C), using n=3 mice per group. For the analysis in (B), two-way ANOVA was followed by Bonferroni's post-hoc pairwise comparisons. In (C), one-way ANOVA was used due to the absence of the WT Trod. control group, followed by Bonferroni's post-hoc pairwise comparisons. *p-value < 0.05, mean values are reported, error bars represent SEM.

5. Discussion

Herein, it was investigated whether there are differences in AD-associated anxiety phenotypes between the hAPP-J20 and PS19 AD mouse models at ages of 6 months and 8 months. It was also examined whether PTP1B has a role to play in the manifestation of these anxiety-related behaviours in AD. Using the open field and elevated plus maze anxiety-testing paradigms, a unique age-based dimorphism was found in the onset of an anti-anxiety behavioural profile between these two mouse lines, with J20 mice exhibiting early onset of this phenotype and PS19 mice displaying late onset. It was also found that selective drug-based inhibition of PTP1B and genetic neuronal ablation of PTP1B can both normalize these behavioural abnormalities.

In the J20 mouse model, this inappropriately reduced anxiety phenotype appears between WT and transgenic mice at the younger age group of 6 months. In the EPM, which is a primary anxiety assay and is a more powerful test for anxiety than the OF, young J20 mice aged 6 months expended more time in open arms of the EPM and entered the open arms at a higher relative frequency compared to WT littermates[76]. This is consistent with other studies which have noted these phenotypes in J20 mice as early as 2 months, continuing to about 7 months of age[79,80]. At 6 months, this phenotype occurred exclusively in J20 mice, with PS19 mice of the same age showing no difference in anxiety-related behaviour. This behavioural abnormality in J20 mice had extinguished in the 8-month cohort. It must be noted that although this anti-anxious behaviour was observed in the EPM experiments for 6-month- old J20 mice, it was not observed in OF tests. This could be a result of differing strain backgrounds for the J20 and PS19 mice, perhaps making the J20 mouse line slightly more resilient to stressors (i.e. since a phenotype could only be observed in the EPM and not in OF). The abnormally reduced anxiety in J20 mice in the EPM could be interpreted as reduced cautiousness/ lowered risk assessment, which could understandably be maladaptive to the survival of the animals. One way to validate this theory would be to observe the frequency of stretch-attend posture (SAP) in these mice, which would need to be tracked manually from video recordings of the mice in the EPM or OF. SAP is a frequently used measure of risk assessment,

particularly in the EPM [125,126]. In humans, this rodent behaviour could resemble disinhibition, which is often observed in AD patients and can have devastating effects on their livelihood[127]. APP function and disruption of the cholinergic system, because of its role in behavioural inhibition, have been proposed as underlying contributors of these anti-anxiety behavioural abnormalities[80]. However, there is no known contribution of PTP1B in these mechanisms[80]. The appearance of these behavioural phenotypes occurs around the same time as prominent neuronal loss in the CA1 hippocampal region in these mice (3 months), which is a region highly implicated in anxiety in AD[36,72,74,75]. Anxiety-related behaviour appears to precede widespread Aβ plaque deposition, which usually occurs around 8 months in J20 mice[38]. This is reminiscent of many reports which have claimed that anxiety occurs in early/prodromal AD in humans and may precede severe AD pathology, including widespread Aβ plaque deposition [36,57,128].

A similar behavioural phenotype was detected in PS19 mice at 8 months of age and was not evident in the younger cohort or in J20 mice of the same age. This aligns with findings from Takeuchi et. al., who observed that PS19 mice spend more time in the open center of the OF arena and spend more time in the open arms of the EPM compared to non-transgenic WT controls[48]. However, Takeuchi et. al. observed these phenotypes in mice at 6 months of age, before these mice developed advanced NFT-like tau pathology[48]. Filamentous tau lesions develop at around 6 months of age, and progressively worsen by 9-12 months and occur in association with profound neuronal loss in the hippocampus and entorhinal cortex[47]. The behavioural abnormalities detected in the 8-month-old PS19 cohort in this report appear to pertain to the timing of this late stage tau pathology. Takeuchi et. al. also observed significant hyper-phosphorylated tau lesions in the prefrontal cortex and amygdala, which may explain the hyperactive and impaired anxiety responses that were seen[48].

The inappropriately lowered anxiety observed in 6-month J20 mice and 8-month PS19 mice, particularly in the EPM, was normalized by 2.5 mg/kg repeated *i.p* injections of the selective PTP1B inhibitor trodusquemine. This was also noted at a higher dosage of the drug. A point to be noted however is that in many instances in the EPM and OF tests, drug treatment was able to reduce/normalize the

amount of time spent in open areas, but not sufficiently able to reduce the relative entries to these regions. This discrepancy could potentially be a result of the mice entering the open areas in short bursts, which would result in lower cumulative duration in these areas but not significantly reduced frequency of entries. This would need to be validated by measuring the time interval between entries and exits from the open arms of the EPM or center of the OF. Nonetheless, trodusquemine showed repeated efficacy in generally normalizing the anti-anxiety baseline phenotype in both J20 and PS19 mouse lines. Our previous study also showed that trodusquemine was able to ameliorate hippocampal neuron loss, and spatial memory deficits in hAPP-J20 mice at 6 months of age[100]. Recently, Limbocker et. al. found that trodusquemine enhances $A\beta_{42}$ oligomerization but significantly reduces the toxicity of these oligomers by preventing them from binding to the surface of neuroblastoma cells[129], thereby reducing the effect of Aβ pathology in AD. How trodusquemine may impact tau pathology has not been previously established. In terms of relevance to anxiety behaviours, Qin et al. published that ablating LMO4, which is an endogenous inhibitor of PTP1B, leads to reduced amygdalar endocannabinoid signaling and consequent increase in stress-induced anxiety behavior, and that trodusquemine administration reversed this increase in anxiety behaviour[103]. Although this present study identifies an anti-anxiety baseline phenotype in J20 and PS19 mice rather than the anxiogenic phenotype observed by Qin et. al in LMO4 knockout mice, trodusquemine reversed anxiety-related behavioural abnormalities in both scenarios. This suggests that unleashed activity of PTP1B may play a role in anxiety-related behaviour and in AD pathogenesis, and that trodusquemine could be a potential therapeutic. However, trodusquemine has been shown to cause weight loss in rodent models[100,116]. Thus, an optimal dosage which leads to minimal weight loss and maximal effect on improving behavioural deficits and pathology must be determined. Weight of PS19 mice before and after 2.5 mg/kg drug treatment should be monitored, as this has not been previously investigated.

In EPM experiments of J20 and PS19 mice treated with ENT-03 at 6 months of age, it was established that this drug also reverses the anti-anxiety phenotype observed in J20 and PS19, similarly to Trodusquemine. This effect could not be observed in PS19 mice because they exhibit the behavioural

phenotype at an older age, for which experiments have not yet been completed. The therapeutic effects observed with mice treated with ENT-03 further consolidate the idea that PTP1B inhibition may be important for targeting anxiety-related behaviours in AD.

As an extension of these experiments, it was next investigated whether neuronal PTP1B, in particular, is involved in these behaviours. Using CamK2α-Cre-driven neuronal ablation of PTP1B, we created knockout models in the J20 and PS19 mouse lines, at 6 and 8 months of age respectively (J20 nPKO and PS19 nPKO). As was observed with drug-based PTP1B inhibition, PTP1B knockout in J20 mice at 6 months of age normalized the anti-anxiety phenotype observed in diseased J20 counterparts. PTP1B ablation in PS19 mice at 8 months had a similar rescue effect on anxiety-related behaviour. Together, these findings further reinforced the theory that PTP1B may play a role in these behaviours.

Many studies have also noted hyperactivity as a distinct phenotype in J20 and PS19 transgenic mice [48,80]. Hyperactivity, as measured primarily by the OF test, can be likened to the exacerbation of activity observed in human AD patients in late afternoon and evening time, termed sundowning syndrome[130]. In contrast to former research, this hyperactivity phenotype was not observed in this present study in any of the OF experiments. It could be possible that rather than a 10-minute testing period, a longer testing period would be required to distinguish a phenotype in these mice. Another possible alteration could be to monitor ambulatory activity as a parameter in addition to total distance moved.

Thus far, a major limitation of these behavioural studies is that a WT trodusquemine-treated group could not be included for the trodusquemine related OF and EPM experiments at a 2.5 mg/kg dosage, which is an important control group. This control group is critical because it would have allowed the use of two-way ANOVA to statistically test for genotype effect, treatment effect, and possible interaction between these effects, which is a more powerful analysis than the one-way ANOVA analysis that was used. However, it should be pointed out that a prior study showed no effect of trodusquemine at the same dosage on either EPM or OF performance compared to vehicle-treated WT mice[103]. Another major limitation is linked to behavioural studies involving the neuronal PTP1B KO model in the J20

background, where only 4 mice constituted the J20 nPKO group. Thus, the results in this experiment must be interpreted with caution. In future, when more of these mice are generated from breeding, they should be included in this group for assessment to increase statistical power of these results. Another future initiative for this project could be to study the effect of PTP1B blockade in mouse models of AD that display anxious behaviour at baseline, such as the APPxPS1 mouse line which exhibits task-dependent hyperlocomotion and increased anxiety behaviour[131]. If PTP1B inhibition can rescue these behaviours, it would add further validity to the proposition that this protein is indeed involved in the cellular mechanisms underlying the behavioural abnormalities.

Overall, these behavioural studies demonstrate a potential role of PTP1B in anxiety-related behaviours in the J20 and PS19 mouse models of AD. However, a mechanistic link between PTP1B hyperactivity and anxiety-related behaviours remains to be elucidated in these mouse models. One possible mechanism underlying these behaviours could be altered endocannabinoid (eCB) signalling. A large body of previous studies have validated that the eCB system, particularly within the amygdala, is a major regulator of acquired fear, anxiety and stress-coping behaviours[103,132–134]. Although the eCB system is widely distributed throughout the brain, localized eCB signalling within the hippocampus, prefrontal cortex, amygdala and hypothalamus are more relevant in the context of anxiety and stress-coping behaviours[132]. The previous study from our laboratory demonstrated that hyperactive PTP1B directly de-phosphorylates the mGluR5 receptor, which negatively impacts the production of the endocannabinoid, 2-AG, in glutamatergic neurons of the basolateral amygdala[103]. Anxiety-related behaviour has been linked in particular to retrograde eCB signalling to the CB1R endocannabinoid receptor, particularly by 2-AG[103,132]. Upon depolarization (via mGluR5 or mGluR1), post-synaptic neurons synthesize and release 2-AG in an activity-dependent manner, which in turn binds in a retrograde fashion to CB1Rs which are located on presynaptic membranes, inhibiting neurotransmitter release from both presynaptic glutamatergic and GABAergic synapses[132,134]. Qin et al. noted that PTP1B's inhibition of the mGluR5 receptor exclusively causes a collapse of 2-AG synthesis, and does not affect the other major endocannabinoid, anandamide (AEA)[103]. Qin et al. also noted that this impairment of 2-AG in the BLA

led to anxious behaviour in mice. In many models of AD, including J20 and PS19 models, the commonly observed anxiety-related behavioural deficit has been abnormally lowered anxious behaviour in both the open field test and the elevated plus maze test[48,80]. Thereby, it may be possible that, in opposition to what was observed by Qin et al., the baseline anti-anxiety behaviour in AD mice involves elevated levels of 2-AG, and PTP1B may play a role in this elevation.

One possible mechanism by which there can be increased 2-AG eCB at synapses could be through lowered expression of enzymes that degrade 2-AG and increased expression of enzymes that synthesize these eCBs. 2-AG is post-synaptically synthesized "on-demand" by diacylglycerol lipase-α (DAGLα) and primarily catabolized by the enzyme monoacylglycerol lipase (MAGL), which is located at the presynaptic terminal or on astrocytes[132]. Recent reports have shown that deficiency in DAGLα leads to reduced 2-AG brain levels and to increased anxiety-like behaviour, which was rescued by pharmacological inhibition of MAGL with JZL184[135,136]. Overexpression of MAGL leads to decreased 2-AG levels and increased anxiety-like behaviour[137]. Whereas, JZL184-mediated inhibition of MAGL in wild-type mice led to anxiolytic effects under basal conditions, under increased aversive conditions, and after chronic unpredictable stress[132]. Thus a major avenue of future incentive for this project could be to complete a large-scale RNA sequencing study in order scan for differences in the expression of these key enzymes between WT and diseased mice in anxiety-related brain regions, such as the amygdala. Furthermore, it would be important to investigate whether PTP1B blockade influences the expression of these enzymes. Another important investigation would be to observe whether the interaction between PTP1B and the mGluR5 receptor is altered in these two AD mouse models, as was observed in the LMO4 KO mouse model by Qin et al.

Following behavioural experiments, tau pathology in the PS19 mouse model and the effect of PTP1B blockade on this pathology was observed, which has not been tested previously. Yoshiyama et al. showed that filamentous tau lesions develop at around 6 months of age, and progressively worsen by 9-12 months and occur in association with profound neuronal loss in the hippocampus and entorhinal cortex[47].

In the IHC experiments of this report, it was observed that pTau burden in the hippocampal CA1 region became more severe with age in PS19 mice. Severe pTau burden was also noted in the BLA. In PS19 mice, these areas also exhibited increased neuroinflammation, as assessed by Iba1 and GFAP signal. Both phospho-tau burden and neuroinflammation were rescued by trodusquemine treatment, suggesting PTP1B as a potential therapeutic target for tau pathology. This complements the observations of Ricke et al., who showed that PTP1B ablation can reduce Aβ plaque size in the hippocampal CA3 region of 6-month-old J20 mice[100]. Ricke et al. also noted that neurodegeneration and neuroinflammation in J20 mice, which was also rescued by trodusquemine treatment[100]. However, in PS19 mice, notable neurodegeneration was not apparent in hippocampal CA1 or in the amygdala at 8 months. Although, this may become evident at an even later stage, as suggested by Yoshiyama et al. Since hippocampal and amygdalar regions have been highly implicated in anxiety-related behaviours, increased tau burden and neuroinflammatory responses in these areas in the 8–month-old PS19 mice may contribute to the behavioural abnormalities that occurred. It would be interesting to see in future whether the behavioural disinhibition observed in PS19 mice at 8 months persists at a later age (e.g. 12 months), as neurodegeneration becomes more severe.

In addition to IHC studies, immunoblotting experiments were also completed to characterize levels of PTP1B, pTau (S202/T205), total Tau, p-GSK3β (S9), and total GSK3β protein in all groups of the 8-month PS19 mouse cohort. PTP1B levels were assessed to validate the PTP1B KO and PS19 nPKO mouse lines. PTP1B levels were nearly diminished in the KO mouse lines as compared to WT and PS19 counterparts, while trodusquemine treatment had no effect on PTP1B level. This validated that PTP1B protein expression is indeed halted in the KO mouse lines and replicates the observations of PTP1B levels in the J20 nPKO mouse line observed by Ricke et al[100].

Next, the levels of RIPA-soluble pTau and total Tau were quantified using human tau-specific antibodies, and it was found that WT and nPKO control mice do not express any human pTau or total Tau, as expected. The ratio of pTau to total Tau is significantly higher in PS19 mice, and this was rescued

by trodusquemine treatment or by neuronal PTP1B ablation. A limitation here is that the levels of formic acid-extracted insoluble hyper-phosphorylated tau, which are the main constituents of larger oligomers and NFTs, were not analyzed. Traditionally, NFTs have been heavily linked to neuronal death and their accumulation has been positively correlated with cognitive decline in AD, more so than Aβ plaques [14,138]. Neurons with NFT burden also abnormally sequester proteins which are necessary for proper cell function such as synaptic proteins and calcium-binding proteins, and thereby, neuronal function of other surrounding cells are compromised[139–141]. However, significant research has also suggested that soluble tau may have a toxic role as well, which increases the relevance of the experiments of this report. Several studies have now shown that alterations in phosphorylation, somatodendritic localization, or conformation of tau serve as the beginning of the early pathological cascade in AD [142–145]. These changes can induce loss of dendritic spines, impaired trafficking of organelles, and cell death[138]. In mouse models of tau pathology, correlation has been found between soluble tau species and synaptic dysfunction[138].

Overall, the findings of these pTau/Tau Western blotting experiments and IHC experiments complement the results of Ricke et al. and suggest that unleashed PTP1B activity may have a role in tau pathology in addition to it's role in Aβ pathology. On the contrary, Kanno et al. recently found that in rat hippocampal tissue, sole PTP1B inhibition by orthovanadate does not sufficiently lower tau phosphorylation or reduce GSK3β activity. However, knock-down of PTP1B in combination with knock-in of PKCε did have a therapeutic effect of reducing phospho-tau burden[102]. However, orthovanadate is not entirely selective to PTP1B specifically, but targets many kinds of protein tyrosine phosphatases. Perhaps, suppression of tau phosphorylation would have been more effective if a selective PTP1B inhibitor like trodusquemine had been used in Kanno et al.'s study. The exact mechanism by which trodusquemine reduces pTau burden remains to be elucidated. The findings here show that trodusquemine reduces soluble pTau as well as insoluble pTau aggregates (in IHC studies). Clearance of soluble pTau would be the preliminary step to prevent further aggregation, and the findings here show that trodusquemine significantly reduces soluble pTau levels. This could potentially be occurring via PTP1B's indirect interaction with GSK3β, the major tau kinase. Kanno et al. previously showed that PTP1B

inhibition activated GSK3β via the IRS-1/P13K/PDK1/Akt signalling pathway. This pathway could be at play as a mechanism by which trodusquemine's inhibition of PTP1B reduces pTau burden in this mouse model.

In the final set of immunoblotting experiments, I investigated the p-GSK3β/GSK3β ratio in 8-month PS19 mice to assess the activity of the tau molecular cascade. GSK3β is a major tau kinase and is constitutively active. Phosphorylation of GSK3β at the Serine 9 (S9) position renders the protein inactive and it is no longer able to phosphorylate downstream substrates[146]. PTP1B ablation has been linked indirectly to increased phosphorylation/inactivation of GSK3β[101]. The results of Ricke et al. showed that the J20 mouse model of AD exhibited significantly lowered p-GSK3β/GSK3β ratio compared to WT mice, suggesting that GSK3β is in an "unleashed" state in these diseased mice[100]. This ratio is significantly increased in J20-Troduquemine-treated mice and J20 nPKO mice compared to J20 mice, similar to levels seen in WT mice[100]. This suggested that increased PTP1B activity was contributing to the "unleashed" activity of GSK3β in J20 mice[100]. The findings of this report using PS19 mice at 8 months of age showed no difference in p-GSK3β/ GSK3β ratio between WT and PS19 mice. PTP1B inhibition by trodusquemine had no effect and PTP1B genetic ablation actually led to lowered p-GSK3β/ GSK3β ratio. These findings are inconsistent with what was noted by Gum et al. and Ricke et al[100,101]. It could indeed be that these PS19 mice do not show the lowered p-GSK3β/ GSK3β ratio phenotype observed in J20 mice. However, IHC experiment results show increased phospho-Tau levels in PS19 mice at 8 months of age, potentially indicating increased activity of the tau cascade. Ideally, this should translate to lowered p-GSK3β/ GSK3β ratio in these PS19 mice in WB experiments (i.e. GSK3β is more active and p-tau phosphorylation is increased). One possible explanation for why expected results in these WB experiments were not achieved could be that, because whole-hemisphere brain samples were used, the GSK3β protein became overly diluted in the samples used. In the adult mouse brain, GSK3β is highly expressed in the cerebral cortex and hippocampus[147]. Thus, using whole-hemisphere samples instead of specific regions could have caused the p- GSK3β and GSK3β proteins to be diluted out in the samples.

This may be leading to lack of differential expression of these proteins between the different groups in the PS19 cohort.

6. Conclusions

In this project, a distinct age-based difference in the onset of an inappropriately lowered anxiety response in the hAPP-J20 and PS19 mouse models of AD was established. It was also found that PTP1B may play an important role in these anxiety-related symptoms, since its blockade by drug and genetic ablation methods was able to normalize behavioural abnormalities. Finally, tau pathology in the PS19 mouse model was studied and it was observed that unleashed PTP1B may contribute to tau pathology and neuroinflammation in anxiety-related brain areas such as the amygdala and hippocampal CA1 region, as PTP1B inhibition had strong therapeutic effects. Since, neuropsychiatric symptoms of AD, particularly anxiety, have not been well investigated and their treatment has largely occurred in dissociation from AD treatment, the findings of this research can shed light on the underlying mechanism of anxiety in AD and suggest trodusquemine as a feasible drug to reverse or, at least, improve symptoms.

7. References

1. Selkoe DJ, Hardy J. The amyloid hypothesis of Alzheimer's disease at 25 years. *EMBO Mol Med*. 2016;8(6):595-608. doi:10.15252/emmm.201606210

2. Van Der Flier WM, Scheltens P. Epidemiology and risk factors of dementia. *Neurol Pract*. 2005;76(SUPPL. 5):2-7. doi:10.1136/jnnp.2005.082867

3. Scheltens P, Blennow K, Breteler MMB, et al. Alzheimer's disease. *Lancet*. 2016;388(10043):505-517. doi:10.1016/S0140-6736(15)01124-1

4. LaFerla FM, Green KN, Oddo S. Intracellular amyloid-β in Alzheimer's disease. *Nat Rev Neurosci*. 2007;8(7):499-509. doi:10.1038/nrn2168

5. Ballard C, Gauthier S, Corbett A, Brayne C, Aarsland D, Jones E. Alzheimer's disease. *Lancet*. 2011;377(9770):1019-1031. doi:10.1016/S0140-6736(10)61349-9

6. Norton S, Matthews FE, Barnes DE, Yaffe K, Brayne C. Potential for primary prevention of Alzheimer's disease: An analysis of population-based data. *Lancet Neurol*. 2014;13(8):788-794. doi:10.1016/S1474-4422(14)70136-X

7. Gottesman RF, Schneider ALC, Albert M, et al. Midlife hypertension and 20-year cognitive change: The atherosclerosis risk in communities neurocognitive study. *JAMA Neurol*. 2014;71(10):1218-1227. doi:10.1001/jamaneurol.2014.1646

8. Genin E, Hannequin D, Wallon D, et al. APOE and Alzheimer disease: A major gene with semi-dominant inheritance. *Mol Psychiatry*. 2011;16(9):903-907. doi:10.1038/mp.2011.52

9. Guerreiro R, Hardy J. Genetics of Alzheimer's Disease. *Neurotherapeutics*. 2014;11(4):732-737. doi:10.1007/s13311-014-0295-9

10. Hardy JA, Higgins GA. Alzheimer's disease: The amyloid cascade hypothesis. *Science (80-)*. 1992;256(5054):184-185. doi:10.1126/science.1566067

11. Koffie RM, Hyman BT, Spires-Jones TL. Alzheimer's disease: Synapses gone cold. *Mol Neurodegener*. 2011;6(1):1-9. doi:10.1186/1750-1326-6-63

12. Perez-Nievas BG, Stein TD, Tai HC, et al. Dissecting phenotypic traits linked to human resilience to Alzheimer's pathology. *Brain*. 2013;136(8):2510-2526. doi:10.1093/brain/awt171

13. Arriagada P V., Marzloff K, Hyman BT. Distribution of Alzheimer–type pathologic changes in nondemented elderly individuals matches the pattern in Alzheimer's disease. *Neurology*. 1992;42(9):1681-1688. doi:10.1212/wnl.42.9.1681

14. Giannakopoulos P, Herrmann FR, Bussière T, et al. Tangle and neuron numbers, but not amyloid load, predict cognitive status in Alzheimer's disease. *Neurology*. 2003;60(9):1495-1500. doi:10.1212/01.WNL.0000063311.58879.01

15. Ingelsson M, Fukumoto H, Newell KL, et al. Early AB accumulation and progressive synaptic loss, gliosis, and tangle formation in AD brain. *Neurology*. 2004;62(6):925-931. doi: 10.1212/01.wnl.0000115115.98960.37.

16. Goedert M, Spillantini MG. A Century of Alzheimer's Disease. *Acad Manag Rev*.

2006;314(5800):777-781. doi:10.1126/science.1132814.

17. Murphy MP, Levine H. Alzheimer's Disease and the Beta-Amyloid Peptide. *J Alzheimer's Dis*. 2010;19(1):1-17. doi:10.3233/JAD-2010-1221.Alzheimer

18. Jarrett JT, Berger EP, Lansbury PT. The Carboxy Terminus of the β Amyloid Protein Is Critical for the Seeding of Amyloid Formation: Implications for the Pathogenesis of Alzheimer's Disease. *Biochemistry*. 1993;32(18):4693-4697. doi:10.1021/bi00069a001

19. Thal DR, Rüb U, Orantes M, Braak H. Phases of Aβ-deposition in the human brain and its relevance for the development of AD. *Neurology*. 2002;58(12):1791-1800. doi:10.1212/WNL.58.12.1791

20. Serrano-Pozo A, Frosch MP, Masliah E, Hyman BT. Neuropathological alterations in Alzheimer disease. *Cold Spring Harb Perspect Med*. 2011;1(1):1-23. doi:10.1101/cshperspect.a006189

21. Woodhouse A, West AK, Chuckowree JA, Vickers JC, Dickson TC. Does β-amyloid plaque formation cause structural injury to neuronal processes? *Neurotox Res*. 2005;7(1-2):5-15. doi:10.1007/BF03033772

22. Le R, Cruz L, Urbanc B, et al. Plaque-induced abnormalities in neurite geometry in transgenic models of Alzheimer disease: Implications for neural system disruption. *J Neuropathol Exp Neurol*. 2001;60(8):753-758. doi:10.1093/jnen/60.8.753

23. Spires TL, Meyer-Luehmann M, Stern EA, et al. Dendritic spine abnormalities in amyloid precursor protein transgenic mice demonstrated by gene transfer and intravital multiphoton microscopy. *J Neurosci*. 2005;25(31):7278-7287. doi:10.1523/JNEUROSCI.1879-05.2005

24. Stern EA, Bacskai BJ, Hickey GA, Attenello FJ, Lombardo JA, Hyman BT. Cortical synaptic integration in vivo is disrupted by amyloid-β plaques. *J Neurosci*. 2004;24(19):4535-4540. doi:10.1523/JNEUROSCI.0462-04.2004

25. McLellan ME, Kajdasz ST, Hyman BT, Bacskai BJ. In vivo imaging of reactive oxygen species specifically associated with thioflavine S-positive amyloid plaques by multiphoton microscopy. *J Neurosci*. 2003;23(6):2212-2217. doi:10.1523/jneurosci.23-06-02212.2003

26. Serrano-Pozo A, Mielke ML, Gómez-Isla T, et al. Reactive glia not only associates with plaques but also parallels tangles in Alzheimer's disease. *Am J Pathol*. 2011;179(3):1373-1384. doi:10.1016/j.ajpath.2011.05.047

27. Goure WF, Krafft GA, Jerecic J, Hefti F. Targeting the proper amyloid-beta neuronal toxins: A path forward for Alzheimer's disease immunotherapeutics. *Alzheimer's Res Ther*. 2014;6(4):1-15. doi:10.1186/alzrt272

28. Sakono M, Zako T. Amyloid oligomers: Formation and toxicity of Aβ oligomers. *FEBS J*. 2010;277(6):1348-1358. doi:10.1111/j.1742-4658.2010.07568.x

29. Benilova I, Karran E, De Strooper B. The toxic Aβ oligomer and Alzheimer's disease: An emperor in need of clothes. *Nat Neurosci*. 2012;15(3):349-357. doi:10.1038/nn.3028

30. Klyubin I, Cullen WK, Hu NW, Rowan MJ. Alzheimers disease Aβ assemblies mediating rapid disruption of synaptic plasticity and memory. *Mol Brain*. 2012;5(1):1. doi:10.1186/1756-6606-5-25

31. Shankar GM, Li S, Mehta TH, et al. Amyloid-β protein dimers isolated directly from Alzheimer's

brains impair synaptic plasticity and memory. *Nat Med*. 2008;14(8):837-842. doi:10.1038/nm1782

32. Cleary JP, Walsh DM, Hofmeister JJ, et al. Natural oligomers of the amyloid-β protein specifically disrupt cognitive function. *Nat Neurosci*. 2005;8(1):79-84. doi:10.1038/nn1372

33. Reed MN, Hofmeister JJ, Jungbauer L, et al. Cognitive effects of cell-derived and synthetically derived Aβ oligomers. *Neurobiol Aging*. 2011;32(10):1784-1794. doi:10.1016/j.neurobiolaging.2009.11.007

34. Poling A, Morgan-Paisley K, Panos JJ, et al. Oligomers of the amyloid-β protein disrupt working memory: Confirmation with two behavioral procedures. *Behav Brain Res*. 2008;193(2):230-234. doi:10.1016/j.bbr.2008.06.001

35. Mucke L, Masliah E, Yu G, Mallory M, Rockenstein E. High-Level Neuronal Expression of Aβ1–42 in Wild-Type.Synaptotoxicity without Plaque Formation.pdf. *J Neurosci*. 2000;20(11):4050-4058. doi:10.1523/JNEUROSCI.20-11-04050.2000.

36. Wright AL, Zinn R, Hohensinn B, et al. Neuroinflammation and Neuronal Loss Precede Aβ Plaque Deposition in the hAPP-J20 Mouse Model of Alzheimer's Disease. *PLoS One*. 2013;8(4). doi:10.1371/journal.pone.0059586

37. Cheng IH, Scearce-Levie K, Legleiter J, et al. Accelerating amyloid-β fibrillization reduces oligomer levels and functional deficits in Alzheimer disease mouse models. *J Biol Chem*. 2007;282(33):23818-23828. doi:10.1074/jbc.M701078200

38. Hong S, Beja-Glasser VF, Nfonoyim BM, et al. Complement and microglia mediate early synapse loss in Alzheimer mouse models. *Science (80-)*. 2016;352(6286):712-716. doi:10.1126/science.aad8373.

39. Saganich MJ, Schroeder BE, Galvan V, Bredesen DE, Koo EH, Heinemann SF. Deficits in synaptic transmission and learning in amyloid precursor protein (APP) transgenic mice require C-terminal cleavage of APP. *J Neurosci*. 2006;26(52):13428-13436. doi:10.1523/JNEUROSCI.4180-06.2006

40. Green C, Sydow A, Vogel S, et al. Functional networks are impaired by elevated tau-protein but reversible in a regulatable Alzheimer's disease mouse model. *Mol Neurodegener*. 2019;14(1):1-13. doi:10.1186/s13024-019-0316-6

41. Liao K, Guo M, Niu F, Yang L, Callen SE, Buch S. Cocaine-mediated induction of microglial activation involves the ER stress-TLR2 axis. *J Neuroinflammation*. 2016;13(1):1-16. doi:10.1186/s12974-016-0501-2

42. Hooper C, Killick R, Lovestone S. The GSK3 hypothesis of Alzheimer's disease. *J Neurochem*. 2008;104(6):1433-1439. doi:10.1111/j.1471-4159.2007.05194.x

43. Takashima A. GSK-3 is essential in the pathogenesis of Alzheimer's disease. *J Alzheimer's Dis*. 2006;9(SUPPL. 3):309-317. doi:10.3233/jad-2006-9s335

44. Arnold SE, Hyman BT, Flory J, Damasio AR, Van Hoesen GW. The topographical and neuroanatomical distribution of neurofibrillary tangles and neuritic plaques in the cerebral cortex of patients with alzheimer's disease. *Cereb Cortex*. 1991;1(1):103-116. doi:10.1093/cercor/1.1.103

45. Braak H, Alafuzoff I, Arzberger T, Kretzschmar H, Tredici K. Staging of Alzheimer disease-associated neurofibrillary pathology using paraffin sections and immunocytochemistry. *Acta*

Neuropathol. 2006;112(4):389-404. doi:10.1007/s00401-006-0127-z

46. Goodwin LO, Splinter E, Davis TL, et al. Large-scale discovery of mouse transgenic integration sites reveals frequent structural variation and insertional mutagenesis. *Genome Res*. 2019;29(3):494-505. doi:10.1101/gr.233866.117

47. Yoshiyama Y, Higuchi M, Zhang B, et al. Synapse Loss and Microglial Activation Precede Tangles in a P301S Tauopathy Mouse Model. *Neuron*. 2007;53(3):337-351. doi:10.1016/j.neuron.2007.01.010

48. Takeuchi H, Iba M, Inoue H, et al. P301S mutant human tau transgenic mice manifest early symptoms of human tauopathies with dementia and altered sensorimotor gating. *PLoS One*. 2011;6(6). doi:10.1371/journal.pone.0021050

49. Anderson RM, Hadjichrysanthou C, Evans S, Wong MM. Why do so many clinical trials of therapies for Alzheimer's disease fail? *Lancet*. 2017;390(10110):2327-2329. doi:10.1016/S0140-6736(17)32399-1

50. Lyketsos CG, Carrillo MC, Ryan JM, et al. Neuropsychiatric symptoms in Alzheimer's disease. *Alzheimer's Dement*. 2011;7(5):532-539. doi:10.1016/j.jalz.2011.05.2410

51. Zhao QF, Tan L, Wang HF, et al. The prevalence of neuropsychiatric symptoms in Alzheimer's disease: Systematic review and meta-analysis. *J Affect Disord*. 2016;190:264-271. doi:10.1016/j.jad.2015.09.069

52. Binetti G, Mega MS, Magni E, et al. Behavioral Disorders in Alzheimer Disease: A Transcultural Perspective. *Arch Neurol.* 1998;55(4):539–544. doi:10.1001/archneur.55.4.539

53. Jost BC, Grossberg GT. The evolution of psychiatric symptoms in Alzheimer's disease: A natural history study. *J Am Geriatr Soc*. 1996;44(9):1078-1081. doi:10.1111/j.1532-5415.1996.tb02942.x

54. Lyketsos CG, Lopez O, Jones B, Fitzpatrick AL, Breitner J, Dekosky S. Prevalence of Neuropsychiatric Symptoms in Dementia and Mild Cognitive Impairement. *Jama*. 2002;288(12):1475-1483. doi:10.1001/jama.288.12.1475

55. Porter VR, Buxton WG, Fairbanks LA, et al. Frequency and characteristics of anxiety among patients with Alzheimer's disease and related dementias. *J Neuropsychiatry Clin Neurosci*. 2003;15(2):180-186. doi:10.1176/jnp.15.2.180

56. Ferretti L, McCurry SM, Logsdon R, Gibbons L, Teri L. Anxiety and Alzheimer's Disease. *Journal of Geriatric Psychiatry and Neurology*. 2001;14(1):52-58. doi:10.1177/089198870101400111

57. Teri L, Ferretti LE, Gibbons LE, et al. Anxiety in alzheimer's disease: prevalence and comorbidity. *Journals Gerontol - Ser A Biol Sci Med Sci*. 1999;54(7):348-352. doi:10.1093/gerona/54.7.M348

58. Ringman JM, Liang LJ, Zhou Y, et al. Early behavioural changes in familial Alzheimer's disease in the Dominantly Inherited Alzheimer Network. *Brain*. 2015;138(4):1036-1045. doi:10.1093/brain/awv004

59. Ringman JM, Gylys KH, Medina LD, et al. Biochemical, neuropathological, and neuroimaging characteristics of early-onset Alzheimer's disease due to a novel PSEN1 mutation. *Neurosci Lett*. 2011;487(3):287-292. doi:10.1016/j.neulet.2010.10.039

60. Kwak YT, Yang Y, Koo M-S. Anxiety in Dementia. *Dement Neurocognitive Disord*. 2017;16(2):33. doi:10.12779/dnd.2017.16.2.33

61. Chemerinski E, Petracca G, Manes F, Leiguarda R, Starkstein SE. Prevalence and correlates of anxiety in Alzheimer's disease. *Depress Anxiety*. 1998;7(4):166-170. doi:10.1002/(SICI)1520-6394(1998)7:4<166::AID-DA4>3.0.CO;2-8

62. Visser PJ, Verhey F, Knol DL, et al. Prevalence and prognostic value of CSF markers of Alzheimer's disease pathology in patients with subjective cognitive impairment or mild cognitive impairment in the DESCRIPA study: a prospective cohort study. *Lancet Neurol*. 2009;8(7):619-627. doi:10.1016/S1474-4422(09)70139-5

63. Hashimoto H, Monserratt L, Nguyen P, et al. Anxiety and regional cortical glucose metabolism in patients with Alzheimer's disease. *J Neuropsychiatry Clin Neurosci*. 2006;18(4):521-528. doi:10.1176/jnp.2006.18.4.521

64. Sultzer DL, Mahler ME, Mandelkern MA, et al. The relationship between psychiatric symptoms and regional cortical metabolism in Alzheimer's disease. *J Neuropsychiatry Clin Neurosci*. 1995;7(4):476-484. doi:10.1176/jnp.7.4.476

65. Salat DH, Kaye JA, Janowsky JS. Selective preservation and degeneration within the prefrontal cortex in aging and Alzheimer disease. *Arch Neurol*. 2001;58(9):1403-1408. doi:10.1001/archneur.58.9.1403

66. Vertes RP. Differential Projections of the Infralimbic and Prelimbic Cortex in the Rat. *Synapse*. 2004;51(1):32-58. doi:10.1002/syn.10279

67. Lindberg O, Westman E, Karlsson S, et al. Is the subcallosal medial prefrontal cortex a common site of atrophy in Alzheimer's disease and frontotemporal lobar degeneration? *Front Aging Neurosci*. 2012;4(OCT):1-8. doi:10.3389/fnagi.2012.00032

68. Roozendaal B, McEwen BS, Chattarji S. Stress, memory and the amygdala. *Nat Rev Neurosci*. 2009;10(6):423-433. doi:10.1038/nrn2651

69. Vogt LJK, Hyman BT, Van Hoesen GW, Damasio AR. Pathological alterations in the amygdala in Alzheimer's disease. *Neuroscience*. 1990;37(2):377-385. doi:10.1016/0306-4522(90)90408-V

70. Tye KM, Prakash R, Kim SY, et al. Amygdala circuitry mediating reversible and bidirectional control of anxiety. *Nature*. 2011;471(7338):358-362. doi:10.1038/nature09820

71. Cuenod C-A, Denys A, Michot J-L, et al. Amygdala Atrophy in Alzheimer's Disease. *Arch Neurol*. 1993;50(9):941-945. doi:10.1001/archneur.1993.00540090046009

72. Jimenez JC, Su K, Goldberg AR, et al. Anxiety Cells in a Hippocampal-Hypothalamic Circuit. *Neuron*. 2018;97(3):670-683.e6. doi:10.1016/j.neuron.2018.01.016

73. Bannerman DM, Deacon RMJ, Offen S, Friswell J, Grubb M, Rawlins JNP. Double dissociation of function within the hippocampus: Spatial memory and hyponeophagia. *Behav Neurosci*. 2002;116(5):884-901. doi:10.1037/0735-7044.116.5.884

74. West MJ, Coleman PD, Flood DG, Troncoso JC. Differences in the pattern of hippocampal neuronal loss in normal ageing and Alzheimer's disease. *Lancet*. 1994;344(8925):769-772. doi:10.1016/s0140-6736(94)92338-8

75. Braak H, Braak E. Neuropathological stageing of Alzheimer-related changes. *Acta Neuropathol*.

1991;82:239-259. doi:10.1109/ICINIS.2015.10

76. Walf AA, Frye CA. The use of the elevated plus maze as an assay of anxiety-related behaviour in rodents. *Nat Protoc*. 2007;2(2):322-328. doi:10.1038/nprot.2007.44.The

77. Pellow S, Chopin P, File SE, Briley M. Validation of open : closed arm entries in an elevated plus-maze as a measure of anxiety in the rat. *J Neurosci Methods*. 1985;14(3):149-167. doi:10.1016/0165-0270(85)90031-7

78. Seibenhener ML, Wooten MC. Use of the open field maze to measure locomotor and anxiety-like behavior in mice. *J Vis Exp*. 2015;(96):1-6. doi:10.3791/52434

79. Harris JA, Devidze N, Halabisky B, et al. Many neuronal and behavioral impairments in transgenic mouse models of Alzheimer's disease are independent of caspase cleavage of the amyloid precursor protein. *J Neurosci*. 2010;30(1):372-381. doi:10.1523/JNEUROSCI.5341-09.2010

80. Webster SJ, Bachstetter AD, Nelson PT, Schmitt FA, Van Eldik LJ. Using mice to model Alzheimer's dementia: An overview of the clinical disease and the preclinical behavioral changes in 10 mouse models. *Front Genet*. 2014;5(APR):1-23. doi:10.3389/fgene.2014.00088

81. Scattoni ML, Gasparini L, Alleva E, Goedert M, Calamandrei G, Spillantini MG. Early behavioural markers of disease in P301S tau transgenic mice. *Behav Brain Res*. 2010;208(1):250-257. doi:10.1016/j.bbr.2009.12.002

82. Tonks NK. Protein tyrosine phosphatases - From housekeeping enzymes to master regulators of signal transduction. *FEBS J*. 2013;280(2):346-378. doi:10.1111/febs.12077

83. Krishnan N, Fu C, Pappin DJ, Tonks NK. Biochemistry: H 2S-induced sulfhydration of the phosphatase PTP1B and its role in the endoplasmic reticulum stress response. *Sci Signal*. 2011;4(203). doi:10.1126/scisignal.2002329

84. Frangioni J V., Beahm PH, Shifrin V, Jost CA, Neel BG. The nontransmembrane tyrosine phosphatase PTP-1B localizes to the endoplasmic reticulum via its 35 amino acid C-terminal sequence. *Cell*. 1992;68(3):545-560. doi:10.1016/0092-8674(92)90190-N

85. Feldhammer M, Uetani N, Miranda-Saavedra D, Tremblay ML. Ptp1b: A simple enzyme for a complex world. *Crit Rev Biochem Mol Biol*. 2013;48(5):430-445. doi:10.3109/10409238.2013.819830

86. Krishnan N, Bonham CA, Rus IA, et al. Harnessing insulin-and leptin-induced oxidation of PTP1B for therapeutic development. *Nat Commun*. 2018;9(1). doi:10.1038/s41467-017-02252-2

87. Elchebly M, Payette P, Michaliszyn E, et al. Increased insulin sensitivity and obesity resistance in mice lacking the protein tyrosine phosphatase-1B gene. *Science (80-)*. 1999;283(5407):1544-1548. doi:10.1126/science.283.5407.1544

88. Cheng A, Uetani N, Simoncic PD, et al. Attenuation of leptin action and regulation of obesity by protein tyrosine phosphatase 1B. *Dev Cell*. 2002;2(4):497-503. doi:10.1016/S1534-5807(02)00149-1

89. Zabolotny JM, Bence-Hanulec KK, Stricker-Krongrad A, et al. PTP1B regulates leptin signal transduction in vivo. *Dev Cell*. 2002;2(4):489-495. doi:10.1016/S1534-5807(02)00148-X

90. Pandey NR, Zhou X, Qin Z, et al. The LIM domain only 4 protein is a metabolic responsive

inhibitor of protein tyrosine phosphatase 1B that controls hypothalamic leptin signaling. *J Neurosci*. 2013;33(31):12647-12655. doi:10.1523/JNEUROSCI.0746-13.2013

91. Pandey NR, Zhou X, Zaman T, et al. LMO4 is required to maintain hypothalamic insulin signaling. *Biochem Biophys Res Commun*. 2014;450(1):666-672. doi:10.1016/j.bbrc.2014.06.026

92. Bedse G, Di Domenico F, Serviddio G, Cassano T. Aberrant insulin signaling in Alzheimer's disease: Current knowledge. *Front Neurosci*. 2015;9(MAY):1-13. doi:10.3389/fnins.2015.00204

93. Bonda DJ, Stone JG, Torres SL, et al. Dysregulation of Leptin Signaling in Alzheimer Disease: Evidence for Neuronal Leptin Resistance. 2015;128(1):1-19. doi:10.1111/jnc.12380.Dysregulation

94. Bomfim TR, Forny-Germano L, Sathler LB, et al. An anti-diabetes agent protects the mouse brain from defective insulin signaling caused by Alzheimer's disease- associated Aβ oligomers. *J Clin Invest*. 2012;122(4):1339-1353. doi:10.1172/JCI57256

95. Bonda DJ, Stone JG, Torres SL, et al. Dysregulation of leptin signaling in Alzheimer disease: Evidence for neuronal leptin resistance. *J Neurochem*. 2014;128(1):162-172. doi:10.1111/jnc.12380

96. Steen E, Terry BM, Rivera EJ, et al. Impaired insulin and insulin-like growth factor expression and signaling mechanisms in Alzheimer's disease - Is this type 3 diabetes? *J Alzheimer's Dis*. 2005;7(1):63-80. doi:10.3233/JAD-2005-7107

97. De La Monte SM. Insulin resistance in Alzheimer's disease. *Transl Res*. 2017;183(8):26-40. doi:10.1016/j.trsl.2016.12.005

98. Fuentes F, Zimmer D, Atienza M, et al. Protein tyrosine phosphatase PTP1B is involved in hippocampal synapse formation and learning. *PLoS One*. 2012;7(7). doi:10.1371/journal.pone.0041536

99. Zhang L, Qin Z, Sharmin F, et al. Tyrosine phosphatase PTP1B impairs presynaptic NMDA receptor-mediated plasticity in a mouse model of Alzheimer's disease. *Neurobiol Dis*. 2021;156:105402. doi:10.1016/j.nbd.2021.105402

100. Ricke KM, Cruz SA, Qin Z, et al. Neuronal Protein Tyrosine Phosphatase 1B Hastens Amyloid β-Associated Alzheimer's Disease in Mice. *J Neurosci*. 2020;40(7):1581-1593. doi:10.1523/JNEUROSCI.2120-19.2019

101. Gum RJ, Gaede LL, Koterski SL, et al. Reduction of protein tyrosine phosphatase 1B increases insulin-dependent signaling in ob/ob mice. *Diabetes*. 2003;52(1):21-28. doi:10.2337/diabetes.52.1.21

102. Kanno T, Tsuchiya A, Tanaka A, Nishizaki T. Combination of PKCε Activation and PTP1B Inhibition Effectively Suppresses Aβ-Induced GSK-3β Activation and Tau Phosphorylation. *Mol Neurobiol*. 2016;53(7):4787-4797. doi:10.1007/s12035-015-9405-x

103. Qin Z, Zhou X, Pandey NR, et al. Chronic Stress Induces Anxiety via an Amygdalar Intracellular Cascade that Impairs Endocannabinoid Signaling. *Neuron*. 2015;85(6):1319-1331. doi:10.1016/j.neuron.2015.02.015

104. Mendes NF, Castro G, Guadagnini D, et al. Knocking down amygdalar PTP1B in diet-induced obese rats improves insulin signaling/action, decreases adiposity and may alter anxiety behavior. *Metabolism*. 2017;70:1-11. doi:10.1016/j.metabol.2017.01.029

105. Scheltens P, De Strooper B, Kivipelto M, et al. Alzheimer's disease. *Lancet*. 2021;397(10284):1577-1590. doi:10.1016/S0140-6736(20)32205-4

106. van Dyck CH. Anti-Amyloid-β Monoclonal Antibodies for Alzheimer's Disease: Pitfalls and Promise. *Biol Psychiatry*. 2017;83(4):311-319. doi:10.1016/j.biopsych.2017.08.010

107. Wang X, Sun G, Feng T, et al. Sodium oligomannate therapeutically remodels gut microbiota and suppresses gut bacterial amino acids-shaped neuroinflammation to inhibit Alzheimer's disease progression. *Cell Res*. 2019;29(10):787-803. doi:10.1038/s41422-019-0216-x

108. Ngandu T, Lehtisalo J, Solomon A, et al. A 2 year multidomain intervention of diet, exercise, cognitive training, and vascular risk monitoring versus control to prevent cognitive decline in at-risk elderly people (FINGER): A randomised controlled trial. *Lancet*. 2015;385(9984):2255-2263. doi:10.1016/S0140-6736(15)60461-5

109. Solomon A, Turunen H, Ngandu T, et al. Effect of the apolipoprotein e genotype on cognitive change during a multidomain lifestyle intervention a subgroup analysis of a randomized clinical trial. *JAMA Neurol*. 2018;75(4):462-470. doi:10.1001/jamaneurol.2017.4365

110. Imfeld P, Bodmer M, Jick SS, Meier CR. Benzodiazepine Use and Risk of Developing Alzheimer's Disease or Vascular Dementia: A Case–Control Analysis. *Drug Saf*. 2015;38(10):909-919. doi:10.1007/s40264-015-0319-3

111. Buffett-Jerrott S, Stewart S. Cognitive and Sedative Effects of Benzodiazepine Use. *Curr Pharm Des*. 2005;8(1):45-58. doi:10.2174/1381612023396654

112. Chen PL, Lee WJ, Sun WZ, Oyang YJ, Fuh JL. Risk of Dementia in Patients with Insomnia and Long-term Use of Hypnotics: A Population-based Retrospective Cohort Study. *PLoS One*. 2012;7(11). doi:10.1371/journal.pone.0049113

113. Wu CS, Wang SC, Chang IS, Lin KM. The association between dementia and long-term use of benzodiazepine in the elderly: Nested case-control study using claims data. *Am J Geriatr Psychiatry*. 2009;17(7):614-620. doi:10.1097/JGP.0b013e3181a65210

114. Feldman H, Gauthier S, Hecker J, Vellas B, Subbiah P, Whalen E. A 24-week, randomized, double-blind study of donepezil in moderate to severe Alzheimer's disease. *Neurology*. 2001;57(4):613-620. doi:10.1212/WNL.57.4.613

115. Mintzer J, Faison W, Street JS, Sutton VK, Breier A. Olanzapine in the treatment of anxiety symptoms due to Alzheimer's disease: A post hoc analysis. *Int J Geriatr Psychiatry*. 2001;16(SUPPL. 1). doi:10.1002/1099-1166(200112)16:1+<::aid-gps568>3.0.co;2-m

116. Lantz KA, Hart SGE, Planey SL, et al. Inhibition of PTP1B by trodusquemine (MSI-1436) causes fat-specific weight loss in diet-induced obese mice. *Obesity*. 2010;18(8):1516-1523. doi:10.1038/oby.2009.444

117. Zhang L, Qin Z, Ricke KM, Cruz SA, Stewart AFR, Chen HH. Hyperactivated PTP1B phosphatase in parvalbumin neurons alters anterior cingulate inhibitory circuits and induces autism-like behaviors. *Nat Commun*. 2020;11(1):1-15. doi:10.1038/s41467-020-14813-z

118. Rao MN, Shinnar AE, Noecker LA, et al. Aminosterols from the dogfish shark Squalus acanthias. *J Nat Prod*. 2000;63(5):631-635. doi:10.1021/np990514f

119. Zasloff M, Williams JI, Chen Q, et al. A spermine-coupled cholesterol metabolite from the shark

with potent appetite suppressant and antidiabetic properties. *Int J Obes*. 2001;25(5):689-697. doi:10.1038/sj.ijo.0801599

120. Ahima RS, Patel HR, Takahashi N, Qi Y, Hileman SM, Zasloff MA. Appetite Suppression and Weight Reduction by a Centrally Active Aminosterol. *Diabetes*. 2002;51(7):2099-2104. doi:10.2337/diabetes.51.7.2099

121. Roitman MF, Wescott S, Cone JJ, McLane MP, Wolfe HR. MSI-1436 reduces acute food intake without affecting dopamine transporter activity. *Pharmacol Biochem Behav*. 2010;97(1):138-143. doi:10.1016/j.pbb.2010.05.010

122. Nguyen LK, Matallanas D, Croucher DR, Von Kriegsheim A, Kholodenko BN. Signalling by protein phosphatases and drug development: A systems-centred view. *FEBS J*. 2013;280(2):751-765. doi:10.1111/j.1742-4658.2012.08522.x

123. Casanova E, Fehsenfeld S, Mantamadiotis T, et al. A CamKIIα iCre BAC allows brain-specific gene inactivation. *Genesis*. 2001;31(1):37-42. doi:10.1002/gene.1078

124. Malia TJ, Teplyakov A, Ernst R, et al. Epitope mapping and structural basis for the recognition of phosphorylated tau by the anti-tau antibody AT8. *Proteins Struct Funct Bioinforma*. 2016;84(4):427-434. doi:10.1002/prot.24988

125. Nunes-de-Souza RL, Canto-de-Souza A, Rodgers RJ. Effects of intra-hippocampal infusion of WAY-100635 on plus-maze behavior in mice: Influence of site of injection and prior test experience. *Brain Res*. 2002;927(1):87-96. doi:10.1016/S0006-8993(01)03335-2

126. Macrì S, Adriani W, Chiarotti F, Laviola G. Risk taking during exploration of a plus-maze is greater in adolescent than in juvenile or adult mice. *Anim Behav*. 2002;64(4):541-546. doi:10.1006/anbe.2002.4004

127. Chung JA, Cummings JL. Neurobehavioral and neuropsychiatric symptoms in Alzheimer's disease: Characteristics and treatment. *Neurol Clin*. 2000;18(4):829-846. doi:10.1016/S0733-8619(05)70228-0

128. Palmer K, Berger AK, Monastero R, Winblad B, Bäckman L, Fratiglioni L. Predictors of progression from mild cognitive impairment to Alzheimer disease. *Neurology*. 2007;68(19):1596-1602. doi:10.1212/01.wnl.0000260968.92345.3f

129. Limbocker R, Chia S, Ruggeri FS, et al. Trodusquemine enhances Aβ 42 aggregation but suppresses its toxicity by displacing oligomers from cell membranes. *Nat Commun*. 2019;10(1):1-13. doi:10.1038/s41467-018-07699-5

130. Vitiello MV, Bliwise DL, Prinz PN. Sleep in Alzheimer's disease and the sundown syndrome. *Neurology*. 1992;42(7 Suppl 6):83-94.

131. Cheng D, Logge W, Low JK, Garner B, Karl T. Novel behavioural characteristics of the APPSwe/PS1ΔE9 transgenic mouse model of Alzheimer's disease. *Behav Brain Res*. 2013;245:120-127. doi:10.1016/j.bbr.2013.02.008

132. Lutz B, Marsicano G, Maldonado R, Hillard CJ. The endocannabinoid system in guarding against fear, anxiety and stress. *Nat Rev Neurosci*. 2015;16(12):705-718. doi:10.1038/nrn4036

133. Zou S, Kumar U. Cannabinoid receptors and the endocannabinoid system: Signaling and function in the central nervous system. *Int J Mol Sci*. 2018;19(3). doi:10.3390/ijms19030833

134. Castillo PE, Younts TJ, Chávez AE, Hashimotodani Y. Endocannabinoid Signaling and Synaptic Function. *Neuron*. 2012;76(1):70-81. doi:10.1016/j.neuron.2012.09.020

135. Jenniches I, Ternes S, Albayram O, et al. Anxiety, Stress, and Fear Response in Mice with Reduced Endocannabinoid Levels. *Biol Psychiatry*. 2016;79(10):858-868. doi:10.1016/j.biopsych.2015.03.033

136. Shonesy BC, Bluett RJ, Ramikie TS, et al. Genetic Disruption of 2-Arachidonoylglycerol Synthesis Reveals a Key Role for Endocannabinoid Signaling in Anxiety Modulation. *Cell Rep*. 2014;9(5):1644-1653. doi:10.1016/j.celrep.2014.11.001

137. Guggenhuber S, Romo-Parra H, Bindila L, et al. Impaired 2-AG signaling in hippocampal glutamatergic neurons: Aggravation of anxiety-like behavior and unaltered seizure susceptibility. *Int J Neuropsychopharmacol*. 2016;19(2):1-13. doi:10.1093/ijnp/pyv091

138. Kopeikina KJ, Hyman BJ, Spires-Jones TL. Soluble forms of tau are toxic in alzheimer's disease. *Transl Neurosci*. 2012;3(3):223-233. doi:10.2478/s13380-012-0032-y

139. Coleman PD, Yao PJ. Synaptic slaughter in Alzheimer's disease. *Neurobiol Aging*. 2003;24(8):1023-1027. doi:10.1016/j.neurobiolaging.2003.09.001

140. Bezprozvanny I, Mattson MP. Neuronal calcium mishandling and the pathogenesis of Alzheimer's disease. *Trends Neurosci*. 2008;31(9):454-463. doi:10.1016/j.tins.2008.06.005

141. Furukawa K, Wang Y, Yao PJ, et al. Alteration in calcium channel properties is responsible for the neurotoxic action of a familial frontotemporal dementia tau mutation. *J Neurochem.* 2003;87(2):427-436. doi:10.1046/j.1471-4159.2003.02020.x

142. Eckermann K, Mocanu MM, Khlistunova I, et al. The β-propensity of tau determines aggregation and synaptic loss in inducible mouse models of tauopathy. *J Biol Chem*. 2007;282(43):31755-31765. doi:10.1074/jbc.M705282200

143. Mocanu MM, Nissen A, Eckermann K, et al. The potential for β-structure in the repeat domain of tau protein determines aggregation, synaptic decay, neuronal loss, and coassembly with endogenous Tau in inducible mouse models of tauopathy. *J Neurosci*. 2008;28(3):737-748. doi:10.1523/JNEUROSCI.2824-07.2008

144. Brunden KR, Trojanowski JQ, Lee VM. Evidence that non-fibrillar tau causes pathology linked to neurodegeneration and behavioral impairments. *J Alzheimers Dis*. 2008;14(4):393-399. doi:10.3233/jad-2008-14406

145. Li X, Kumar Y, Zempel H, Mandelkow EM, Biernat J, Mandelkow E. Novel diffusion barrier for axonal retention of Tau in neurons and its failure in neurodegeneration. *EMBO J*. 2011;30(23):4825-4837. doi:10.1038/emboj.2011.376

146. Beurel E, Grieco SF, Jope RS. Glycogen synthase kinase-3 (GSK3): regulation, actions, and diseases. *Pharmacol Ther*. 2015;0:114-131. doi:10.1016/j.pharmthera.2014.11.016. Glycogen

147. Yao HB, Shaw PC, Wong CC, Wan DCC. Expression of glycogen synthase kinase-3 isoforms in mouse tissues and their transcription in the brain. *J Chem Neuroanat*. 2002;23(4):291-297. doi:10.1016/S0891-0618(02)00014-5

8. Supplementary Figures

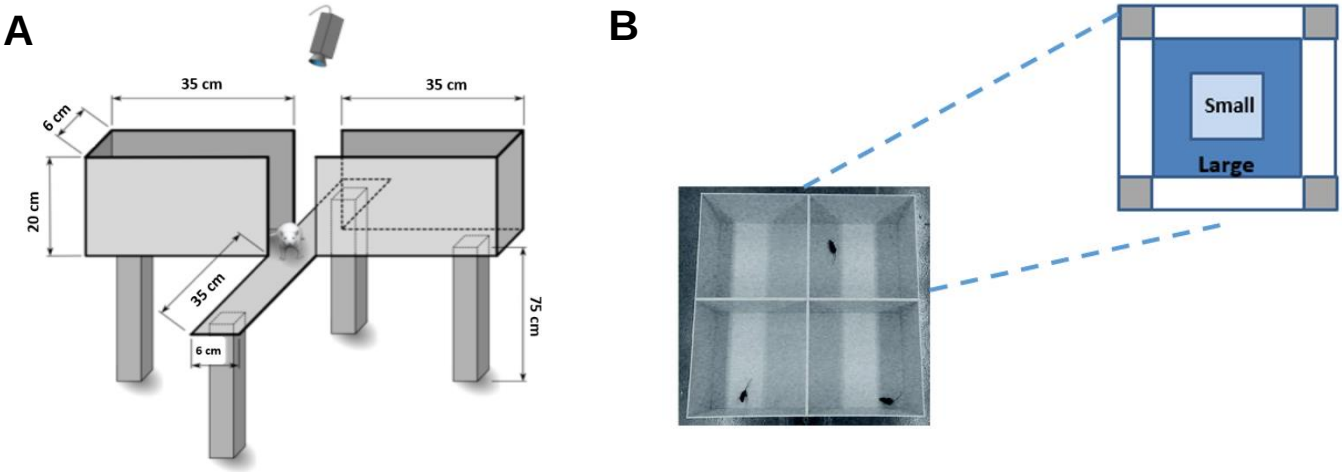

Supplementary Figure 1. Representative diagrams of elevated plus maze (EPM) and open field Test (OF). The EPM is a plus-shaped maze, elevated 75 cm from the ground, with two open arms (6 cm x 35cm) and two wall-enclosed arms (6cm x 35 cm x 20 cm). Prior to testing, mice were habituated in the experiment room for 45-60 minutes and monitored for 10 minutes during testing period (A). The OF test consists of a box-like arena without a roof, with dimensions of 50 cm (length) x 50 cm (width) x 38 cm (height). Prior to testing, mice were habituated in the experiment room for 45-60 minutes and monitored for 10 minutes during testing period (B).

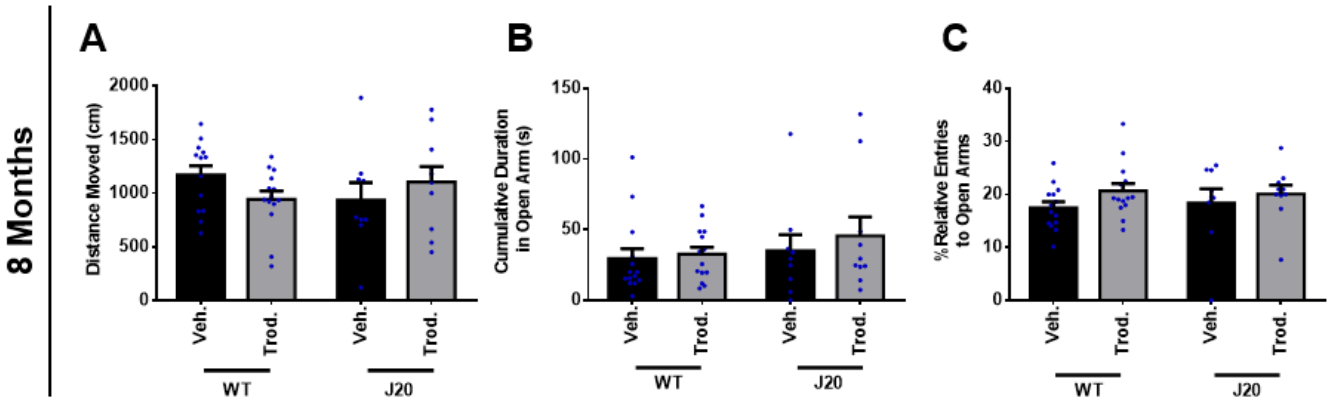

Supplementary Figure 2. No anxiety-related behavioural abnormalities of J20 mice at 8 months of age in EPM test, 5.0 mg/kg dosage of trodusquemine had no effect. No phenotype was detected in distance moved (A) or anxiety-related parameters when comparing all groups (B-C). Trodusquemine treatment had no significant effect. For A-C, n= 14, 14, 9, 10, respectively. Data depicts mean ± SEM. For each analysis, one-way ANOVA was followed by Bonferroni's post-hoc pairwise comparisons. *p-value ≤ 0.05; **p-value ≤ 0.01; ***p-value ≤ 0.001; ****p-value ≤ 0.0001.

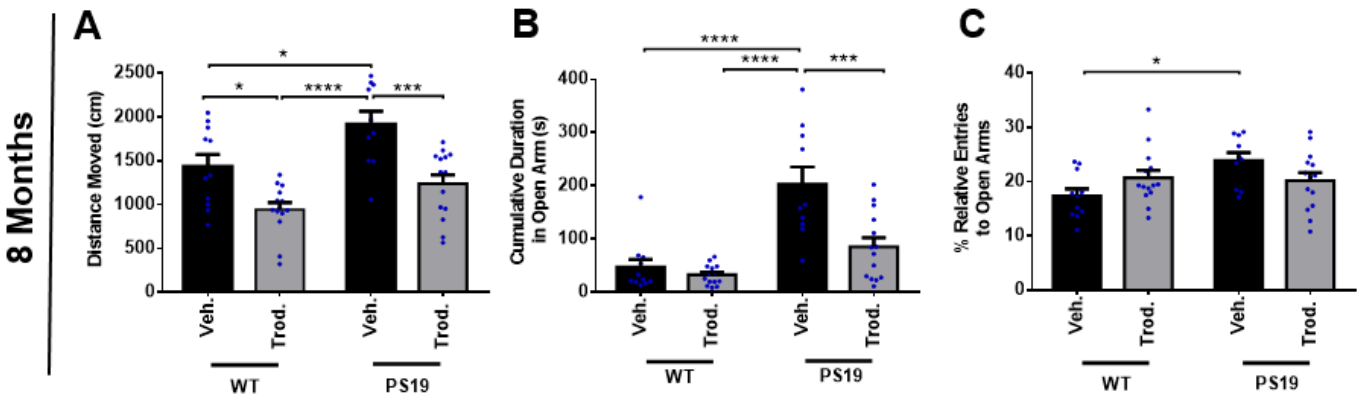

Supplementary Figure 3. Selective inhibition of PTP1B via 5.0 mg/kg dosage of trodusquemine ameliorated inappropriately lowered anxious response in PS19 mice at 8 months of age in EPM test. PS19 Veh. mice moved a greater total distance in the maze as compared to WT Veh. and WT trod.-treated mice, and this was ameliorated by trodusquemine treatment (A). Compared to WT-Veh. mice, WT trod. -treated mice moved a lower distance in the maze (A). PS19 Veh. mice expended more time in open arms of the maze compared to WT Veh. and WT Trod. counterparts, and this was rescued in the PS19 Trod. group (B). PS19 mice also entered the open arms of the EPM more than WT mice, but this was not rescued by trodusquemine treatment (C). For A-C, n= 11, 14, 10, 14, respectively. Data depicts mean ± SEM. For each analysis, one-way ANOVA was followed by Bonferroni's post-hoc pairwise comparisons. *p-value ≤ 0.05; **p-value ≤ 0.01; ***p-value ≤ 0.001; ****p-value ≤ 0.0001.

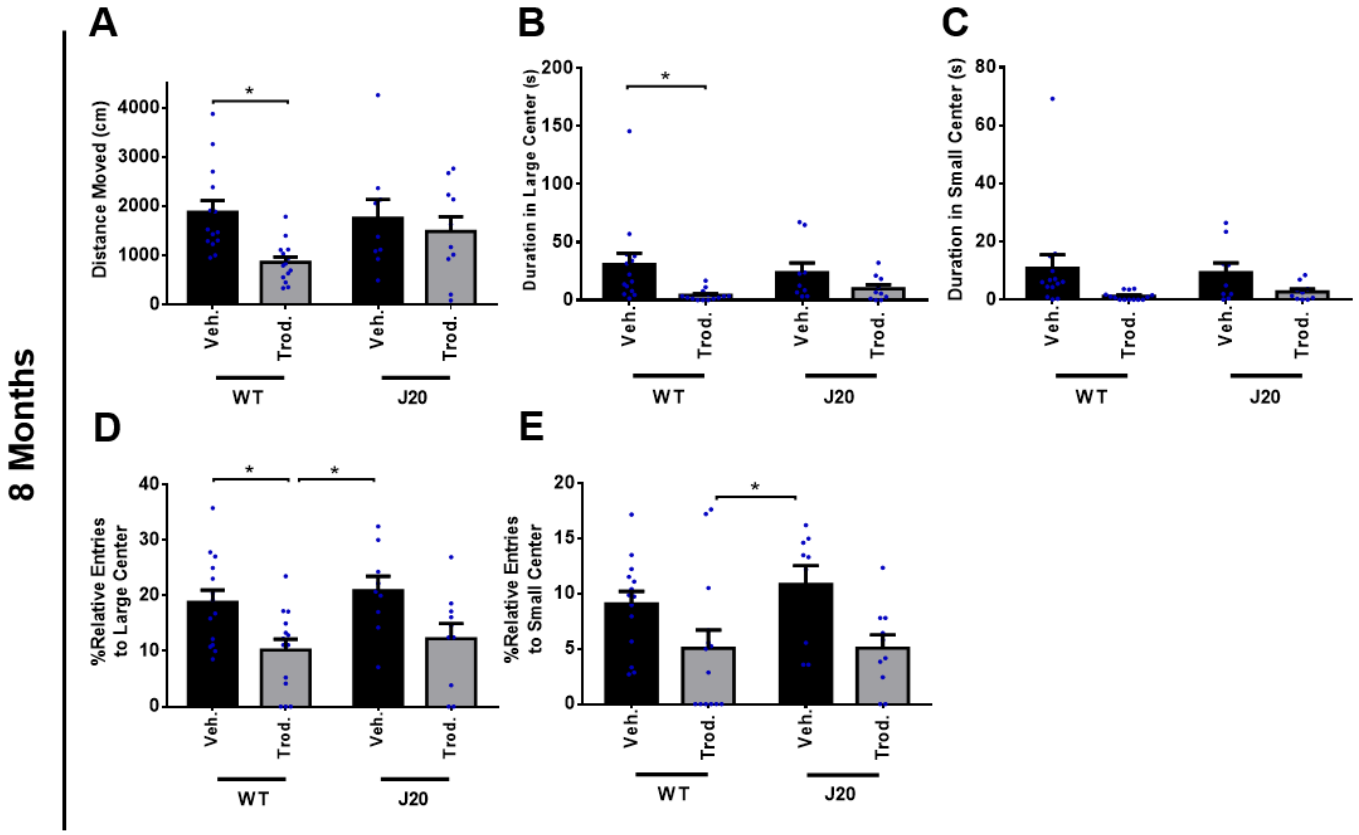

Supplementary Figure 4. No anxiety-related behavioural abnormalities in J20 mice at 8 months of age in OF test, 5.0 mg/kg dosage of trodusquemine had no effect. WT trod.-treated mice moved a lower total distance, spent less time in the large center, and entered the large center at a lower frequency than WT Veh. mice (A, B, D). No phenotype was detected in distance moved (A) or anxiety-related parameters when comparing WT Veh. and PS19 Veh. mice (B-E). Trodusquemine treatment had no significant effect. For A-E, n= 14, 14, 9, 10, respectively. Data depicts mean ± SEM. For each analysis, one-way ANOVA was followed by Bonferroni's post-hoc pairwise comparisons. *p-value ≤ 0.05; **p-value ≤ 0.01; ***p-value ≤ 0.001; ****p-value ≤ 0.0001.

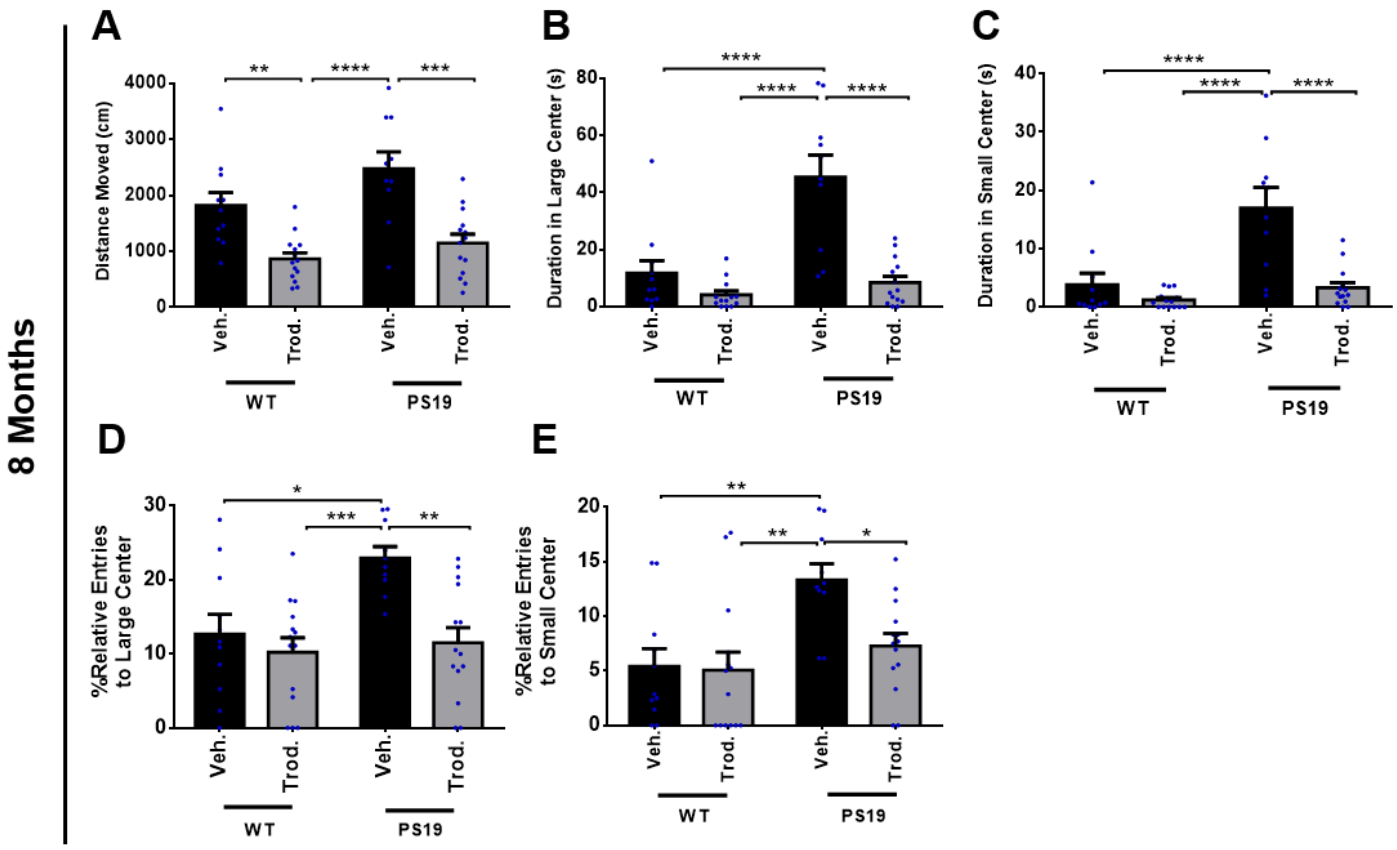

Supplementary Figure 5. Selective inhibition of PTP1B via 5.0 mg/kg dosage of trodusquemine ameliorated inappropriately lowered anxious response in PS19 mice at 8 months of age in OF test. No statistically significant phenotype in the distance moved in the arena was detected between WT Veh. and PS19 Veh., although WT trod.- treated mice moved a lower total distance than WT Veh. mice (A). PS19 mice spent more time in the large and small centers of the OF arena, and entered these central regions more than WT Veh. and WT trod. mice (B-E). This was rescued in the PS19 trod.- treated group (B-E). For A-E, n = 11, 14, 10, 14, respectively. Data depicts mean ± SEM. For each analysis, one-way ANOVA was followed by Bonferroni's post-hoc pairwise comparisons. *p-value ≤ 0.05; **p-value ≤ 0.01; ***p-value ≤ 0.001; ****p-value ≤ 0.0001.

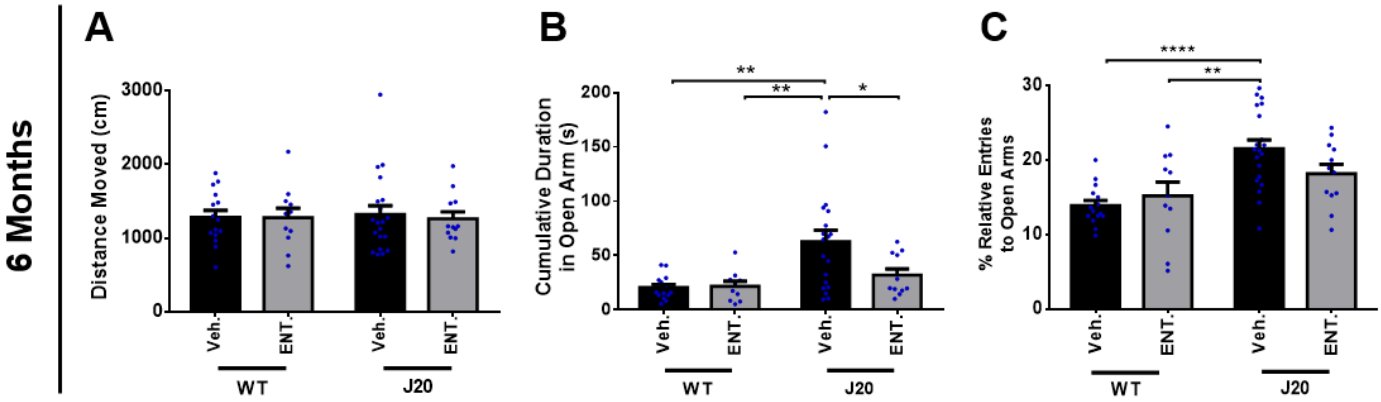

Supplementary Figure 6. Selective inhibition of PTP1B by 2.5 mg/kg dosage of ENT-03 ameliorated inappropriately lowered anxious response in J20 mice aged 6 months in EPM test. No phenotype was detected in the distance moved in the maze between groups (A). J20 mice expended more time in the open arms of the maze compared to WT Veh. and WT ENT03-treated mice, and this was normalized in the J20 ENT03-treated group (B). Similarly, J20 mice also entered the open arms more frequently than WT Veh. and WT ENT03-treated counterparts, although this was not sufficiently rescued in the J20 ENT03-treated group. For A and C, n= 15, 13, 20, 12, respectively. For B, n= 14, 10, 19, 11, respectively. 5 outlier values were removed from data in (B). Data depicts mean ± SEM. For each analysis, one-way ANOVA was followed by Tukey's post-hoc pairwise comparisons. *p-value ≤ 0.05; **p-value ≤ 0.01; ***p-value ≤ 0.001; ****p-value ≤ 0.0001.

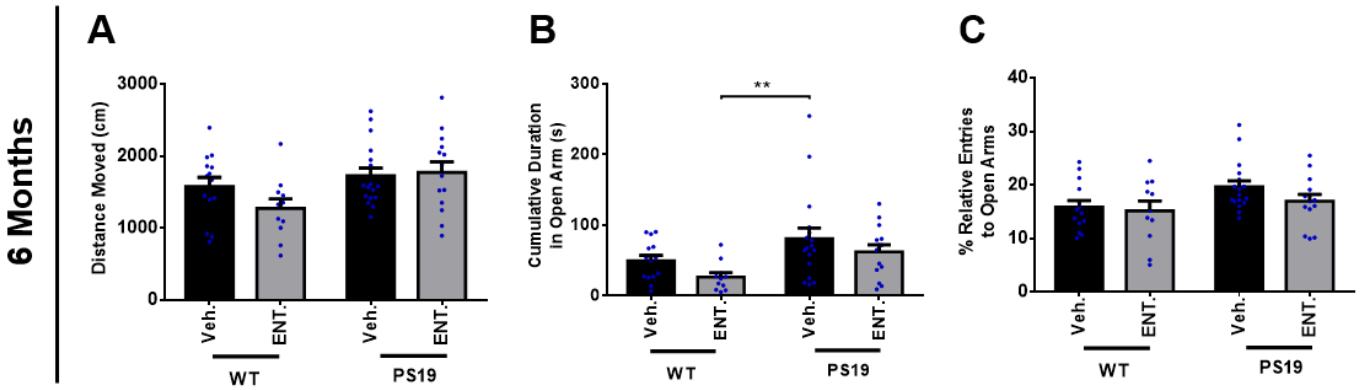

Supplementary Figure 7. No anxiety-related behavioural abnormalities in PS19 mice aged 6 months in EPM test, selective inhibition of PTP1B by 2.5 mg/kg dosage of ENT-03 did not have any effect. No phenotype was detected in distance moved (A) or anxiety-related parameters in the EPM between WT Veh. mice and PS19 Veh. mice, and administration of ENT-03 had no effect on any anxiety-related parameters of the EPM test (B, C). For A-C, n= 14, 13, 17, 14, respectively. Data depicts mean ± SEM. For each analysis, two-way ANOVA was followed by Tukey's post-hoc pairwise comparisons, *p-value < 0.05, mean values are reported, error bars represent SEM.

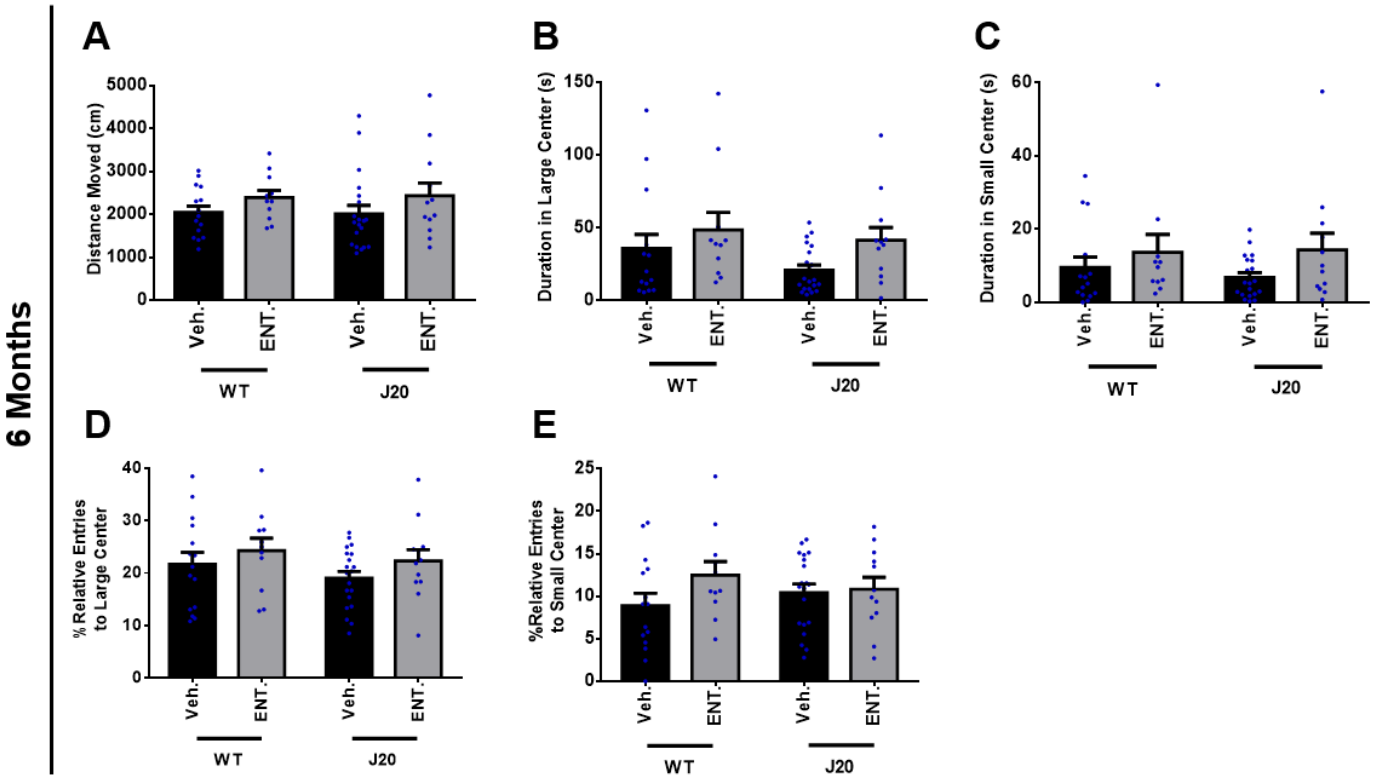

Supplementary Figure 8. No anxiety-related behavioural abnormalities in J20 mice at 6 months of age in OF test, selective inhibition of PTP1B by 2.5 mg/kg dosage of ENT-03 had no effect. No phenotype was detected in the distance moved or anxiety-related behaviour in OF between WT Veh.-treated mice and J20 Veh.- treated mice (A-E). Treatment with ENT-03 did not have significant effects on behaviour in any of the OF parameters assessed (A-E). For A-E, n= 15, 11, 20, 12, respectively. Data depicts mean ± SEM. For each analysis, two-way ANOVA was followed by Tukey's post-hoc pairwise comparisons, *p-value < 0.05, mean values are reported, error bars represent SEM.

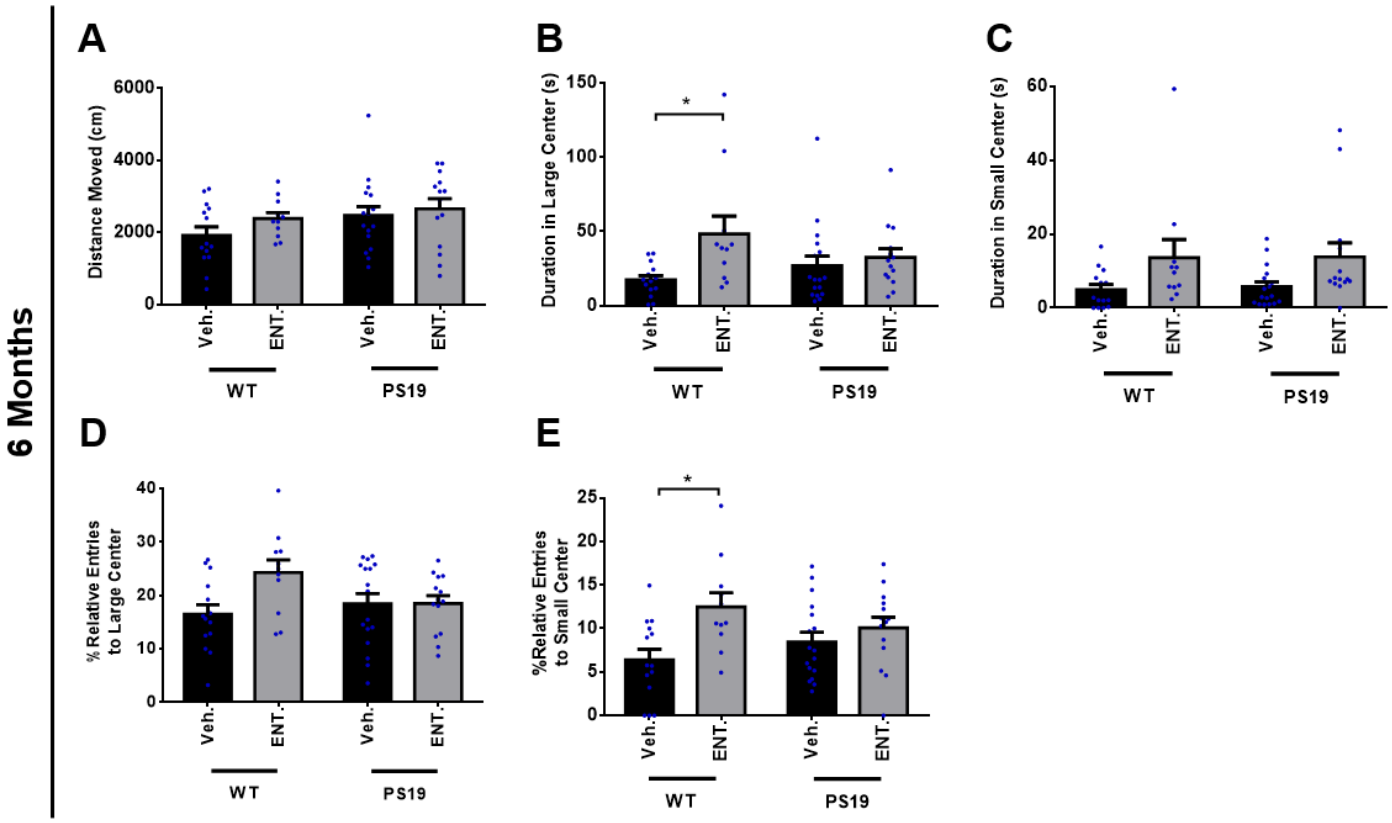

Supplementary Figure 9. No anxiety-related behavioural abnormalities in PS19 mice at 6 months of age in OF test, selective inhibition of PTP1B by 2.5 mg/kg dosage of ENT-03 had no effect. No phenotype was detected in the distance moved or anxiety-related behaviour in OF between WT Veh.-treated mice and PS19 Veh.- treated mice (A-E). Treatment with ENT-03 did not have significant effects on behaviour in any of the OF parameters assessed (A-E). For A-E, n= 14, 11, 17, 14, respectively. Data depicts mean ± SEM. For each analysis, two-way ANOVA was followed by Tukey's post-hoc pairwise comparisons, *p-value < 0.05, mean values are reported, error bars represent SEM.

9. Tables

Table 1. PCR Primers			
Gene	**PCR Product Band Size (bp)**	**Primer Name**	**Primer Sequence**
PTP1B flx	WT: 206 Flx: 327	PTP1Bflx-F	5'-TGC TCA CTC ACC CTG CTA CAA-3'
		PTP1Bflx-R	5'-GAA ATG GCT CAC TCC TAC TGG-3'
PS19 Transgene	Transgene: 450 Control: 200	PS19 A	5'-GGT ATT AGC CTA TGG GGG ACA C-3'
		PS19 B	5'-GGC ATC TCA GCA ATG TCT CC-3'
		PS19 C	5'-CAA ATG TTG CTT GTC TGG TG-3'
		PS19 D	5'-GTC AGT CGA GTG GAC AGT TT-3'
APP Transgene	Transgene: 360 Control: 200	oIMR 2044	5'-GGT GAG TTT GTA AGT GAT GCC-3'
		oIMR 2045	5'-TCT TCT TCT TCC ACC TCA GC-3'
		oIMR 8744	5'-CAA ATG TTG CTT GTC TGG TG -3'
		oIMR 8745	5'-GTC AGT CGA GTG CAC AGT TT -3'
CamK-Cre	Mutant: 522	iCre - F	5'-GAC AGG CAG GCC TTC TCT GAA -3'
		iCre-R	5'-CTT CTC CAC ACC AGC TGT GGA-3'

Table 1. List of PCR primers used for genotyping. Flx indicates flox site. F indicates forward primer; R indicates reverse primer.

Table 2 Statistical analysis of behavioural experiments															
				Main effect					Post hoc						
Figure	**Brief description**	**n**	**DESCRIPTIVE STATS**	**Test**	**Factor**	**F value**	**P value**	**Signficant?**	**Test**	**Description**	**t value**	**q value**	**P value**	**Signficant?**	**Mark**
Figure $1A_1$	6 mo. EPM, Distance Moved	15,20,14,17	Mean ± SEM	One-Way ANOVA	Genotype	1.895	0.1395	No	N/A						
Figure $1A_2$	6 mo. EPM, Duration in Open Arms	15,20,14,17	Mean ± SEM	One-Way ANOVA	Genotype	4.684	0.0052	Yes	Bonferroni	WT Veh. vs. J20 Veh.	2.923		0.0145	Yes	*
										WT Veh. vs. PS19 Veh.	1.846		0.2089	No	
										J20 Veh. vs. PS19 Veh.	0.699		>0.9999	No	
Figure $1A_3$	6 mo. EPM, %Rel. Ent. To Open Arms.	15,20,14,17	Mean ± SEM	One-Way ANOVA	Genotype	10.2	<0.0001	Yes	Bonferroni	WT Veh. vs. J20 Veh.	5.012		<0.0001	Yes	****
										WT Veh. vs. PS19 Veh.	2.327		0.0697	No	
										J20 Veh. vs. PS19 Veh.	1.255		0.6421	No	
Figure $1B_1$	8 mo. EPM, Distance Moved	14,9,11,10	Mean ± SEM	One-Way ANOVA	Genotype	9.673	<0.0001	Yes	Bonferroni	WT Veh. vs. J20 Veh.	1.294		0.6096	No	
										WT Veh. vs. PS19 Veh.	2.594		0.0396	Yes	*
										J20 Veh. vs. PS19 Veh.	5.007		< 0.0001	Yes	****
Figure $1B_2$	8 mo. EPM, Duration in Open Arms	14,9,11,10	Mean ± SEM	One-Way ANOVA	Genotype	20.57	< 0.0001	Yes	Bonferroni	WT Veh. vs. J20 Veh.	0.222		> 0.9999	No	
										WT Veh. vs. PS19 Veh.	6.029		< 0.0001	Yes	****
										J20 Veh. vs. PS19 Veh.	6.183		< 0.0001	Yes	****
Figure $1B_3$	8 mo. EPM, %Rel. Ent. To Open Arms.	14,9,11,10	Mean ± SEM	One-Way ANOVA	Genotype	3.683	0.0197	Yes	Bonferroni	WT Veh. vs. J20 Veh.	0.402		> 0.9999	No	
										WT Veh. vs. PS19 Veh.	2.853		0.0205	Yes	*
										J20 Veh. vs. PS19 Veh.	2.283		0.0835	No	
Figure $2A_1$	6 mo. OF, Distance Moved	15,20,14,17	Mean ± SEM	One-Way ANOVA	Genotype	1.373	0.2594	No	N/A						
Figure $2A_2$	Duration in Large Center	15,20,14,17	Mean ± SEM	One-Way ANOVA	Genotype	1.577	0.2039	No	N/A						
Figure $2A_3$	6 mo. OF, Duration in Small Center	15,20,14,17	Mean ± SEM	One-Way ANOVA	Genotype	1.143	0.3387	No	N/A						
Figure $2A_4$	6 mo. OF, %Rel. Ent. To Large Center	15,20,14,17	Mean ± SEM	One-Way ANOVA	Genotype	1.283	0.2882	No	N/A						
Figure $2A_5$	6 mo. OF, %Rel. Ent. To Small Center	15,20,14,17	Mean ± SEM	One-Way ANOVA	Genotype	2.001	0.123	No	N/A						
Figure $2B_1$	8 mo. OF, Distance Moved	14,9,11,10	Mean ± SEM	One-Way ANOVA	Genotype	1.303	0.2867	No	N/A						
Figure $2B_2$	8 mo. OF, Duration in Large Center	14,9,11,10	Mean ± SEM	One-Way ANOVA	Genotype	2.73	0.0565	Marginal	Bonferroni	WT Veh. vs. J20 Veh.	0.594		> 0.9999	No	
										WT Veh. vs. PS19 Veh.	2.799		0.0235	Yes	*
										J20 Veh. vs. PS19 Veh.	1.717		0.2814	No	
Figure $2B_3$	8 mo. OF, Duration in Small Center	14,9,11,10	Mean ± SEM	One-Way ANOVA	Genotype	1.939	0.1388	No	N/A						
Figure $2B_4$	8 mo. OF, %Rel. Ent. To Large Center	14,9,11,10	Mean ± SEM	One-Way ANOVA	Genotype	3.576	0.0221	Yes	Bonferroni	WT Veh. vs. J20 Veh.	0.638		> 0.9999	No	
										WT Veh. vs. PS19 Veh.	3.083		0.0111	Yes	*
										J20 Veh. vs. PS19 Veh.	0.581		> 0.9999	No	
Figure $2B_5$	8 mo. OF, %Rel. Ent. To Small Center	14,9,11,10	Mean ± SEM	One-Way ANOVA	Genotype	4.963	0.0051	Yes	Bonferroni	WT Veh. vs. J20 Veh.	0.852		> 0.9999	No	
										WT Veh. vs. PS19 Veh.	3.741		0.0017	Yes	**
										J20 Veh. vs. PS19 Veh.	1.112		0.8187	No	

Table 2. Summarized statistical analyses of all behavioural experiments.

Continues on next page…

Figure $3A_1$	6 mo. J20 EPM Med. Trod., Distance Moved	15,20,18	Mean ± SEM	One-Way ANOVA	Treatment	0.7487	0.4782	No	N/A						
Figure $3A_2$	6 mo. J20 EPM Med. Trod., Duration in Open Arms	15,20,18	Mean ± SEM	One-Way ANOVA	Treatment	8.632	0.0006	Yes	Bonferroni	WT Veh. vs. J20 Veh.	3.699		0.0016	Yes	**
										WT Veh. vs. J20 Trod.	0.496		> 0.9999	No	
										J20 Veh. vs. J20 Trod.	3.356		0.0046	Yes	**
Figure $3A_3$	6 mo. J20 EPM Med. Trod., %Rel. Ent. To Open Arms	15,20,18	Mean ± SEM	One-Way ANOVA	Treatment	12.74	< 0.0001	Yes	Bonferroni	WT Veh. vs. J20 Veh.	5.043		< 0.0001	Yes	****
										WT Veh. vs. J20 Trod.	2.659		0.0315	Yes	*
										J20 Veh. vs. J20 Trod.	2.441		0.0548	No	
Figure $3B_1$	8 mo. J20 EPM Med. Trod., Distance Moved	14,9,11	Mean ± SEM	One-Way ANOVA	Treatment	1.363	0.2708	No	N/A						
Figure $3B_2$	8 mo. J20 EPM Med. Trod., Duration in Open Arms	14,9,11	Mean ± SEM	One-Way ANOVA	Treatment	0.3358	0.7173	No	N/A						
Figure $3B_3$	8 mo. J20 EPM Med. Trod., %Rel. Ent. To Open Arms	14,9,11	Mean ± SEM	One-Way ANOVA	Treatment	3.391	0.0466	Yes	Bonferroni	WT Veh. vs. J20 Veh.	0.392		> 0.9999	No	
										WT Veh. vs. J20 Trod.	2.505		0.0531	No	
										J20 Veh. vs. J20 Trod.	1.873		0.2114	No	
Figure $4A_1$	6 mo. PS19 EPM Med. Trod. , Distance Moved	14,17,14	Mean ± SEM	One-Way ANOVA	Treatment	1.373	0.2644	No	N/A						
Figure $4A_2$	6 mo. PS19 EPM Med. Trod., Duration in Open Arms	14,17,14	Mean ± SEM	One-Way ANOVA	Treatment	1.534	0.2274	No	N/A						
Figure $4A_3$	6 mo. PS19 EPM Med. Trod., %Rel. Ent. To Open Arms	14,17,14	Mean ± SEM	One-Way ANOVA	Treatment	4.084	0.024	Yes	Bonferroni	WT Veh. vs. PS19 Veh.	2.295		0.0804	No	
										WT Veh. vs. PS19 Trod.	0.249		> 0.9999	No	
										PS19 Veh. vs. PS19 Tro	2.556		0.0429	Yes	*
Figure $4B_1$	8 mo. PS19 EPM Med. Trod., Distance Moved	11,10,12	Mean ± SEM	One-Way ANOVA	Treatment	2.386	0.1093	No							
Figure $4B_2$	8 mo. PS19 EPM Med. Trod., Duration in Open Arms	11,10,12	Mean ± SEM	One-Way ANOVA	Treatment	14.2	< 0.0001	Yes	Bonferroni	WT Veh. vs. PS19 Veh.	5.211		< 0.0001	Yes	****
										WT Veh. vs. PS19 Trod.	1.628		0.3421	No	
										PS19 Veh. vs. PS19 Tro	3.731		0.0024	Yes	**
Figure $4B_3$	8 mo. PS19 EPM Med. Trod., %Rel. Ent. To Open Arms	11,10,12	Mean ± SEM	One-Way ANOVA	Treatment	6.802	0.0037	Yes	Bonferroni	WT Veh. vs. PS19 Veh.	3.629		0.0031	Yes	**
										WT Veh. vs. PS19 Trod.	1.238		0.6763	No	
										PS19 Veh. vs. PS19 Tro	2.497		0.0548	No	

Continues on next page…

Supplementary Figure 2A	8 mo. J20 EPM High Trod., Distance Moved	14,14,9, 10	Mean ± SEM	Two-Way ANOVA	Interaction	3.133	0.0838	No	N/A						
					Genotype	0.11	0.7417	No	N/A						
					Treatment	0.06971	0.793	No	N/A						
Supplementary Figure 2B	8 mo. J20 EPM High Trod., Duration in Open Arms	14,14,9, 10	Mean ± SEM	Two-Way ANOVA	Interaction	0.1676	0.6842	No	N/A						
					Genotype	1.052	0.3108	No	N/A						
					Treatment	0.605	0.4409	No	N/A						
Supplementary Figure 2C	8 mo. J20 EPM High Trod., %Rel. Ent. To Open Arms	14,14,9, 10	Mean ± SEM	Two-Way ANOVA	Interaction	0.2068	0.6516	No	N/A						
					Genotype	0.00814	0.9285	No	N/A						
					Treatment	2.155	0.1494	No	N/A						
Supplementary Figure 3A	8 mo. PS19 EPM High Trod., Distance Moved	11,14,10,14	Mean ± SEM	Two-Way ANOVA	Interaction	0.6664	0.4186	No	Bonferroni	WT Veh. Vs. WT Trod.	3.051		0.0229	Yes	*
										WT Veh. vs. PS19 Veh.	2.775		0.0481	Yes	*
					Genotype	11.43	0.0015	Yes		WT Veh. vs. PS19 Trod.	1.213		> 0.9999	No	
										WT Trod. vs. PS19 Veh.	5.897		< 0.0001	Yes	****
					Treatment	25.72	< 0.0001	Yes		WT Trod. vs. PS19 Trod.	1.96		0.3375	No	
										PS19 Veh. vs. PS19 Tro	4.108		0.001	Yes	***
Supplementary Figure 3B	8 mo. PS19 EPM High Trod., Duration in Open Arms	11,14,10,14	Mean ± SEM	Two-Way ANOVA	Interaction	8.068	0.0067	Yes	Bonferroni	WT Veh. Vs. WT Trod.	0.572		> 0.9999	No	
										WT Veh. vs. PS19 Veh.	5.687		< 0.0001	Yes	****
					Genotype	33.19	< 0.0001	Yes		WT Veh. vs. PS19 Trod.	1.522		0.8105	No	
										WT Trod. vs. PS19 Veh.	6.558		< 0.0001	Yes	****
					Treatment	13.24	0.0007	Yes		WT Trod. vs. PS19 Trod.	2.232		0.1837	No	
										PS19 Veh. vs. PS19 Tro	4.52		0.0003	Yes	***
Supplementary Figure 3C	8 mo. PS19 EPM High Trod., %Rel. Ent. To Open Arms	11,14,10,14	Mean ± SEM	Two-Way ANOVA	Interaction	6.067	0.0177	Yes	Bonferroni	WT Veh. Vs. WT Trod.	1.661		0.622	No	
										WT Veh. vs. PS19 Veh.	3.022		0.0248	Yes	*
					Genotype	4.441	0.0407	Yes		WT Veh. vs. PS19 Trod.	1.406		0.9997	No	
										WT Trod. vs. PS19 Veh.	1.572		0.7371	No	
					Treatment	0.02144	0.8842	No		WT Trod. vs. PS19 Trod.	0.272		> 0.9999	No	
										PS19 Veh. vs. PS19 Tro	1.821		0.4519	No	

Continues on next page…

Figure $5A_1$	6 mo. J20 OF Med. Trod., Distance Moved	15, 20, 18	Mean ± SEM	One-Way ANOVA	Treatment	0.0079	0.9921	No	N/A						
Figure $5A_2$	6 mo. J20 OF Med. Trod., Duration in Large Center	15, 20, 18	Mean ± SEM	One-Way ANOVA	Treatment	1.625	0.2072	No	N/A						
Figure $5A_3$	6 mo. J20 OF Med. Trod., Duration in Small Center	15, 20, 18	Mean ± SEM	One-Way ANOVA	Treatment	0.3642	0.6966	No	N/A						
Figure $5A_4$	6 mo. J20 OF Med. Trod., %Rel. Ent. in Large Center	15, 20, 18	Mean ± SEM	One-Way ANOVA	Treatment	1.399	0.2564	No	N/A						
Figure $5A_5$	6 mo. J20 OF Med. Trod., %Rel. Ent. in Small Center	15, 20, 18	Mean ± SEM	One-Way ANOVA	Treatment	0.6679	0.5173	No	N/A						
Figure $5B_1$	8 mo. J20 OF Med. Trod., Distance Moved	14, 9, 11	Mean ± SEM	One-Way ANOVA	Treatment	0.1367	0.8728	No	N/A						
Figure $5B_2$	8 mo. J20 OF Med. Trod., Duration in Large Center	14, 9, 11	Mean ± SEM	One-Way ANOVA	Treatment	0.1438	0.8666	No	N/A						
Figure $5B_3$	8 mo. J20 OF Med. Trod., Duration in Small Center	14, 9, 11	Mean ± SEM	One-Way ANOVA	Treatment	0.06601	0.9363	No	N/A						
Figure $5B_4$	8 mo. J20 OF Med. Trod., %Rel. Ent. in Large Center	14, 9, 11	Mean ± SEM	One-Way ANOVA	Treatment	0.282	0.7562	No	N/A						
Figure $5B_5$	8 mo. J20 OF Med. Trod., %Rel. Ent. in Small Center	14, 9, 11	Mean ± SEM	One-Way ANOVA	Treatment	0.4738	0.6271	No	N/A						
Figure $6A_1$	6 mo. PS19 OF Med. Trod., Distance Moved	14, 17, 14	Mean ± SEM	One-Way ANOVA	Treatment	3.718	0.0326	Yes	Bonferroni	WT Veh. vs. PS19 Veh.	1.747		0.2638	No	
										WT Veh. vs. PS19 Trod.	2.699		0.0299	Yes	*
										PS19 Veh. vs. PS19 Tro	1.079		0.8599	No	
Figure $6A_2$	6 mo. PS19 OF Med. Trod., Duration in Large Center	14, 17, 14	Mean ± SEM	One-Way ANOVA	Treatment	2.28	0.1148	No	N/A						
Figure $6A_3$	6 mo. PS19 OF Med. Trod., Duration in Small Center	14, 17, 14	Mean ± SEM	One-Way ANOVA	Treatment	3.213	0.0503	Marginal	Bonferroni	WT Veh. vs. PS19 Veh.	0.373		> 0.9999	No	
										WT Veh. vs. PS19 Trod.	2.332		0.0738	No	
										PS19 Veh. vs. PS19 Tro	2.069		0.1343	No	
Figure $6A_4$	6 mo. PS19 OF Med. Trod., %Rel. Ent. in Large Center	14, 17, 14	Mean ± SEM	One-Way ANOVA	Treatment	1.05	0.359	No	N/A						
Figure $6A_5$	6 mo. PS19 OF Med. Trod., %Rel. Ent. in Small Center	14, 17, 14	Mean ± SEM	One-Way ANOVA	Treatment	3.288	0.0471	Yes	Bonferroni	WT Veh. vs. PS19 Veh.	1.293		0.6092		
										WT Veh. vs. PS19 Trod.	2.564		0.0421		*
										PS19 Veh. vs. PS19 Tro	1.392		0.5138		
Figure $6B_1$	8 mo. PS19 OF Med. Trod., Distance Moved	11, 10, 12	Mean ± SEM	One-Way ANOVA	Treatment	1.584	0.2218	No	N/A						
Figure $6B_2$	8 mo. PS19 OF Med. Trod., Duration in Large Center	11, 10, 12	Mean ± SEM	One-Way ANOVA	Treatment	8.328	0.0013	Yes	Bonferroni	WT Veh. vs. PS19 Veh.	4.044		0.001	Yes	**
										WT Veh. vs. PS19 Trod.	1.539		0.4028	No	
										PS19 Veh. vs. PS19 Tro	2.626		0.0404	Yes	*
Figure $6B_3$	8 mo. PS19 OF Med. Trod., Duration in Small Center	11, 10, 12	Mean ± SEM	One-Way ANOVA	Treatment	6.286	0.0052	Yes	Bonferroni	WT Veh. vs. PS19 Veh.	3.467		0.0048	Yes	**
										WT Veh. vs. PS19 Trod.	1.083		0.8623	No	
										PS19 Veh. vs. PS19 Tro	2.482		0.0567	No	
Figure $6B_4$	8 mo. PS19 OF Med. Trod., %Rel. Ent. in Large Center	11, 10, 12	Mean ± SEM	One-Way ANOVA	Treatment	6.113	0.0059	Yes	Bonferroni	WT Veh. vs. PS19 Veh.	3.355		0.0065	Yes	**
										WT Veh. vs. PS19 Trod.	2.526		0.0512	No	
										PS19 Veh. vs. PS19 Tro	0.961		> 0.9999	No	
Figure $6B_5$	8 mo. PS19 OF Med. Trod., %Rel. Ent. in Small Center	11, 10, 12	Mean ± SEM	One-Way ANOVA	Treatment	7.222	0.0028	Yes	Bonferroni	WT Veh. vs. PS19 Veh.	3.711		0.0025	Yes	**
										WT Veh. vs. PS19 Trod.	1.14		0.7897	No	
										PS19 Veh. vs. PS19 Tro	2.676		0.0359	Yes	*

Continues on next page…

Supplementary Figure 4A	8 mo. J20 OF High Trod., Distance Moved	14,14,9,10	Mean ± SEM	Two-Way ANOVA	Interaction	2.177	0.1474	No	Bonferroni	WT Veh. Vs. WT Trod.	3.177		0.0165	Yes	*
										WT Veh. vs. J20 Veh.	0.326		> 0.9999	No	
					Genotype	1.013	0.3198	No		WT Veh. vs. J20 Trod.	1.117		> 0.9999	No	
										WT Trod. vs. J20 Veh.	2.484		0.1017	No	
					Treatment	6.563	0.014	Yes		WT Trod. vs. J20 Trod.	1.783		0.4898	No	
										J20 Veh. vs. J20 Trod.	0.703		> 0.9999	No	
Supplementary Figure 4B	8 mo. J20 OF High Trod., Duration in Large Center	14,14,9,10	Mean ± SEM	Two-Way ANOVA	Interaction	0.8349	0.3659	No	Bonferroni	WT Veh. Vs. WT Trod.	2.965		0.0295	Yes	*
										WT Veh. vs. J20 Veh.	0.691		> 0.9999	No	
					Genotype	0.00615	0.9378	No		WT Veh. vs. J20 Trod.	2.107		0.246	No	
										WT Trod. vs. J20 Veh.	1.932		0.3595	No	
					Treatment	8.145	0.0066	Yes		WT Trod. vs. J20 Trod.	0.6		> 0.9999	No	
										J20 Veh. vs. J20 Trod.	1.256		> 0.9999	No	
Supplementary Figure 4C	8 mo. J20 OF High Trod., Duration in Small Center	14,14,9,10	Mean ± SEM	Two-Way ANOVA	Interaction	0.2362	0.6295	No	Bonferroni	WT Veh. Vs. WT Trod.	2.399		0.1249	No	
										WT Veh. vs. J20 Veh.	0.346		> 0.9999	No	
					Genotype	0.00011	0.9918	No		WT Veh. vs. J20 Trod.	1.849		0.4283	No	
										WT Trod. vs. J20 Veh.	1.777		0.4957	No	
					Treatment	6.567	0.014	Yes		WT Trod. vs. J20 Trod.	0.342		> 0.9999	No	
										J20 Veh. vs. J20 Trod.	1.345		> 0.9999	No	
Supplementary Figure 4D	8 mo. J20 OF High Trod., %Rel. Ent. in Large Center	14,14,9,10	Mean ± SEM	Two-Way ANOVA	Interaction	0.00019	0.9891	No	Bonferroni	WT Veh. Vs. WT Trod.	2.876		0.0375	Yes	*
										WT Veh. vs. J20 Veh.	0.614		> 0.9999	No	
					Genotype	0.7536	0.3902	No		WT Veh. vs. J20 Trod.	2.011		0.3034	No	
										WT Trod. vs. J20 Veh.	3.158		0.0174	Yes	*
					Treatment	13.45	0.0007	Yes		WT Trod. vs. J20 Trod.	0.614		> 0.9999	No	
										J20 Veh. vs. J20 Trod.	2.384		0.1298	No	
Supplementary Figure 4E	8 mo. J20 OF High Trod., %Rel. Ent. in Small Center	14,14,9,10	Mean ± SEM	Two-Way ANOVA	Interaction	0.3434	0.5609	No	Bonferroni	WT Veh. Vs. WT Trod.	2.135		0.231	No	
										WT Veh. vs. J20 Veh.	0.824		> 0.9999	No	
					Genotype	0.3562	0.5537	No		WT Veh. vs. J20 Trod.	1.941		0.3528	No	
										WT Trod. vs. J20 Veh.	2.712		0.0574	No	
					Treatment	10.88	0.002	Yes		WT Trod. vs. J20 Trod.	0.008		> 0.9999	No	
										J20 Veh. vs. J20 Trod.	2.515		0.0943	No	

Continues on next page…

Supplementary Figure 5A	8 mo. PS19 OF High Trod., Distance Moved	11,14,10,14	Mean ± SEM	Two-Way ANOVA	Interaction	0.9236	0.3417	No	Bonferroni	WT Veh. Vs. WT Trod.	3.484		0.0067	Yes	**
										WT Veh. vs. PS19 Veh.	2.227		0.1859	No	
					Genotype	5.797	0.0202	Yes		WT Veh. vs. PS19 Trod.	2.447		0.1102	No	
										WT Trod. vs. PS19 Veh.	5.741		< 0.0001	Yes	****
					Treatment	33.88	< 0.0001	Yes		WT Trod. vs. PS19 Trod.	1.106		> 0.9999	No	
										PS19 Veh. vs. PS19 Tro	4.731		0.0001	Yes	***
Supplementary Figure 5B	8 mo. PS19 OF High Trod., Duration in Large Center	11,14,10,14	Mean ± SEM	Two-Way ANOVA	Interaction	13.37	0.0007	Yes	Bonferroni	WT Veh. Vs. WT Trod.	1.353		> 0.9999	No	
										WT Veh. vs. PS19 Veh.	5.533		< 0.0001	Yes	****
					Genotype	22.22	< 0.0001	Yes		WT Veh. vs. PS19 Trod.	0.594		> 0.9999	No	
										WT Trod. vs. PS19 Veh.	7.156		< 0.0001	Yes	****
					Treatment	30.72	< 0.0001	Yes		WT Trod. vs. PS19 Trod.	0.809		> 0.9999	No	
										PS19 Veh. vs. PS19 Tro	6.418		< 0.0001	Yes	****
Supplementary Figure 5C	8 mo. PS19 OF High Trod., Duration in Small Center	11,14,10,14	Mean ± SEM	Two-Way ANOVA	Interaction	9.648	0.0033	Yes	Bonferroni	WT Veh. Vs. WT Trod.	1.052		> 0.9999	No	
										WT Veh. vs. PS19 Veh.	4.872		< 0.0001	Yes	****
					Genotype	18.18	0.0001	Yes		WT Veh. vs. PS19 Trod.	0.222		> 0.9999	No	
										WT Trod. vs. PS19 Veh.	6.165		< 0.0001	Yes	****
					Treatment	20.91	< 0.0001	Yes		WT Trod. vs. PS19 Trod.	0.885		> 0.9999	No	
										PS19 Veh. vs. PS19 Tro	5.358		< 0.0001	Yes	****
Supplementary Figure 5D	8 mo. PS19 OF High Trod., %Rel. Ent. in Large Center	11,14,10,14	Mean ± SEM	Two-Way ANOVA	Interaction	4.453	0.0404	Yes	Bonferroni	WT Veh. Vs. WT Trod.	0.829		> 0.9999	No	
										WT Veh. vs. PS19 Veh.	3.192		0.0155	Yes	*
					Genotype	7.388	0.0093	Yes		WT Veh. vs. PS19 Trod.	0.393		> 0.9999	No	
										WT Trod. vs. PS19 Veh.	4.175		0.0008	Yes	***
					Treatment	10.67	0.0021	Yes		WT Trod. vs. PS19 Trod.	0.465		> 0.9999	No	
										PS19 Veh. vs. PS19 Tro	3.751		0.003	Yes	**
Supplementary Figure 5E	8 mo. PS19 OF High Trod., %Rel. Ent. in Small Center	11,14,10,14	Mean ± SEM	Two-Way ANOVA	Interaction	3.544	0.0662	No	Bonferroni	WT Veh. Vs. WT Trod.	0.17		> 0.9999	No	
										WT Veh. vs. PS19 Veh.	3.454		0.0073	Yes	**
					Genotype	11.17	0.0017	Yes		WT Veh. vs. PS19 Trod.	0.876		> 0.9999	No	
										WT Trod. vs. PS19 Veh.	3.811		0.0025	Yes	**
					Treatment	4.496	0.0395	Yes		WT Trod. vs. PS19 Trod.	1.115		> 0.9999	No	
										PS19 Veh. vs. PS19 Tro	2.793		0.0459	Yes	*

Continues on next page…

Supplementary Figure 6A	6 mo. J20 EPM Med. Hu1436, Distance Moved	15,13,20, 12	Mean ± SEM	Two-Way ANOVA	Interaction	0.04885	0.8259	No	N/A						
					Genotype	0.00864	0.9263	No							
					Treatment	0.07283	0.7883	No							
Supplementary Figure 6B	6 mo. J20 EPM Med. Hu1436, Duration in Open Arms	14, 10, 19, 11 NOTE: 5 outliers removed	Mean ± SEM	Two-Way ANOVA	Interaction	3.498	0.0673	No	Tukey	WT Veh. Vs. WT Hu.		0.138	0.9997	No	
										WT Veh. vs. J20 Veh.		5.551	0.0015	Yes	**
					Genotype	9.344	0.0036	Yes		WT Veh. vs. J20 Hu.		1.31	0.7908	No	
										WT Hu. vs. J20 Veh.		4.859	0.0064	Yes	**
					Treatment	2.98	0.0905	No		WT Hu. vs. J20 Hu.		1.078	0.8711	No	
										J20 Veh. vs. J20 Hu.		3.767	0.0492	Yes	*
Supplementary Figure 6C	6 mo. J20 EPM Med. Hu1436, %Rel. Ent. to Open Arms	15,13,20, 12	Mean ± SEM	Two-Way ANOVA	Interaction	3.329	0.0736	No	Tukey	WT Veh. Vs. WT Hu.		0.9873	0.8973	No	
										WT Veh. vs. J20 Veh.		6.687	< 0.0001	Yes	****
					Genotype	17.34	0.0001	Yes		WT Veh. vs. J20 Hu.		3.316	0.1007	No	
										WT Hu. vs. J20 Veh.		5.041	0.0042	Yes	**
					Treatment	0.6353	0.4289	No		WT Hu. vs. J20 Hu.		2.137	0.4379	No	
										J20 Veh. vs. J20 Hu.		2.738	0.2253	No	
Supplementary Figure 7A	6 mo. PS19 EPM Med. Hu1436, Distance Moved	14, 13, 17, 14	Mean ± SEM	Two-Way ANOVA	Interaction	1.907	0.1732	No	Tukey	WT Veh. Vs. WT Trod.		2.28	0.3809	No	
										WT Veh. vs. PS19 Veh.		1.228	0.8212	No	
					Genotype	6.448	0.0141	Yes		WT Veh. vs. PS19 Trod.		1.537	0.6991	No	
										WT Trod. vs. PS19 Veh.		3.519	0.0736	No	
					Treatment	1.042	0.3121	No		WT Trod. vs. PS19 Trod.		3.721	0.0528	No	
										PS19 Veh. vs. PS19 Trod.		0.3818	0.993	No	
Supplementary Figure 7B	6 mo. PS19 EPM Med. Hu1436, Duration in Open Arms	14, 13, 17, 14	Mean ± SEM	Two-Way ANOVA	Interaction	0.04103	0.8403	No	Tukey	WT Veh. Vs. WT Trod.		1.897	0.5415	No	
										WT Veh. vs. PS19 Veh.		2.855	0.1945	No	
					Genotype	8.387	0.0055	Yes		WT Veh. vs. PS19 Trod.		1.114	0.8597	No	
										WT Trod. vs. PS19 Veh.		4.637	0.0098	Yes	**
					Treatment	3.223	0.0784	No		WT Trod. vs. PS19 Trod.		2.941	0.1732	No	
										PS19 Veh. vs. PS19 Trod.		1.688	0.6336	No	
Supplementary Figure 7C	6 mo. J20 EPM Med. Hu1436, %Rel. Ent. to Open Arms	14, 13, 17, 14	Mean ± SEM	Two-Way ANOVA	Interaction	0.5237	0.4725	No	Tukey	WT Veh. Vs. WT Trod.		0.5188	0.9829	No	
										WT Veh. vs. PS19 Veh.		2.966	0.1675	No	
					Genotype	4.306	0.0429	Yes		WT Veh. vs. PS19 Trod.		0.8145	0.9388	No	
										WT Trod. vs. PS19 Veh.		3.307	0.1025	No	
					Treatment	1.613	0.2097	No		WT Trod. vs. PS19 Trod.		1.283	0.8011	No	
										PS19 Veh. vs. PS19 Trod.		2.113	0.4483	No	

Continues on next page…

Supplementary Figure 8A	6 mo. J20 OF Med. Hu1436, Distance Moved	15, 11, 20, 12	Mean ± SEM	Two-Way ANOVA	Interaction	0.02972	0.8638	No	N/A						
					Genotype	0.00052	0.9819	No							
					Treatment	3.163	0.081	No							
Supplementary Figure 8B	6 mo. J20 OF Med. Hu1436, Duration in Large Center	15, 11, 20, 12	Mean ± SEM	Two-Way ANOVA	Interaction	0.2184	0.6422	No	Tukey	WT Veh. Vs. WT Hu.		1.48	0.7228	No	
										WT Veh. vs. J20 Veh.		2.005	0.4941	No	
					Genotype	1.764	0.1897	No		WT Veh. vs. J20 Hu.		0.6698	0.9646	No	
										WT Hu. vs. J20 Veh.		3.39	0.0898	No	
					Treatment	4.033	0.0496	Yes		WT Hu. vs. J20 Hu.		0.7865	0.9445	No	
										J20 Veh. vs. J20 Hu.		2.586	0.2715	No	
Supplementary Figure 8C	6 mo. J20 OF Med. Hu1436, Duration in Small Center	15, 11, 20, 12	Mean ± SEM	Two-Way ANOVA	Interaction	0.2678	0.6069	No	N/A						
					Genotype	0.09519	0.7589	No							
					Treatment	3.275	0.0759	No							
Supplementary Figure 8D	6 mo. J20 OF Med. Hu1436, %Rel. Ent. in Large Center	15, 11, 20, 12	Mean ± SEM	Two-Way ANOVA	Interaction	0.029	0.8654	No	N/A						
					Genotype	1.333	0.2533	No							
					Treatment	2.146	0.1487	No							
Supplementary Figure 8E	6 mo. J20 OF Med. Hu1436, %Rel. Ent. in Small Center	15, 11, 20, 12	Mean ± SEM	Two-Way ANOVA	Interaction	1.394	0.2429	No	N/A						
					Genotype	0.00263	0.9593	No							
					Treatment	2.16	0.1474	No							

Continues on next page…

Supplementary Figure 9A	6 mo. PS19 OF Med. Hu1436, Distance Moved	14, 11, 17, 14	Mean ± SEM	Two-Way ANOVA	Interaction	0.3317	0.5671	No	N/A						
					Genotype	2.739	0.104	No							
					Treatment	1.695	0.1987	No							
Supplementary Figure 9B	6 mo. PS19 OF Med. Hu1436, Duration in Large Center	14, 11, 17, 14	Mean ± SEM	Two-Way ANOVA	Interaction	3.175	0.0806	No	Tukey	WT Veh. Vs. WT Trod.		4.149	0.0249	Yes	*
										WT Veh. vs. PS19 Veh.		1.408	0.7524	No	
					Genotype	0.2051	0.6525	No		WT Veh. vs. PS19 Trod.		2.161	0.4285	No	
										WT Trod. vs. PS19 Veh.		3.006	0.1585	No	
					Treatment	6.699	0.0125	Yes		WT Trod. vs. PS19 Trod.		2.121	0.4448	No	
										PS19 Veh. vs. PS19 Trod.		0.8547	0.9302	No	
Supplementary Figure 9C	6 mo. PS19 OF Med. Hu1436, Duration in Small Center	14, 11, 17, 14	Mean ± SEM	Two-Way ANOVA	Interaction	0.01068	0.9181	No	Tukey	WT Veh. Vs. WT Trod.		2.824	0.2024	No	
										WT Veh. vs. PS19 Veh.		0.287	0.997	No	
					Genotype	0.02802	0.8677	No		WT Veh. vs. PS19 Trod.		3.075	0.144	No	
										WT Trod. vs. PS19 Veh.		2.673	0.2449	No	
					Treatment	8.244	0.0059	Yes		WT Trod. vs. PS19 Trod.		0.0608	> 0.9999	No	
										PS19 Veh. vs. PS19 Trod.		2.933	0.1751	No	
Supplementary Figure 9D	6 mo. PS19 OF Med. Hu1436, %Rel. Ent. in Large Center	14, 11, 17, 14	Mean ± SEM	Two-Way ANOVA	Interaction	4.053	0.0493	Yes	Tukey	WT Veh. Vs. WT Trod.		3.85	0.0424	Yes	*
										WT Veh. vs. PS19 Veh.		1.086	0.8684	No	
					Genotype	0.9769	0.3275	No		WT Veh. vs. PS19 Trod.		1.066	0.8746	No	
										WT Trod. vs. PS19 Veh.		2.995	0.1609	No	
					Treatment	4.17	0.0462	Yes		WT Trod. vs. PS19 Trod.		2.85	0.1957	No	
										PS19 Veh. vs. PS19 Trod.		0.03041	> 0.9999	No	
Supplementary Figure 9E	6 mo. PS19 OF Med. Hu1436, %Rel. Ent. in Small Center	14, 11, 17, 14	Mean ± SEM	Two-Way ANOVA	Interaction	3.106	0.0839	No	Tukey	WT Veh. Vs. WT Trod.		4.54	0.0118	Yes	*
										WT Veh. vs. PS19 Veh.		1.738	0.6117	No	
					Genotype	0.01503	0.9029	No		WT Veh. vs. PS19 Trod.		2.932	0.1755	No	
										WT Trod. vs. PS19 Veh.		3.106	0.1377	No	
					Treatment	9.119	0.0039	Yes		WT Trod. vs. PS19 Trod.		1.789	0.5888	No	
										PS19 Veh. vs. PS19 Trod.		1.333	0.7822	No	

Continues on next page…

Figure 7A	6 mo. EPM J20 PTP1B ablation, Distance Moved	20, 11, 15, 4	Mean ± SEM	Two-Way ANOVA	Interaction	3.357	0.0734	No	N/A						
					Genotype	0.5117	0.478	No							
					Treatment	0.01301	0.9097	No							
Figure 7B	6 mo. EPM J20 PTP1B ablation, Duration in Open Arms	20, 11, 15, 4	Mean ± SEM	Two-Way ANOVA	Interaction	9.078	0.0042	Yes	Bonferroni	WT vs. nPKO	0.421		> 0.9999	No	
										WT vs. J20	5.503		< 0.0001	Yes	****
					Genotype	6.473	0.0144	Yes		WT vs. J20 nPKO	0.001		> 0.9999	No	
										nPKO vs. J20	4.337		0.0005	Yes	***
					Treatment	6.482	0.0143	Yes		nPKO vs. J20 nPKO	0.272		> 0.9999	No	
										J20 vs. J20 nPKO	3.341		0.01	Yes	**
Figure 7C	6 mo. EPM J20 PTP1B ablation, Duration in Open Arms	20, 11, 15, 4	Mean ± SEM	Two-Way ANOVA	Interaction	4.099	0.0487	Yes	Bonferroni	WT vs. nPKO	1.285		> 0.9999	No	
										WT vs. J20	6.018		< 0.0001	Yes	****
					Genotype	16.42	0.0002	Yes		WT vs. J20 nPKO	2.133		0.2298	No	
										nPKO vs. J20	3.963		0.0015	Yes	**
					Treatment	0.3579	0.5526	No		nPKO vs. J20 nPKO	1.175		> 0.9999	No	
										J20 vs. J20 nPKO	1.576		0.7306	No	
Figure 8A	8 mo. EPM PS19 PTP1B ablation, Distance Moved	16, 12, 10, 15	Mean ± SEM	Two-Way ANOVA	Interaction	13.33	0.0006	Yes	Bonferroni	WT vs. nPKO	1.176		> 0.9999	No	
										WT vs. PS19	2.939		0.03	Yes	*
					Genotype	0.3459	0.5592	No		WT vs. PS19 nPKO	1.133		> 0.9999	No	
										nPKO vs. PS19	1.719		0.5517	No	
					Treatment	4.182	0.0462	Yes		nPKO vs. PS19 nPKO	2.211		0.1906	No	
										PS19 vs. PS19 nPKO	3.9		0.0018	Yes	**
Figure 8B	8 mo. EPM PS19 PTP1B ablation, Duration in Open Arms	16, 12, 10, 15	Mean ± SEM	Two-Way ANOVA	Interaction	18.5	< 0.0001	Yes	Bonferroni	WT vs. nPKO	0.019		> 0.9999	No	
										WT vs. PS19	6.462		< 0.0001	Yes	****
					Genotype	25.18	< 0.0001	Yes		WT vs. PS19 nPKO	0.577		> 0.9999	No	
										nPKO vs. PS19	6.067		< 0.0001	Yes	****
					Treatment	18.28	< 0.0001	Yes		nPKO vs. PS19 nPKO	0.517		> 0.9999	No	
										PS19 vs. PS19 nPKO	5.872		< 0.0001	Yes	****
Figure 8C	8 mo. EPM PS19 PTP1B ablation, %Rel. Ent. To Open Arms	16, 12, 10, 15	Mean ± SEM	Two-Way ANOVA	Interaction	4.734	0.0344	Yes	Bonferroni	WT vs. nPKO	0.081		> 0.9999	No	
										WT vs. PS19	3.85		0.0021	Yes	**
					Genotype	11.41	0.0014	Yes		WT vs. PS19 nPKO	1.021		> 0.9999	No	
										nPKO vs. PS19	3.552		0.0051	Yes	**
					Treatment	4.264	0.0443	Yes		nPKO vs. PS19 nPKO	0.867		> 0.9999	No	
										PS19 vs. PS19 nPKO	2.903		0.0331	Yes	*

Continues on next page…

Figure 9A	6 mo. OF J20 PTP1B ablation, Distance Moved	20, 11, 15, 4	Mean ± SEM	Two-Way ANOVA	Interaction	1.84E-05	0.9966	No	N/A						
					Genotype	3.238	0.0785	No							
					Treatment	1.951	0.1692	No							
Figure 9B	6 mo. OF J20 PTP1B ablation, Duration in Large Center	20, 11, 15, 4	Mean ± SEM	Two-Way ANOVA	Interaction	0.2996	0.5868	No	N/A						
					Genotype	0.07827	0.7809	No							
					Treatment	0.231	0.6331	No							
Figure 9C	6 mo. OF J20 PTP1B ablation, Duration in Small Center	20, 11, 15, 4	Mean ± SEM	Two-Way ANOVA	Interaction	0.00692	0.9341	No	N/A						
					Genotype	0.0528	0.8193	No							
					Treatment	0.07237	0.7891	No							
Figure 9D	6 mo. OF J20 PTP1B ablation, %Rel. Ent. to Large Center	20, 11, 15, 4	Mean ± SEM	Two-Way ANOVA	Interaction	0.6377	0.4286	No	N/A						
					Genotype	0.2962	0.5889	No							
					Treatment	1.238	0.2716	No							
Figure 9E	6 mo. OF J20 PTP1B ablation, %Rel. Ent. to Small Center	20, 11, 15, 4	Mean ± SEM	Two-Way ANOVA	Interaction	0.6377	0.4286	No	N/A						
					Genotype	0.2962	0.5889	No							
					Treatment	1.238	0.2716	No							

Continues on next page…

Figure 10A	8 mo. OF PS19 PTP1B ablation, Distance Moved	16, 12, 10, 15	Mean ± SEM	Two-Way ANOVA	Interaction	19.61	< 0.0001	Yes	Bonferroni	WT vs. nPKO	2.66		0.0631	No	
										WT vs. PS19	2.516		0.0912	No	
					Genotype	0.6411	0.4272	No		WT vs. PS19 nPKO	1.24		> 0.9999	No	
										nPKO vs. PS19	0.004		> 0.9999	No	
					Treatment	0.6309	0.4308	No		nPKO vs. PS19 nPKO	3.774		0.0026	Yes	**
										PS19 vs. PS19 nPKO	3.576		0.0048	Yes	**
Figure 10B	8 mo. OF PS19 PTP1B ablation, Duration in Large Center	16, 12, 10, 15+(	Mean ± SEM	Two-Way ANOVA	Interaction	15.16	0.0003	Yes	Bonferroni	WT vs. nPKO	2.109		0.2405	No	
										WT vs. PS19	4.343		0.0004	Yes	***
					Genotype	5.616	0.0218	Yes		WT vs. PS19 nPKO	1.055		> 0.9999	No	
										nPKO vs. PS19	2.208		0.1916	No	
					Treatment	1.026	0.3161	No		nPKO vs. PS19 nPKO	1.1		> 0.9999	No	
										PS19 vs. PS19 nPKO	3.36		0.0091	Yes	**
Figure 10C	8 mo. OF PS19 PTP1B ablation, Duration in Small Center	16, 12, 10, 15+(	Mean ± SEM	Two-Way ANOVA	Interaction	19.54	< 0.0001	Yes	Bonferroni	WT vs. nPKO	2.058		0.2694	No	
										WT vs. PS19	4.414		0.0003	Yes	***
					Genotype	3.781	0.0576	No		WT vs. PS19 nPKO	0.261		> 0.9999	No	
										nPKO vs. PS19	2.319		0.1475	No	
					Treatment	2.587	0.1142	No		nPKO vs. PS19 nPKO	1.787		0.4807	No	
										PS19 vs. PS19 nPKO	4.128		0.0009	Yes	***
Figure 10D	8 mo. OF PS19 PTP1B ablation, %Rel. Ent. To Large Center	16, 12, 10, 15+(	Mean ± SEM	Two-Way ANOVA	Interaction	4.966	0.0305	Yes	Bonferroni	WT vs. nPKO	0.799		> 0.9999	No	
						4.967				WT vs. PS19	2.622		0.0697	No	
					Genotype	4.968	0.1269	No		WT vs. PS19 nPKO	0.323		> 0.9999	No	
										nPKO vs. PS19	1.756		0.5118	No	
					Treatment	1.294	0.2608	No		nPKO vs. PS19 nPKO	0.488		> 0.9999	No	
										PS19 vs. PS19 nPKO	2.305		0.1528	No	
Figure 10E	8 mo. OF PS19 PTP1B ablation, %Rel. Ent. To Large Center	16, 12, 10, 15+(	Mean ± SEM	Two-Way ANOVA	Interaction	12.76	0.0008	Yes	Bonferroni	WT vs. nPKO	2.132		0.2284	No	
										WT vs. PS19	4.1		0.0009	Yes	***
					Genotype	5.483	0.0233	Yes		WT vs. PS19 nPKO	1.308		> 0.9999	No	
										nPKO vs. PS19	1.959		0.335	No	
					Treatment	0.4345	0.5129	No		nPKO vs. PS19 nPKO	0.888		> 0.9999	No	
										PS19 vs. PS19 nPKO	2.897		0.0337	Yes	*

Continues on next page…

Table 3 Statistical analysis for biochemical experiments														
				Main effect					Post hoc					
Figure	Brief description	n	DESCRIPTIVE STATS	Test	Factor	F value	P value	Signficant? (P-Value < 0.05)	Test	Description	t value	P value	Signficant? (P-Value < 0.05)	Mark
Figure 15B	PTP1B levels, PS19 8 mo. PTP1B level PTP1B ablation model	3,3,3,3	Mean ± SEM	Two-Way ANOVA	Interaction	F (1, 8) = 0.2005	0.6662	No	Bonferroni	WT vs. PTP1B KO	14.08	< 0.0001	Yes	****
										WT vs. PS19	0.5066	> 0.9999	No	
					Genotype	F (1, 8) = 1.355	0.2779	No		WT vs. PS19 PTP1B KO	12.94	< 0.0001	Yes	****
										PTP1B KO vs. PS19	14.58	< 0.0001	Yes	****
					Treatment	F (1, 8) = 378.7	< 0.0001	Yes		PTP1B KO vs. PS19 PTP1B	1.14	> 0.9999	No	
										PS19 vs. PS19 PTP1B KO	13.44	< 0.0001	Yes	****
Figure 15C	PTP1B levels, PS19 8 mo. PTP1B level Med. Trod.	3,3,3,3	Mean ± SEM	One-Way ANOVA	Treatment	0.05906	0.9432	No	N/A					
Figure 16B	pTau levels, PS19 8 mo., KO and Trod	3,3,3	Mean ± SEM	One-Way ANOVA	Treatment	2150	< 0.0001	Yes	Bonferroni	PS19 vs. PS19 nPKO	26.25	0.0029	Yes	**
										PS19 vs. PS19 Trod.	69.61	0.0004	Yes	***
Figure 16C	Tau levels, PS19 8 mo., KO and Trod	3,3,3	Mean ± SEM	One-Way ANOVA	Treatment	0.7302	0.5366	No	N/A					
Figure 16D	pTau/Tau ratio, PS19 mo., KO and Trod	3,3,3	Mean ± SEM	One-Way ANOVA	Treatment	73.65	0.0131	Yes	Bonferroni	PS19 vs. PS19 nPKO	4.134	0.1077	No	
										PS19 vs. PS19 Trod.	167.9	< 0.0001	Yes	****
Figure 17B	PS19 8 mo. p-GSK3B/GSK3B ratio PTP1B ablation model	3,3,3,3	Mean ± SEM	Two-Way ANOVA	Interaction	F (1, 8) = 1.368	0.2758	No	Bonferroni	WT vs. PTP1B KO	1.163	> 0.9999	No	
										WT vs. PS19	0.8437	> 0.9999	No	
					Genotype	F (1, 8) = 5.584	0.0457	Yes		WT vs. PS19 PTP1B KO	3.661	0.0384	Yes	*
										PTP1B KO vs. PS19	0.3189	> 0.9999	No	
					Treatment	F (1, 8) = 7.918	0.0227	Yes		PTP1B KO vs. PS19 PTP1B	2.498	0.2223	No	
										PS19 vs. PS19 PTP1B KO	2.817	0.1356	No	
Figure 17C	PS19 8 mo. p-GSK3B/GSK3B ratio Trod. Treatment	3,3,3,3	Mean ± SEM	One-Way ANOVA	Treatment	0.05906	0.9432	No	N/A					

Table 3. Summarized statistical analyses for Western Blot experiments.